A differential capacitive measurement system used in a dynamic environment

Goossens, J.H.P.M.

Award date:
2000

Eindhoven University of Technology
Department of Electrical Engineering
Control Systems Group

A Differential Capacitive Measurement System Used in a Dynamic Environment.

By: J.H.P.M. Goossens

Professor: Prof. Dr. Ir. P.P.J. van den Bosch

Mentor: Ir. V.M.G. van Acht

Eindhoven, October 2000

The Netherlands

Abstract

A PhD student of the Control Systems group of the department of Electrical Engineering of the Technical University of Eindhoven is designing and building a laser deflection system. This laser deflection system is used for 3D laser interferometer measurements for object tracking. An important part of this laser deflection system is the differential capacitive measurement system. This measurement system measures the orientation and position of a floating mirror that deflects a laser beam.

This report handles about the design and implementation of the differential capacitive measurement system in a dynamic environment. The differential capacitive measurement system in this report has one degree of freedom. The measurement system measures small displacements of a loudspeaker diaphragm (=dynamical environment). The following aspects of the measurement system are investigated.

- Accuracy
- Sensitivity
- Reproducibility
- Resolution
- Signal to noise ratio

Furthermore possible sources of errors are investigated and their contributions to the inaccuracy of the measurement system have been estimated. The measurement system has a resolution of at least 10^{-5} m. A sensitivity of 211mV/mm was realized. The averaged inaccuracy of the measurement system was 8 μm. Based on identified models of the loudspeaker a controller is designed for controlling the displacement of the loudspeaker diaphragm.

Acknowledgement

I would like to use this page of my report, to express my sincere gratitude to the people involved in my thesis.

First of all I would like to thank Prof. Dr. Ir. P.P.J. van den Bosch, who gave me the opportunity for working on this project.

I also would like to thank Ir. V.M.G. van Acht, who coached me during the months I was working on my thesis.

I would like to thank Ir. H. Goossens for his time and effort he has put in the graduation commission.

Special thanks go out to Mr. A.H.A.S. van de Graft and Ing. R.A. Zorge, who helped me with the electronics and the mechanical construction of the differential capacitive measurement system.

I would like to thank the involved employees of the Control Systems Group of the TU/e who all contributed their own part to my thesis.

Finally I would like to thank my family and friends, who supported me during my entire period of study.

Jeffrey Goossens.

Contents

1. Introduction

1.1. Purpose of investigation

For several years the Control Systems group of the department of Electrical Engineering of the Technical University of Eindhoven (TU/e) studies magnetic levitation systems. A PhD student (AIO-4) is designing and building a new laser deflection system for a 3D laser interferometer for object tracking. See figure 1.1. The laser beam from the interferometer is reflected by the laser deflection on the object to be tracked. The returning beam is splitted for the interferometer and the Position Sensitive Device (short PSD). The error signal is the feedback for the laser deflection system. The object position can be calculated using distance measurement from the interferometer and angle measurements from the laser deflection system.

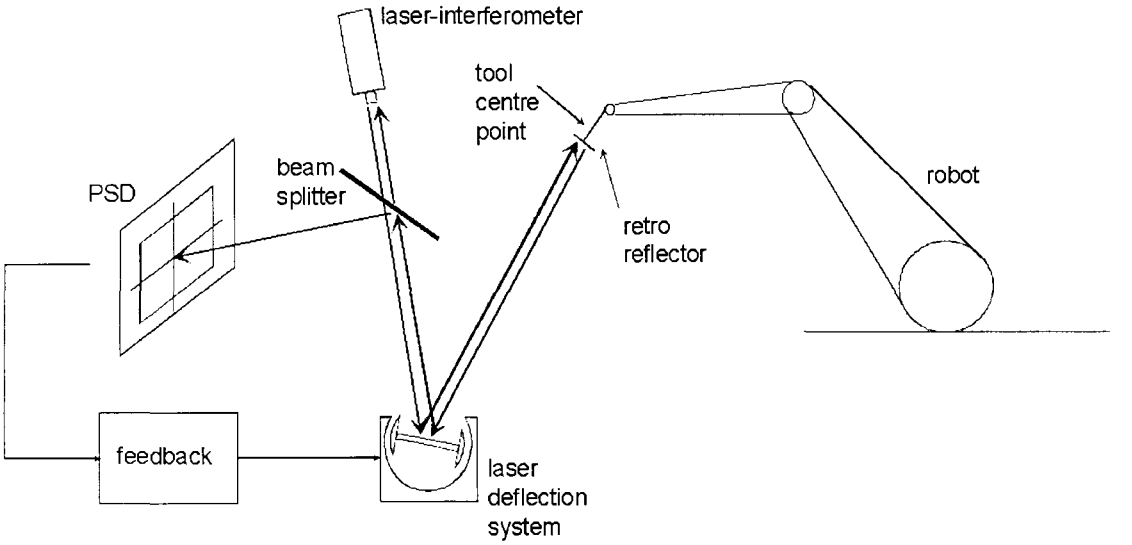

Figure 1-1 Diagram of laser-interferometer.

The laser deflection system consists of a floating mirror, magnetic actuators and a capacitive position/orientation measurement system. The magnetic actuators keep the mirror floating and a controller controls the position and orientation of the mirror. The floating mirror has 5 degrees of freedom. The mirror can move in the X, Y and Z direction and rotate around the X and Y axes. The capacitive position/orientation measurement system measures the location and orientation of the mirror. The rotation around the Z axes is not important because the mirror is symmetrical. This thesis describes the capacitive measurement system.

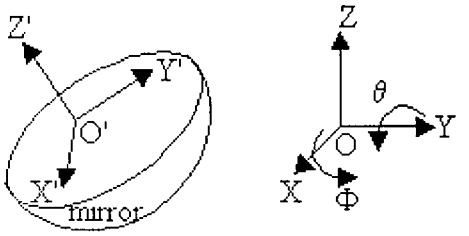

Figure 1-2 Degree of freedoms of orientation and translation of floating mirror.

1.2. Capacitive measurement system

The capacitive measurement system has to meet several requirements:

- Contactless measurement
- 5 degrees of freedom must be measured
- Small
- EMC robust
- Accurate
- Bandwidth of 20 kHz
- Simple and cheap
- Robust

No commercial capacitive measurement systems were available that met all mentioned requirements. Especially the first two requirements were not satisfied by any measurement system. Furthermore no measurement system could measure large rotations around the X and Y axes. This implied that a new capacitive measurement system had to be designed. The assignment for my teaching practice at the Control Systems group was to design and built an experimental capacitive measurement system with 1 degree of freedom. The measurement system had to meet the other above requirements. An experimental capacitive measurement system that could measure a movement in one direction was built. The capacitive sensor consisted of plate capacitors. The experimental capacitive measurement system showed that a resolution of approximately 15 micrometers was possible. [GOO99] Furthermore the principle of operation of the capacitive measurement system has been proven to work.

1.3. Assignment

As a preparation for the laser deflection system with 5 degrees of freedom a similar analogous system has to be designed and built that has 1 degree of freedom. A loudspeaker is a Lorentz motor with 1 degree of freedom. A loudspeaker also consists of a magnetic actuator. The major difference between the laser deflection system and a loudspeaker is that the former is passively unstable and the latter is passively stable.

Now a new capacitive measurement system will be designed. The experimental capacitive measurement system must be redesigned and implemented in a dynamic environment. The capacitive measurement system measures the displacements of the loudspeaker diaphragm with concentric cylinder capacitors. A controller will be designed and built to control the position of the loudspeaker diaphragm. The capacitive measurement system shall be calibrated. The following aspects of the capacitive measurement system shall be investigated:

- Accuracy
- Sensitivity
- Reproducibility
- Resolution
- Signal to noise ratio

1.4.Approach

First the capacitive measurement system needs to be improved in comparison with the experimental measurement system [GOO99] and modified such that the displacements of the diaphragm of the loudspeaker can be measured. The influence of many disturbances that existed in the experimental capacitive measurement system need to be eliminated. When the capacitive measurement system is built the implementation has to be improved such that the differential capacitive measurement system fulfills all requirements. The aspects summed in section 1.3, are investigated for the capacitive measurement system.

The loudspeaker characteristics are identified and a suitable model is formulated. Based on this model a controller will be designed to control the system.

2. Differential capacitive measurement system

2.1. Plate capacitor

An experimental differential capacitive measuring system was already developed, which measured a displacement of a conducting object contactlessly. [GOO99] The conducting object had one degree of freedom. The sensor consisted of plate capacitors. The value for a plate capacitor changes proportionally with the common surface of the plates and inverse proportional with the distance between the plates. In [GOO99] the common surface of the plates changed linearly with the displacement of the conducting object.

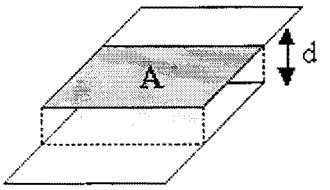

Figure 2-1 Plate capacitor.

The capacitance C of a plate capacitor is given by:

$$C = \frac{\varepsilon_0 \varepsilon_r A}{d} \tag{2.1}$$

[LAA95]

where

C = capacity [F]
ε_0 = dielectric constant [Fm^{-1}]
ε_r = relative dielectric constant
A = common surface of plates [m^2]
d = distance between plates [m]

The experimental system in [GOO99] had a sensitivity of 268 mV/mm. Furthermore the experimental measurement system suffered from lot of disturbances.

2.2. Concentric Cylinder Capacitor

Figure 2-2 shows two concentric cylinders. The capacitance between two concentric cylinders with length L and radius a and b, see figure 2.2 is given by formula 2.2. The Electrical fringing field is neglected.

$$C = \frac{2\pi \varepsilon_o \varepsilon_r}{\ln(b/a)} L \tag{2.2}$$

[LAA95]

where

C = capacity [F]
ε_0 = dielectric constant [Fm^{-1}]
ε_r = relative dielectric constant
ln = natural logarithm
L = common length of cylinder a with cylinder b [m]
b = inside radius outside cylinder [m]
a = outside radius inside cylinder [m]

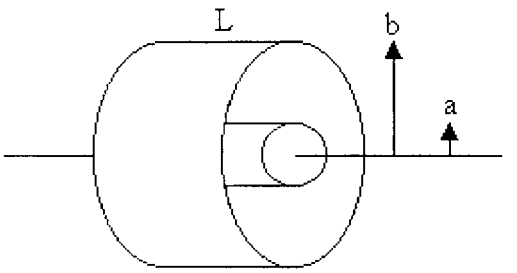

Figure 2-2 Concentric cylinders.

The capacity between two concentric cylinders is proportional with the common length of the concentric cylinders and inverse proportional with the natural logarithmic ratio of radius b and a. Both cylinders are equal in length. In equilibrium the common length is equal to the length of each cylinder. Cylinder A is completely surrounded by cylinder B in equilibrium. A movement of one of the two cylinders in the axial direction implies that the common length decreases and also the capacity value decreases. It is possible to measure displacements with concentric cylinders and convert the information to an electrical quantity. The advanced differential capacitive measurement system uses cylinder capacitors instead of plate capacitors. It is mechanical easier to implement cylinder capacitors rather than plate capacitors on a loudspeaker.

2.3. Mechanical configuration of the differential capacitive sensor

Mechanical configuration

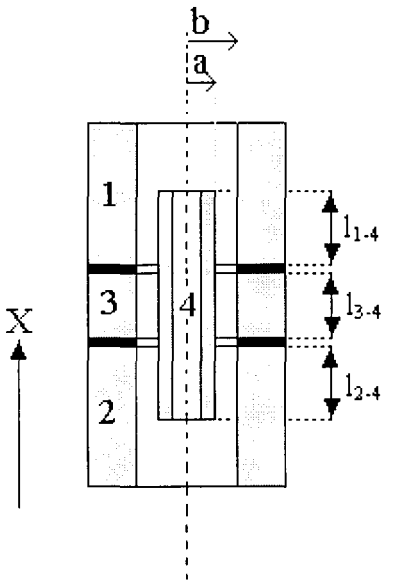

Figure 2-3 Cross-section of cylindrical capacitive sensor with 1 DOF.
Grey area = conducting material
Black area = non-conducting material
White area = air

Figure 2-3 shows a cross-section of the cylindrical differential capacitive sensor with 1 degree of freedom. The grey planes in figure 2-3 are cross-sections of metal cylinders named: cylinder 1, cylinder 2, cylinder 3 and cylinder 4. The black planes are cross-sections of non-conducting rings located between cylinders 1 and 3 and located between cylinders 2 and 3. Cylinder 4 is able to move **only** in the positive as well as in the negative X direction (=axial direction). Between cylinder 4 and cylinders 1, 2 and 3 capacities exist. All capacities are concentric cylinder capacitors. Cylinders 1 and 2 are the input terminals of the sensor. Cylinder 3 is the output terminal of the sensor.

Definitions:

C_{1-4} := concentric cylinder capacity between cylinder 1 and 4
C_{2-4} := concentric cylinder capacity between cylinder 2 and 4
C_{3-4} := concentric cylinder capacity between cylinder 3 and 4

Cylinder 4 is the moving object that may travel in the X-direction until one of the ends of the cylinder passes one of the non-conducting rings. This implies that the capacitor value C_{3-4} is invariant at all times because the common length l_{3-4} and the radiuses a and b are invariant for capacitor C_{3-4}. If cylinder 4 moves in the positive X direction the common length of capacitor C_{1-4} increases while the common length of capacitor C_{2-4} decreases. The capacities C_{1-4} and C_{2-4} respectively increase and decrease in size. For movements of cylinder 4 in the negative X direction the reverse happens. Due to the restriction in movement for cylinder 4 the linear relation between movement and capacity value is always guaranteed. The theoretical origin of the X-axis is defined halfway the length of cylinder 3 in the axial direction (= X direction). The capacitors C_{1-4} and C_{2-4} are equal to the constant C_0 if X=0 (no displacement of

cylinder 4). If cylinder 4 moves in the positive direction the value of $C_{1\text{-}4}$ will linear increase with the displacement X while the value of $C_{2\text{-}4}$ linear decreases with the displacement. For a movement of cylinder 4 in the negative X direction the opposite occurs.

Definitions:

$$C_{1-4} = C_0 + c \cdot X \tag{2.3}$$

$$C_{2-4} = C_0 - c \cdot X \tag{2.4}$$

$$C_{3-4} = C_0 \tag{2.5}$$

Fringe capacity
If cylinder 4 moves near the far ends of its range the above equations must be expanded with a non-linear term. Figure 2-4 shows a partial drawing of two concentric cylinders that have no common length. The electrical fringe field between the ends of the cylinders introduce a small capacity called a fringe capacity. This fringe capacity is also sensitive for displacements hence the electrical fringe field between the two cylinders changes due to displacement of one of the two cylinders in the axial direction. This introduces a small non-linearity to formula 2.2 to 2.4. The introduced additional non-linear term is only important if the linear term (=formula 2.2) is small else this non-linear term can be neglected. The linear term is small if the common length of the cylinder capacity is close to zero. Because it is not possible to calculate the fringe capacitor analytically we neglect this influence. This is a fair assumption if the capacitive measurement system does not operate near the far ends of its range.

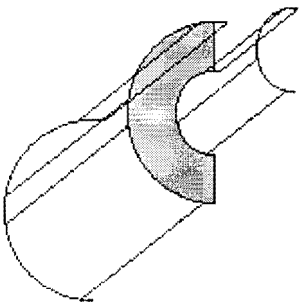

Figure 2-4 Partial drawing of two concentric cylinders.

Influence of eccentricity
The moving cylinder 4 has to be positioned concentrically in the mechanical configuration. The electric field between two concentric cylinders in air is given by formula 2.6:

for $r_a < r < r_b$

$$E = \frac{Q'}{2\pi\varepsilon_0\varepsilon_r r} \tag{2.6}$$

where

E = Electrical field [V/m]
Q' = Charge per length [C/m]
r = Radius [m]

What happens if cylinder 4 is positioned eccentrically? The radial axis of cylinder 4 is parallel with the radial axes of all other cylinders but does not coincide. Due to the shifting of the radial axis of cylinder 4 in the radial direction the radius r is not constant for formula 2.6. At one side the distance between cylinder 4 and the mechanical sensor construction is smaller while at the other side the distance is larger. The Electrical field between cylinder 4 and the mechanical sensor construction is non-uniform.

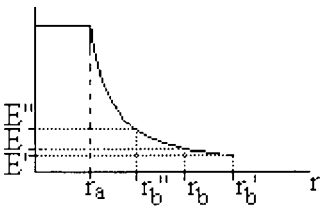

Figure 2-5 Electrical field curve.

Figure 2-5 shows the Electrical field curve of formula 2.6 in air ($r_a < r < r_b$). A smaller gap distance results in a stronger Electrical field while a greater gap distance results in a weaker Electrical field. The loss of electrical field intensity due to a wider radius r_b' is much lesser than the gain of Electrical field intensity due to a smaller radius r_b''.

The potential is defined as:

$$V = \int E dr \tag{2.7}$$

The potential is the surface beneath the electrical field curve. The potential decreases if the gap distance becomes smaller while the potential increases if the gap distance becomes larger. The accumulated result of the eccentricity is that the decrease in potential at one side is larger than the increase in potential at the other side.

$$C = \frac{Q}{V} \tag{2.8}$$

The capacity is calculated with formula 2.8. The potential V is smaller which results to a larger capacitor value. The capacity value is larger but has also a linear relation with the displacement in the axial direction. The capacity per length unit only increased due to the eccentricity. This implies that the linearity of the capacitor sensor is not affected by eccentricity.

What is the influence of cylinder 4 on the systems performance when the axial axis is not parallel to the other axial axes cylinders? Cylinder 4 is positioned asymmetrical in the sensor case. At one end the distance between cylinder 4 and for example cylinder 1 increases while at the other end the distance decreases. The net result of the decrease and increase distance on the capacity value cannot be simply calculated. This can only be numerically analysed and depends on how asymmetrical cylinder 4 is positioned in the sensor case. The linearity between displacement and alteration of the capacitor values will not be valid any more. This asymmetry results in a non linear relation between displacement and capacities.

2.4.Basic principle of capacitive measuring system

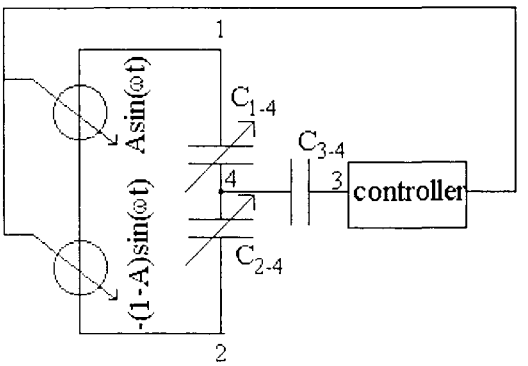

Figure 2-6 Basic principle of differential capacitive measurement system.

Figure 2-6 shows the basic principal of the differential capacitive measurement system. Two variable voltage sources with amplitudes A and –(1-A), with the condition $0 \leq A \leq 1$, are connected with respectively capacitors $C_{1\text{-}4}$ and $C_{2\text{-}4}$. The signals of the voltage sources have the same frequency but have a phase difference of 180 degrees and the ratio of the amplitudes is variable. The magnitude of the changes of the concentric cylinder capacitors $C_{1\text{-}4}$ and $C_{2\text{-}4}$ can be determined from the voltage at point 4. With capacity $C_{3\text{-}4}$ the AC voltage at point 4 is measured contactlessly. The voltage at point 4 is a superposition of the voltages of the variable voltage sources. If we assume that no current flows through capacitor $C_{3\text{-}4}$:

$$V_4(t) = \frac{\frac{1}{j\omega C_{2-4}}}{\frac{1}{j\omega C_{1-4}} + \frac{1}{j\omega C_{2-4}}} A\sin(\omega t) - \frac{\frac{1}{j\omega C_{1-4}}}{\frac{1}{j\omega C_{1-4}} + \frac{1}{j\omega C_{2-4}}} (1-A)\sin(\omega t) \qquad (2.9)$$

$$V_4(t) = \frac{AC_{1-4}\sin(\omega t) - (1-A)C_{2-4}\sin(\omega t)}{C_{1-4} + C_{2-4}} \qquad (2.10)$$

$$V_4(t) = \frac{2AC_0 - C_0 + c \cdot X}{2C_0}\sin(\omega t) \qquad (2.11)$$

[ACH00]

The ratio between capacity $C_{1\text{-}4}$ and $C_{2\text{-}4}$ is related to the displacement. If we control the AC voltage at point 4 to zero by adjusting the amplitudes of the voltage sources there is a linear relation between the controlled amplitude A and the displacement X. A is called the output voltage of the differential capacitive measurement system.

$$\omega \neq 0 \quad \exists A \Rightarrow |V_4(t)| = 0$$
$$A = \tfrac{1}{2} - \frac{c}{2C_0} X \tag{2.12}$$

The controller in figure 2-6 controls the voltage at point 4 back to 0 Volts for all displacements. If the AC voltage at point 4 is equal zero then the AC voltage at point 3 must also be equal to zero. Formula 2.9 states that the linear relation between the displacement X and the controlled voltage A is independent of the frequency of the signals of the variable voltage sources.

2.5.Parasitic capacities

In figure 2-7 the schematics of the differential cylindrical capacitive sensor is depicted and extended with parasitic capacities named: C_{p1} .. C_{p6}. The value C_0 is small so that parasitic capacities cannot be completely neglected. Parasitic capacities exist between every electrical node. The main problem with parasitic capacities is that they cannot be *accurately* calculated.

The parasitic capacities C_{p1}, C_{p2} and C_{p3} have no influence on the voltage $V_4(t)$ if we assume to have ideal voltage sources. The influence of the non idealities of the voltage sources will be discussed in chapter 7. The parasitic capacitors C_{p0} and C_{p4} have no influence on the measurement because the voltages at points 4 and 3 are controlled to zero Volts by the controller. The important parasitic capacitors that have to be taken into account for accurate measurement are parasitic capacitors C_{p5} and C_{p6}. The parasitic capacitors C_{p5} and C_{p6} are functions of the displacement of cylinder 4. The influence of parasitic capacitors C_{p5} and C_{p6} cannot be eliminated by calibration because their influence is not constant. The influence of C_{p5} and C_{p6} can be reduced to an insignificant value by proper guarding the output signal at the output terminal (cylinder 3) of the differential capacitive sensor.

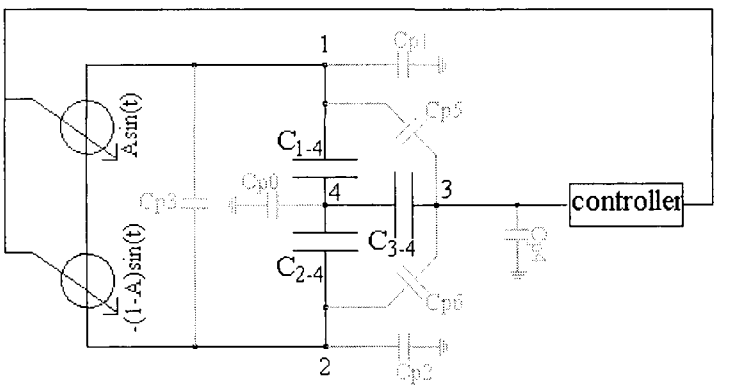

Figure 2-7 Schematics of differential capacitive measuring system.

The Kirchhoff's node equations for points 4 and 3 are respectively:

$$(V_4 - V_1)sC_{1-4} + (V_4 - V_2)sC_{2-4} + (V_4 - V_3)sC_{3-4} + V_4 sC_{p0} = 0 \tag{2.13}$$

$$(V_3 - V_4)sC_{3-4} + (V_3 - V_1)sC_{p5} + (V_3 - V_2)sC_{p6} + V_3 sC_{p4} = 0 \tag{2.14}$$

Solving formula 2.13 for V_4 gives:

$$V_4 = \frac{C_{1-4}V_1 + C_{2-4}V_2 + C_{3-4}V_3}{C_{1-4} + C_{2-4} + C_{3-4} + C_{p0}} \tag{2.15}$$

Solving formula 2.14 and using formula 2.15 gives for V_3:

$$\begin{aligned} V_3 = & \frac{\{C_{1-4}C_{3-4} + C_{p5}(C_{p0} + C_{1-4} + C_{2-4} + C_{3-4})\}}{C_{3-4}(C_{p0} + C_{1-4} + C_{2-4}) + (C_{p4} + C_{p5} + C_{p6})(C_{p0} + C_{1-4} + C_{2-4} + C_{3-4})} V_1 \\ & + \frac{\{C_{2-4}C_{3-4} + C_{p6}(C_{p0} + C_{1-4} + C_{2-4} + C_{3-4})\}}{C_{3-4}(C_{p0} + C_{1-4} + C_{2-4}) + (C_{p4} + C_{p5} + C_{p6})(C_{p0} + C_{1-4} + C_{2-4} + C_{3-4})} V_2 \end{aligned} \tag{2.16}$$

V_3 is called the output voltage of the differential capacitive sensor. If we reduce the value of parasitic capacitor C_{p4}, the output voltage V_3 of the differential capacitive sensor is much more ***sensitive*** for amplitude changes of the voltages V_1 and V_2. C_{p4} is only a variable in the denominator of formula 2.16. With proper guarding the value of capacitor C_{p4} can be reduced.

Reducing capacitor value C_{p0} also increases the sensitivity of the output voltage of the sensor. This is not possible in practice because parasitic capacitor C_{p0} is located between the fixed world and a 'floating' object. Increasing the sensitivity by reducing C_{p0} can be seen by rewriting formula 2.16.

Redefining:

$$\begin{aligned} Q\{C_{1-4}, C_{2-4}, C_{3-4}, C_{p4}, C_{p5}, C_{p6}, V_1, V_2\} := & (C_{1-4}C_{3-4} + C_{p5}(C_{1-4} + C_{2-4} + C_{3-4}))V_1 \\ & + (C_{2-4}C_{3-4} + C_{p6}(C_{1-4} + C_{2-4} + C_{3-4}))V_2 \end{aligned} \tag{2.17}$$

$$\begin{aligned} U\{C_{1-4}, C_{2-4}, C_{3-4}, C_{p4}, C_{p5}, C_{p6}, V_1, V_2\} := & C_{3-4}(C_{1-4} + C_{2-4}) \\ & + (C_{p4} + C_{p5} + C_{p6})(C_{1-4} + C_{2-4} + C_{3-4}) \end{aligned} \tag{2.18}$$

$$V_3 = \frac{C_{p0}(C_{p5}V_1 + C_{p6}V_2) + Q\{C_{1-4}, C_{2-4}, C_{3-4}, C_{p4}, C_{p5}, C_{p6}, V_1, V_2\}}{C_{p0}(C_{3-4} + C_{p4} + C_{p5} + C_{p6}) + U\{C_{1-4}, C_{2-4}, C_{3-4}, C_{p4}, C_{p5}, C_{p6}, V_1, V_2\}} \tag{2.19}$$

Functions Q and U are independent of C_{p0}. Reducing C_{p0} results in an increase of the output voltage V_3 thus a larger sensitivity. The conclusion is that reducing the parasitic capacities C_{p0} and C_{p4} increases the sensitivity. It is only possible to reduce C_{p4} in practice by using a guard.

2.6. Guarding

The parasitic capacitor values C_{p5} and C_{p6} have to be reduced to insignificant values. Because the sensor is symmetrical, only the reduction of the value of parasitic capacitor C_{p5} is discussed but the same things have been done to reduce the value of parasitic capacitor C_{p6}. Parasitic capacitor C_{p5} exists between input terminal 1 and the output terminal 3.

Figure 2-8a shows a partial cross-section of the differential capacitive sensor with a guard ring. Between cylinder 1 and cylinder 3 a conducting ring is located named 'guard'. The parasitic capacitor C_{p5} that existed in the mechanical configuration depicted in figure 2-3 is replaced by two parasitic capacitors in series.
Figure 2-8b shows the new electronic schematic. The first parasitic capacitor is located between cylinder 1 and the guard ring named C_{p5}'. The second parasitic capacitor is located between the guard ring and cylinder 3 named C_{p5}''.

The output signal of the differential capacitive sensor is buffered. The output voltage of the buffer is the same as the voltage at point 4 with the assumption that the capacitors C_{p0} and C_{p4} are neglected. If the parasitic capacitors C_{p0} and C_{p4} cannot be neglected they only attenuate the output signal. Connecting the guard with the output voltage of the buffer implies with the above assumption that the parasitic capacitor C_{p5}'' between the guard ring and cylinder 3 is unimportant because both terminals of the parasitic capacitor are connected to the same voltage. C_{G-4} is the capacitor that exists between the guard ring and cylinder 4 because there isn't any voltage difference between the terminals of C_{G-4} this capacitor has not any influence.

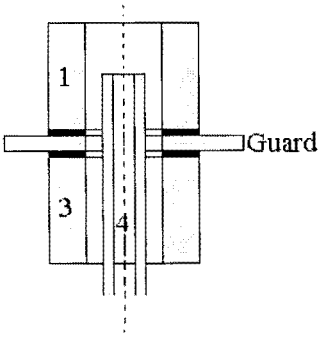

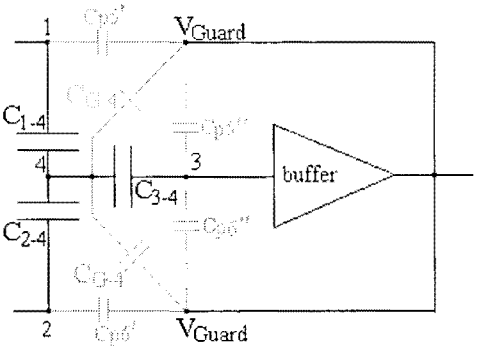

Figure 2-8a Partial mechanical cross-section. b Electronic scheme for guarding.

Grey area = conducting material
Black area = non-conducting material
White area = air

The values of the two parasitic capacitors C_{p5}'' are not important. The input voltage of the buffer is equal the output voltage. The capacitors C_{p5}' and C_{p6}' are connected at both ends with voltage sources that are presumed to be ideal. In chapter 7 the influence of the voltage sources is discussed. This implies that C_{p5}' and C_{p6}' have no influence on the output voltage of the capacitive sensor. The output of the capacitive sensor is surround with guards, which have the same potential as the output of the

capacitive sensor. The parasitic capacitor C_{p4} that exists between the output of the sensor and earth has been reduced due to this guarding.

2.7. Square wave generators

The voltage sources with variable amplitude can also generate square wave signals in contrary to the earlier reported sinusoidal signals. Formula 2.12 stated that the linear relation between controlled amplitude and displacement is independent of the used frequency. A square wave consists of many harmonic sinusoidal signals.

The amplitudes of the square waves are variable and the signals have a phase difference of 180 degrees. The principle mentioned before remains the same. The advantage of square wave signals is that the electronics to generate square wave signals is much easier to realise than sinusoidal signals.

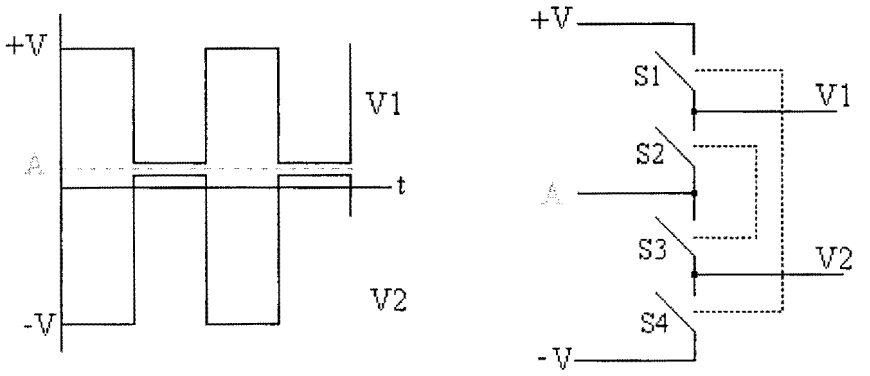

Figure 2-9 Square wave signals and principal scheme.

By switching very fast between different voltages we can generate square wave signals. Figure 2-9 shows the scheme to generate two square wave signals with a phase difference of 180 degrees and variable amplitudes. Closing switches S1 and S4 during the first half period and closing switches S2 and S3 during the second half period results that the switches generate the signals depicted in figure 2-9. The output voltage of the differential capacitive sensor is a superposition of the voltages V_1 and V_2. See formula 2.9. The controller adjusts the voltage A such that the AC output signal of the capacitive sensor is equal to zero Volts. The DC output voltage of the capacitive sensor will be removed by a demodulator.

2.8. Controlled voltage sources

We redefine the output voltage V_3 of the capacitive sensor as functions of F(), G() and H().

Redefinition:

$$F\{C_{p0}, C_{1-4}, C_{2-4}, C_{3-4}, C_{p5}\} := C_{1-4}C_{3-4} + C_{p5}(C_{p0} + C_{1-4} + C_{2-4} + C_{3-4}) \tag{2.20}$$

$$G\{C_{p0}, C_{1-4}, C_{2-4}, C_{3-4}, C_{p6}\} := C_{2-4}C_{3-4} + C_{p6}(C_{p0} + C_{1-4} + C_{2-4} + C_{3-4}) \tag{2.21}$$

$$\begin{aligned} H\{C_{p0}, C_{1-4}, C_{2-4}, C_{3-4}, C_{p4}, C_{p5}, C_{p6}\} := {} & C_{3-4}(C_{p0} + C_{1-4} + C_{2-4}) \\ & + (C_{p4} + C_{p5} + C_{p6})(C_{p0} + C_{1-4} + C_{2-4} + C_{3-4}) \end{aligned} \tag{2.22}$$

$$V_3 = \frac{F\{C_{P0}, C_{1-4}, C_{2-4}, C_{3-4}, C_{p5}\} \cdot V_1 + G\{C_{p0}, C_{1-4}, C_{2-4}, C_{3-4}, C_{p6}\} \cdot V_2}{H\{C_{p0}, C_{1-4}, C_{2-4}, C_{3-4}, C_{p4}, C_{p5}, C_{p6}\}} \tag{2.23}$$

The voltage sources have two states. State 1 is defined as the state in which switches 1 and 4 are closed and switches 2 and 3 are opened. The output voltages of the voltage sources are respectively +V and –V. State 2 is defined as the state in which switches 2 and 3 are closed and switches 1 and 4 are opened. The output voltages of both controlled voltage sources are equal A Volts.

State 1:

$$V_3^1 = \frac{F\{C_{P0}, C_{1-4}, C_{2-4}, C_{3-4}, C_{p5}\} - G\{C_{p0}, C_{1-4}, C_{2-4}, C_{3-4}, C_{p6}\}}{H\{C_{p0}, C_{1-4}, C_{2-4}, C_{3-4}, C_{p4}, C_{p5}, C_{p6}\}} V \tag{2.24}$$

State 2:

$$V_3^2 = \frac{F\{C_{P0}, C_{1-4}, C_{2-4}, C_{3-4}, C_{p5}\} + G\{C_{p0}, C_{1-4}, C_{2-4}, C_{3-4}, C_{p6}\}}{H\{C_{p0}, C_{1-4}, C_{2-4}, C_{3-4}, C_{p4}, C_{p5}, C_{p6}\}} A \tag{2.25}$$

If the voltage at point 3 is equal the voltage at point 4 than no current flows through capacitors C_{p0}, C_{3-4} and C_{p4}. This implies that V_3^1 is equal to V_3^2. The output voltage of the controller is given by:

$$A = \frac{F\{C_{P0}, C_{1-4}, C_{2-4}, C_{3-4}, C_{p5}\} - G\{C_{p0}, C_{1-4}, C_{2-4}, C_{3-4}, C_{p6}\}}{F\{C_{p0}, C_{1-4}, C_{2-4}, C_{3-4}, C_{p5}\} + G\{C_{p0}, C_{1-4}, C_{2-4}, C_{3-4}, C_{p6}\}} V \tag{2.26}$$

The output voltage of the controller is a function of the capacities and the displacement X. The capacities C_{1-4} and C_{2-4} are related to the displacement X. See formulas 2.3 and 2.4.

2.9. Block diagram

The depicted block diagram in figure 2-10 is an improved version of the block diagram of the experimental capacitive measuring system. [GOO99] The block timing controls the switches that generate the square wave signals V_1 and V_2. The output voltage of the differential capacitive sensor is buffered before the amplitude information is extracted. The output signal of the buffer is synchronously demodulated.

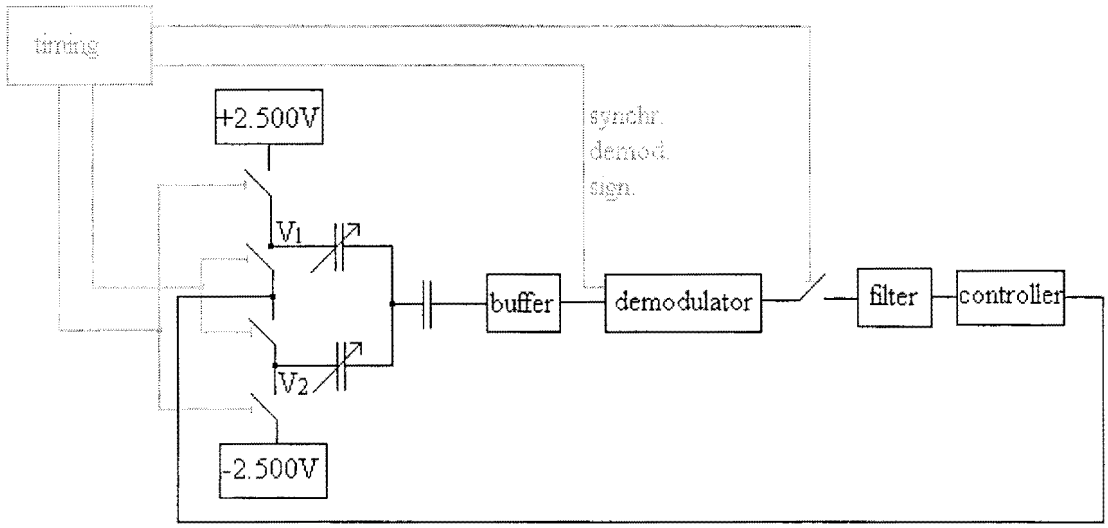

Figure 2-10 Block diagram differential capacitive measurement system.

The timing electronic generate the synchronous demodulation signal. The 'ideal' output signal of the demodulator is the amplitude of the input signal but the demodulator introduces noise and higher order carrier components. A second order low-pass filter eliminates as much noise as possible. The filter has order two because a higher order filter does not improve the signal to noise ratio further because the disturbances are located in the pass-band of the low-pass filter. The output signal of the demodulator has disturbances due to the demodulation. Most of these disturbances are located around the switching moments of the demodulator but the disturbances are in smaller quantities present between two switching moments.

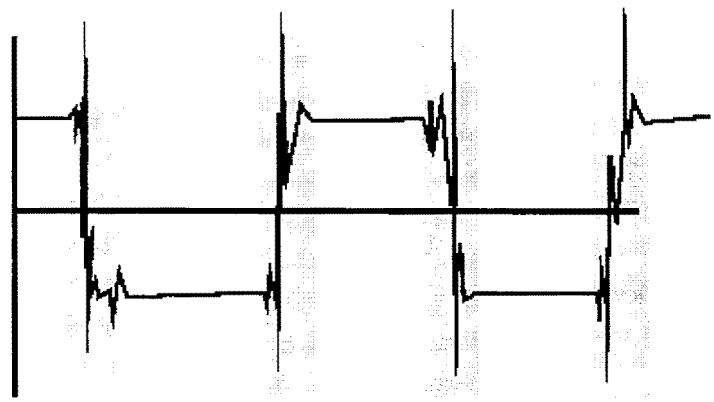

Figure 2-11 Output signal of differential capacitive sensor.

The measured signal of the differential capacitive sensor is not a nice square wave signal. Figure 2-11 shows a realistic impression of the measured signal of the sensor. The output of the capacitive sensor is a superposition of two square wave signals because the flanks of the square wave signals do not have infinite steepness distortion is introduced. The major problem is that the distortion is not averaged to zero. The distortion is mostly present near the flanks and repeats itself. This problem is solved with a switch between demodulator and low-pass filter. When the signal is smooth the switch is closed but when signal has much distortion the switch is opened. The filter keeps its value when the switched is opened.

The switching always occurs on the same moment. The switch is opened and closed at double frequency. The timing electronics also generates the control signal for the switch. The controller controls the voltage sources such that the AC output signal of the differential capacitive sensor is equal to zero.

3. Closed loop transfer function of differential capacitive measuring system

3.1. Transfer function differential capacitive sensor

Formula 2.11 states that the output voltage of the capacitive sensor is independent of the frequency. The transfer function of the differential capacitor sensor is only a gain. For calculating the transfer function of the capacitive sensor we neglect all parasitic capacities and resistances: the influence of capacitors C_{p5} and C_{p6} can be reduced to an insignificant role by proper guarding. Parasitic capacitors C_{p0} and C_{p4} only reduce the sensitivity of the sensor and will be taken later into account. When all parasitic capacities are neglected formulas 2.24 and 2.25 can be simplified to:

In state 1:

$$V_3^1 = \frac{C_{3-4}(C_{1-4} - C_{2-4})}{C_{3-4}(C_{1-4} + C_{2-4})} V \tag{3.1}$$

In state 2:

$$V_3^2 = \frac{C_{3-4}(C_{1-4} + C_{2-4})}{C_{3-4}(C_{1-4} + C_{2-4})} A \tag{3.2}$$

The top-top value of the AC voltage V_3^{tt} is:

$$V_3'' = V_3^2 - V_3^1 = A - \frac{C_{1-4} - C_{2-4}}{C_{1-4} + C_{2-4}} V \tag{3.3}$$

Substituting formulas 3.1 and 3.2 in 3.3 results in:

$$V_3'' = A - \frac{C_0 + cX - (C_0 - cX)}{C_0 + cX + C_0 - cX} = A - \frac{c}{C_0} X \tag{3.4}$$

The transfer function of the sensor is related to the displacement variable X and the voltage A. This only holds with the condition that the parasitic capacities are insignificant. The voltage A is not depending on the variable X in open loop. The parasitic capacitors C_{p0} and C_{p4} only deteriorate the sensitivity. This means that the gains of the transfer function must be adjusted with a factor α. The α value must be between 0 and 1. The transfer functions H_A and H_X are only gains.

$$V_3'' = \alpha A - \alpha \frac{c}{C_0} X \tag{3.5}$$

Definition:

$$H_A = \alpha \tag{3.6}$$

$$H_X = \alpha \frac{c}{C_0} \tag{3.7}$$

Redefinition:

$$V_3'' := H_A \cdot A - H_X \cdot X \tag{3.8}$$

3.2. Transfer function demodulator

The demodulator extracts the amplitude information and phase information from the input signal. This is done by multiplying the input signal with +1 during one half period and multiplying the input signal with –1 during the other half period. The amplitude of the input signal of the demodulator is multiplied with one. The sign of the dc output voltage represents the phase information. A positive dc output voltage represents zero phase shift and a negative dc voltage represents 180 degrees phase shift.

3.3. Transfer function of second order filter

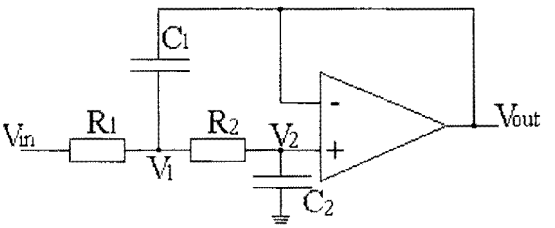

Figure 3-1 Electronic circuitry of a second order filter.

Figure 3-1 shows the electronic circuitry of a second order filter. This electronic circuitry is chosen because the filter needs to have imaginary poles. The reason for imaginary poles is explained in section 3.5. The transfer function is given by:

$$\frac{(V_1 - V_{in})}{R_1} + \frac{(V_1 - V_2)}{R_2} + sC_1(V_1 - V_{out}) = 0 \tag{3.9}$$

$$\frac{(V_2 - V_1)}{R_2} + sC_2V_2 = 0 \tag{3.10}$$

$$V_2 = V_{out} \tag{3.11}$$

$$H_{Filter}(s) = \frac{1}{s^2R_1R_2C_1C_2 + s(R_1C_2 + R_2C_2) + 1} \tag{3.12}$$

3.4. Transfer function controller

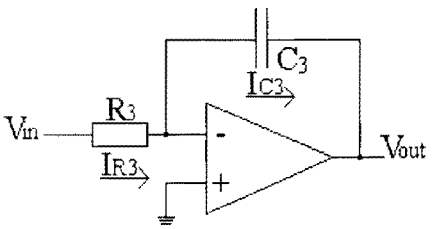

Figure 3-2 Electronic circuitry of an integrator.

The controller is an integrator. The integration action of the controller is necessary to remove a systematic final error. The transfer function of the integrator is given by:

$$H_{controller}(s) = -\frac{1}{sR_3C_3} \tag{3.13}$$

A short integration time results in a fast response but a long integration time results in a more accurate value because the noise is averaged over a longer period. The value of the integration time is a compromise between accuracy and speed.

3.5. Transfer function closed loop measuring system

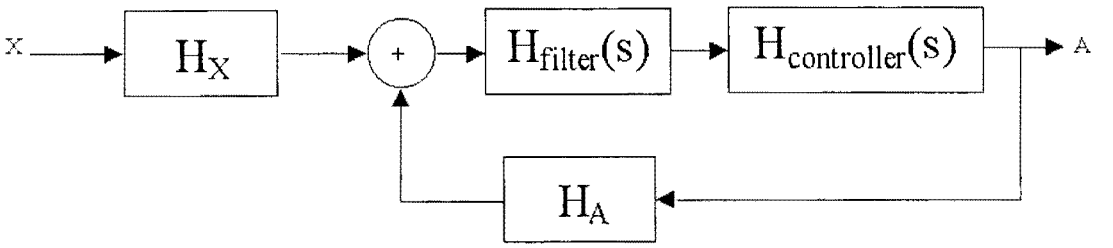

Figure 3-3 Closed loop block diagram.

Figure 3-3 shows the closed loop block diagram of the measurement system. For simplicity we neglected the transfer function of the demodulator because this is a multiplication of the amplitude of the input signal with 1. The transfer function of the closed loop system is given by:

$$H_{system} = \frac{H_X \cdot H_{filter}(s) \cdot H_{controller}(s)}{1 - H_A \cdot H_{Filter}(s) \cdot H_{controller}(s)} \tag{3.14}$$

Substituting formulas 3.12 and 3.13 in 3.14 results in:

$$H_{system}(s) = \frac{c}{C_0} \frac{\alpha}{s^3 R_1 R_2 R_3 C_1 C_2 C_3 + s^2 (R_1 R_3 C_2 C_3 + R_2 R_3 C_2 C_3) + sR_3 C_3 + \alpha} \tag{3.15}$$

The transfer function $H_{system}(s)$ of the closed loop system must satisfy a third order Bessel transfer function or also called a third order low-pass Bessel filter. This implies that imaginary poles are needed. A low-pass Bessel filter has a constant group delay. The group delay is defined as minus the derivative of the phase:

$$\tau_g(\omega) = -\frac{\partial \Phi(\omega)}{\partial \omega} \tag{3.16}$$

A constant group delay means that the delay time between the input signal and output signal of a system is constant for all frequencies in the pass-band. The shape of the input signal shall not be disfigured by the transfer function of the system. If cylinder 4 moves in the X-direction describing a certain pattern than the output voltage of the system will describe that same pattern. When the group delay is not constant for all frequencies in the pass-band then the output signal is disfigured. The Bessel transfer function has a shorter settling time than other transfer functions. The Bessel transfer function is the best compromise between a fast and accurate response.

3.5.1 Bessel transfer function

The coefficients of the closed loop transfer function should satisfy a third order Bessel polynomial. The formula for Bessel polynomials of order n is given by:

$$B_n(s) = \sum_{k=0}^{n} \frac{(2n-k)!}{2^{n-k}\, k!(n-k)!} s^k \tag{3.17}$$

[SUA96]

For a third order Bessel polynomial $B_3(s)$ is:

$$B_3(s) = s^3 + 6s^2 + 15s + 15 \tag{3.18}$$

$$H_{bessel}(j\omega) = \frac{15}{-j\omega^3 - 6\omega^2 + 15j\omega + 15} \tag{3.19}$$

The Bessel transfer function is given by formula 3.19. The Bessel transfer function can be normalized. This means that the cut-off frequency is equal to 1 rad/sec. Index c is short for cut-off frequency and index n is short for normalized frequency.

$$\omega = \omega_n \cdot \omega_c \tag{3.20}$$

$$H_{Bessel}(j\omega_n) = \frac{\frac{15}{\omega_c^3}}{-j\omega_n^3 - 6\frac{\omega_n^2}{\omega_c} + 15j\frac{\omega_n}{\omega_c^2} + \frac{15}{\omega_c^3}} \tag{3.21}$$

Normalization of formula 3.19.

$$\omega_C = \sqrt[3]{15} \tag{3.22}$$

$$H_{Bessel}(j\omega_n) = \frac{1}{-j\omega_n^3 - \frac{6}{\sqrt[3]{15}}\omega_n^2 + j\sqrt[3]{15}\omega_n + 1} \tag{3.23}$$

The differential capacitive measuring system must have a bandwidth of 20 kHz. Denormalization of formula 3.23 with cut-off frequency 20 kHz.

$$H(j\omega)_{Bessel} = \frac{\omega_c^3}{-j\omega^3 - \frac{6}{\sqrt[3]{15}}\omega_c\omega^2 + j\sqrt[3]{15}\omega_c^2\omega + \omega_c^3} \tag{3.24}$$

The cut-off frequency of a Bessel transfer function implies that the phase response is linear for frequencies smaller than the cut-off frequency. For frequencies larger than the cut-off frequency their exists a non-linear relation.

Redefining $H(j\omega)_{Bessel}$:

$$H(j\omega)_{Bessel} = \frac{b_0}{-j\omega^3 - b_2\omega^2 + jb_1\omega + b_0} \tag{3.25}$$

$$b_0 = 1.9844 \cdot 10^{15} \tag{3.26}$$

$$b_1 = 3.8944 \cdot 10^{10} \tag{3.27}$$

$$b_2 = 3.0572 \cdot 10^{5} \tag{3.28}$$

3.5.2 Properties Bessel transfer function

Figure 3-4 shows the amplitude and phase plot of the Bessel transfer function. The cut-off frequency lies at 20 kHz. The closed loop Bessel transfer function has the characteristics of a third order low-pass filter.

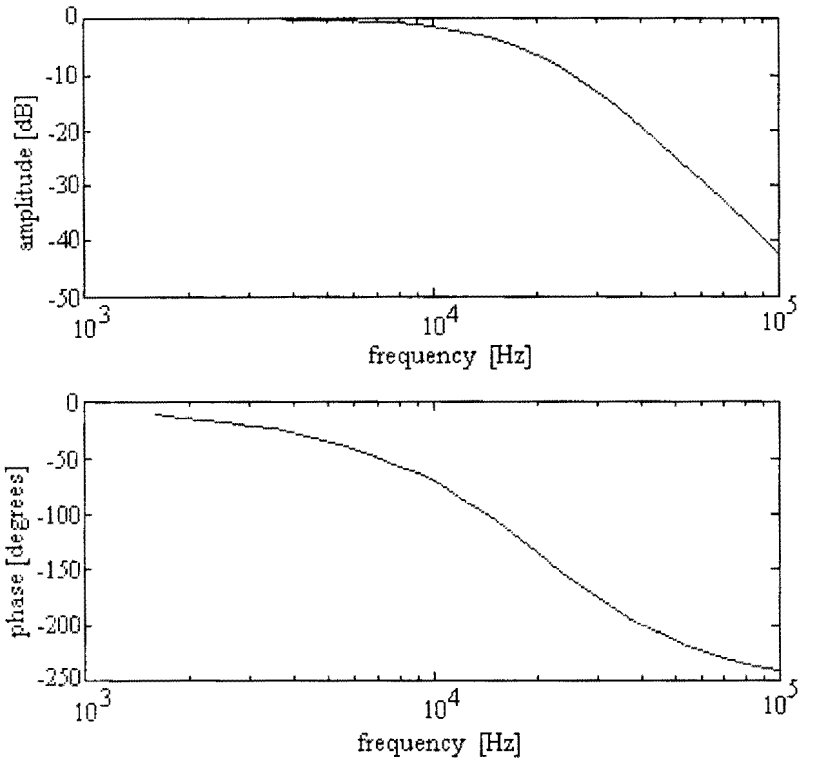

Figure 3-4 Amplitude and phase plot of Bessel transfer function f_c = 20 kHz.

The phase of the Bessel transfer function is given by formula 3.29.

$$\Phi(\omega) = -\arctan\left(\frac{b_1\omega - \omega^3}{b_0 - b_2\omega^2}\right) \tag{3.29}$$

The group delay of the Bessel transfer function is given by formula 3.30.

$$\tau_g(\omega) = -\frac{\partial\Phi(\omega)}{\partial\omega} = \frac{(b_0 - b_2\omega^2)(b_1 - 3\omega^2) + 2b_2\omega(b_1\omega - \omega^3)}{(b_0 - b_2\omega^2)^2 + (b_1\omega - \omega^3)^2} \tag{3.30}$$

Figure 3-5 shows the linear phase frequency curve of the Bessel transfer function. The derivative of the phase is constant for frequencies smaller than 20 kHz. This implies a constant group delay for frequencies smaller than the cut-off frequency of 20 kHz. For frequencies larger than 20 kHz the derivative decreases rapidly.

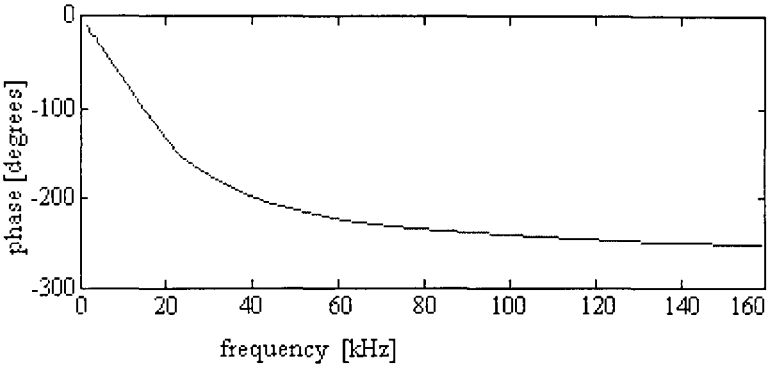

Figure 3-5 Linear phase frequency curve.

Figure 3-6 shows the group delay of the Bessel transfer function. The group delay is constant for all frequencies in the pass-band ($\omega << \omega_C$).

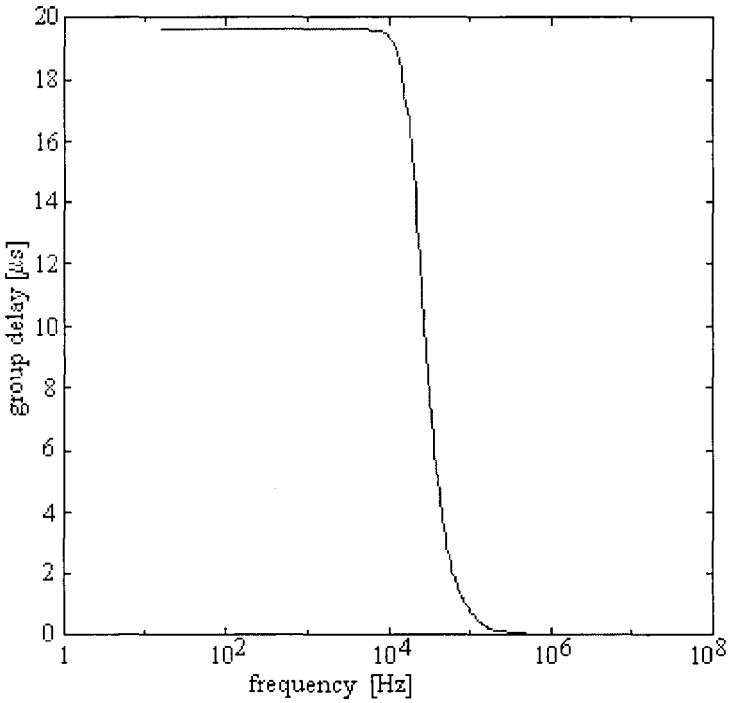

Figure 3-6 Group delay Bessel transfer function.

3.5.3 Dimensioning of the closed loop transfer function

Formula 3.15 is rewritten in the form of formula 3.25 with the assumption that the factor α is equal 1. The influences of capacitors C_{p0} and C_{p4} on the sensitivity of the sensor are assumed to be minimal. This gives the following result:

$$b_0 = \frac{1}{R_1 R_2 R_3 C_1 C_2 C_3} \tag{3.31}$$

$$b_1 = \frac{1}{R_1 R_2 C_1 C_2} \tag{3.32}$$

$$b_2 = \frac{(R_1 + R_2)C_2}{R_1 R_2 C_1 C_2} \tag{3.33}$$

Combining formula 3.30 with formula 3.32 gives:

$$C_3 R_3 = \frac{b_1}{b_0} = 1.962 \cdot 10^{-5} \tag{3.34}$$

If C_3 is chosen to be 10 nF then R_3 must be equal 1962 Ω.
Combining formula 3.31 with formula 3.33 gives:

$$R_1 R_2 C_1 C_2 = \frac{1}{b_0 R_3 C_3} = 2.57 \cdot 10^{-11} \tag{3.35}$$

Combining formula 3.35 with formula 3.33 gives:

$$C_2 (R_1 + R_2) = \frac{b_2}{b_0 R_3 C_3} = 7.85 \cdot 10^{-6} \tag{3.36}$$

The choice was made that R_1 is equal R_2. This results in:

$$C_2 = \frac{7.85 \cdot 10^{-6}}{2R_1} \tag{3.37}$$

The choice was made that C_2 is equal to 1 nF. This implies that R_1=R_2=3634 Ω.
Solving formula 3.34 with all known variables implies that C_1=1.8 nF. Table 3.1 reports the resisters and capacitors values used in the circuitry.

Table 3.1

R_1	3.3 KΩ +330 Ω
R_2	3.3 kΩ +330 Ω
R_3	1.8 kΩ +150 Ω
C_1	1.8 nF
C_2	1 nF
C_3	10 nF

|| := *parallel*
\+ := *serie*

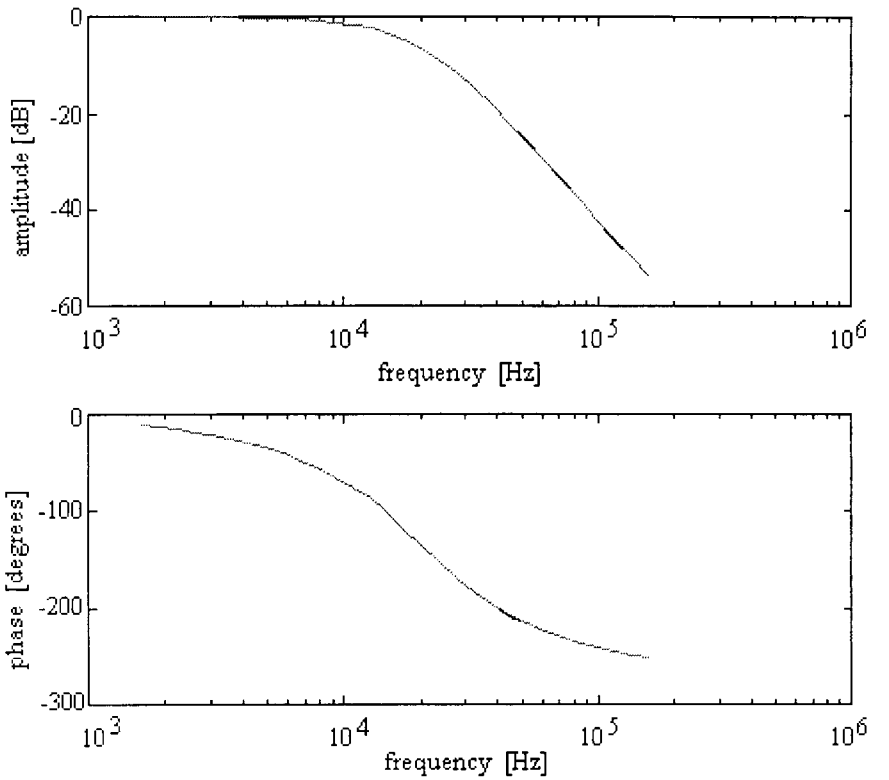

Figure 3-7 Bode diagrams of calculated and implemented Bessel transfer function.

Figure 3-7 shows the bode diagrams of the calculated Bessel transfer function and the implemented Bessel transfer function with the capacitor and resistor values given in table 3.1. There are no noticeable deviations between the two amplitude plots and phase plots. The group delay of the calculated Bessel transfer function and implemented Bessel transfer function coincide if the phase plots are the same. This is the case. The influence of the gain factor α on the Bessel transfer function will be discussed in section 7.3.

4. Electronics of differential capacitive measurement system

4.1. Controllable voltage sources

The controllable voltage sources generate two square waves with a phase difference of 180 degrees and with adjustable amplitude. Figure 2.9 gives a detailed view of the square wave signals. Figure 4-1 shows the electronic scheme for generating square waves with controllable amplitude. A multiplexer (type HEF4053) switches with a frequency of 125 kHz between two voltage levels generating square waves. The 125 kHz clock frequency is 1/16 of the maximum frequency of the most critical component of the measuring system namely the demodulator. The multiplexer needs a symmetrical supply voltage of ± 5V. The 100 nF capacitors in figure 4.1 are to stabilize the supply voltages of the multiplexer.

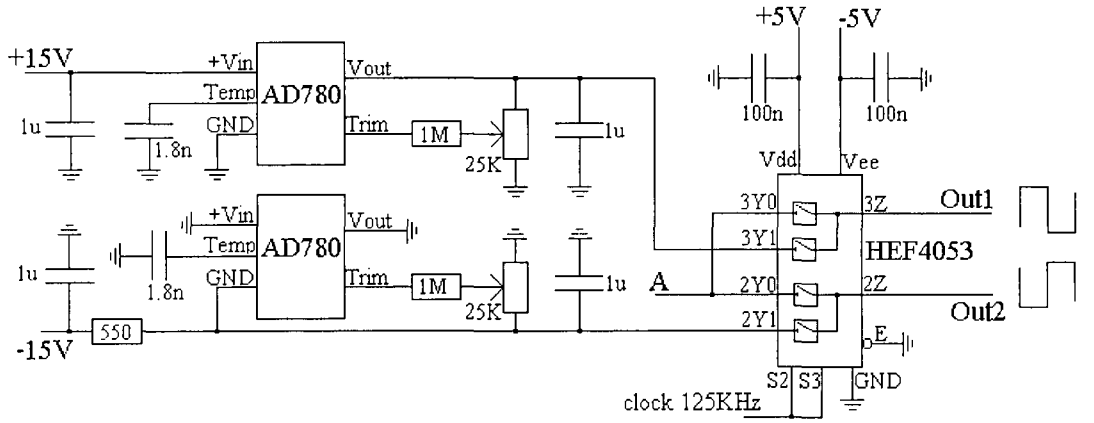

Figure 4-1 Electronic scheme for generating square waves with controllable amplitudes.

The AD780 is a ***high precision*** reference voltage source. The reference voltage source produces a positive or negative reference voltage of 2.500 V. The sign of the reference voltage depends on the external configuration used for the AD780. The 1 μF and 1.8 nF capacitors are needed to ensure a good noise performance of the AD780. With the 1 MΩ resistors and 25KΩ potentiometers the output voltages of the AD780 can be trimmed more accurately. The reference voltage sources have an ultra low temperature drift (typical 3 ppm/°C). The accuracy of the measuring system deteriorates if the amplitudes of the signals change due to temperature drift. The 550 Ω resistor configures the AD780 to supply a reference voltage of –2.500V. The AD780 of the negative reference voltage controls the voltage at the GND terminal to exactly -2.500V.

Signal Out1 of the multiplexer is a square wave signal that is generated by switching between 2.500V and the controlled voltage level A. Signal Out2 is a square wave with a phase difference of 180 degrees compared to signal Out1 and is generated by switching between –2.500V and the controlled voltage level A. With the 125 kHz clock signal all 4 switches of the multiplexer can be turned on and off accordingly.

4.2.Demodulation

The output voltage of the differential capacitive sensor is buffered. The buffer should have the following specifications:

- Low noise performance
- High slew rate
- Wide bandwidth
- High input impedance
- Low input bias current

The low noise performance of the buffer is necessary to realize a good signal to noise ratio. The buffer buffers a square wave signal, which consists of many harmonic sinusoidal signals. To ensure that the output signal of the buffer is also a square wave signal the buffer must have a wide bandwidth to be able to buffer as many higher harmonic sinusoidal signals. A wide bandwidth is also necessary for proper guarding the sensor output signal. The input signal and output signal of the buffer must be exactly the same for guarding. A high slew rate and a wide bandwidth ensure that input and output signal of the buffer are identical. The FET input terminal guarantees that the input bias current of the buffer is small. The sensor output has a negligible load of the input terminal of the buffer. The LH0033 is a very fast buffer and was the only component that complied with above specifications. The LH0033 has a temperature offset drift of 50 μV/°C. This dc offset voltage of the buffer (LH0033) is demodulated outside the pass-band of the measurement system.

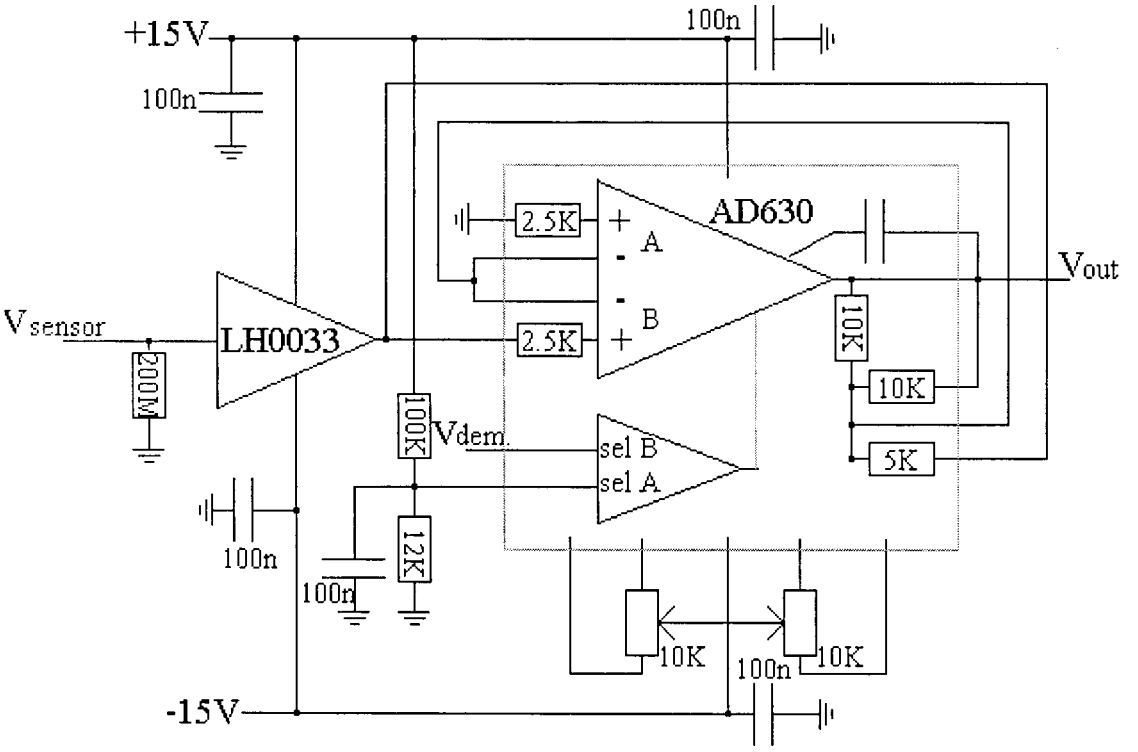

Figure 4-2 Electronic scheme of buffer and demodulator.

Figure 4-2 shows the electronic scheme of buffering and demodulating the output signal of the sensor. The output signal of the sensor is buffered with a fast buffer (type LH0033). The 200 MΩ resistor between the output terminal of the differential

capacitive sensor and ground is necessary to ensure a constant DC voltage at the output of the capacitive sensor. An alternating voltage influences the measurement. The value of this resistor is 200 MΩ so the output of the capacitive sensor has a minimum load. The typical input bias current is 2.5 nA which gives a dc voltage of $(2.5 \cdot 10^{-9} \cdot 200 \cdot 10^{6}) = 0.5$ V at the buffer output. The dc offset voltage of the buffer is small compared to the 0.5 Vdc. The total dc signal is demodulated outside the pass-band of the low-pass filter.

The demodulator (type AD630) synchronously demodulates the buffered sensor signal. The dc input voltage of the demodulator is modulated outside the pass band. This means that the dc output signal of the sensor is unimportant except that the dc voltage level is much smaller than the power supply voltages. The signal that demodulates the input signal of the demodulator is called Vdem. The AD630 is specially chosen because of the capability of recovering signal from 100 dB noise and the channel bandwidth of 2 MHz. A better component is not available.

The basic modes of operation of the demodulator are two fixed gain stages, which can be inserted into the signal path under the control of a sensitive voltage comparator. The demodulator has two stages named A and B. In stage A the input signal is amplified with −1. In stage B the input signal is amplified with +1. The Vdem signal controls the sensitive voltage comparator. The demodulator has internally a compensation capacitor to eliminate some disturbances.

By switching the gain stages of the demodulator accordingly, the dc output signal of the demodulator is equal to the amplitude of the input signal. Furthermore the output signal of the demodulator consists of higher harmonic carrier components, which are removed by a second order filter. The additional trim potentiometers showed in figure 4-2 are to adjust the offset voltage and to adjust the gain factor of the demodulator more accurately. The controller cannot exactly control the AC output voltage of the sensor to zero Volt. There will always be a small AC signal. If the gain factors of the demodulator are not exactly the same, this difference may cause a disturbance.

The voltage divider at the input of the voltage comparator is to ensure that the switching of the stages happens at a positive voltage. The reason will be explained in section 4.4. The additional capacitors of 100 nF are to stabilize the supply voltages.

4.3. Second order filter and controller

As mentioned in section 2.9 the output signal of the sensor is not a nice square wave signal. The output signal of the demodulator contains much distortion at the switching moments of the gain stages. An analogue switch connects and disconnects the output of the demodulator with the input of the second order filter. The analogue switch is implemented with a multiplexer (type HEF4053). Further details about the control signal of the analogue switch will be given in section 4.4.

During the moments when the output signal of the demodulator has spikes, the switch disconnects the signal path between the output of the demodulator and the input of the filter. The output terminal of the multiplexer is connected with an additional capacitor. This capacitor is necessary to ensure that the voltage at the filter input remains constant during the short time period when the filter input is disconnected. At the moments when the output signal of the demodulator is smooth, the signal path to

the input of the filter is closed. A second order filter eliminates further modulation components and noise.

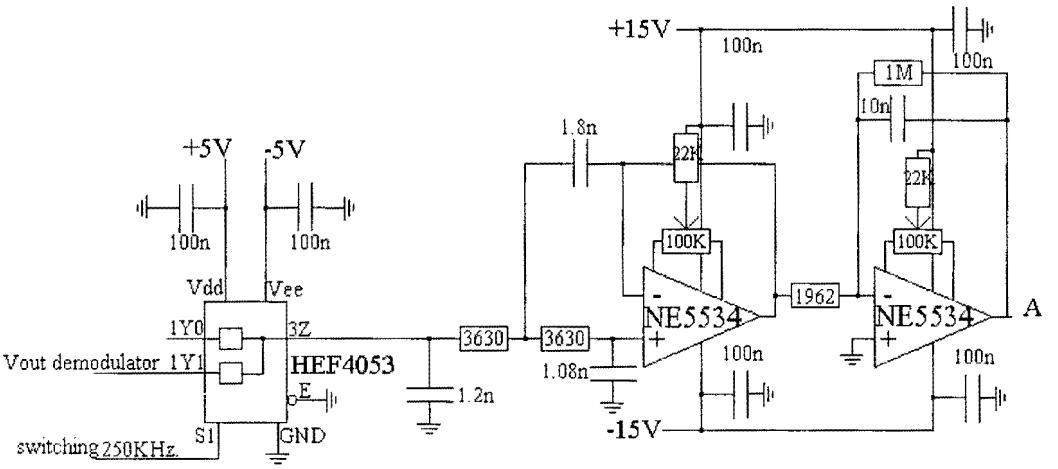

Figure 4-3 Electronic scheme of analogue switch, filter and controller.

Figure 4-3 shows the electronic scheme of the analogue switch, filter and controller. The dimensioning of the resistor and capacitor components has been discussed in section 3.8. The operational amplifiers (type: NE5534) used as buffer and as integrator have a very good noise performance (typical noise 4 nV/Hz.$^{0.5}$), low dc offset drift (typical 5 μV/°C), small input bias currents (2.5 nA) and are very cheap. Further constraints are not important for these operational amplifiers.

The output of the integrator has an additional load of 100 Ω. The output signal of the integrator has less distortion when it is loaded. The dc offset voltage of the operational amplifier are adjusted with the 100 KΩ potentiometers

Whenever control saturation happens, the controller has to stop integrating with the integral control law: otherwise the integrator will keep integrating, and this charge must be removed later, resulting in substantial overshoot. This problem is called integrator windup. This windup can occur when the closed loop of the transfer function is not yet closed. Furthermore the gain of the integrator is not infinite for $\omega = 0$ because of the 1 MΩ resistor. A small dc offset voltage will not cause the system to saturate. The disadvantage of this 1 MΩ resistor is that the final error is no longer 0. In section 7.3. the influence of this final error on the measurements performance is discussed.

A small dc input offset voltage may cause the output signal of the integrator to saturate. The effect of the anti windup is to reduce both the overshoot and the control effort in the feedback system. Omission of this technique may lead to deterioration of response and even instability. [FRA94] The controller has a 1 MΩ resistor parallel to the integrator capacitor. This 1 MΩ limits the maximum gain factor of the integrator.

A low-pass filter (R = 100 Ω C = 1.5 nF) with a cut-off frequency of approximately 1 MHz connects the output of the controller with the adjustable voltage level A of the multiplexer. This additional low-pass filter is necessary to remove additional high frequency disturbances. If this additional low-pass filter is not used the amplifier of

the integrator is severely overloaded by the switching of the multiplexer. This causes a deterioration of the performance of the integration amplifier. The cut-off frequency is high enough that the low-pass filter has negligible influence on the Bessel transfer function of the closed loop system.

4.4. Block timing electronic

The block timing electronic generates the following **external** signals:

1. Signal that control the switches S1, S2, S3 and S4 of the multiplexer.
2. Synchronous demodulation signal
3. Switch signal

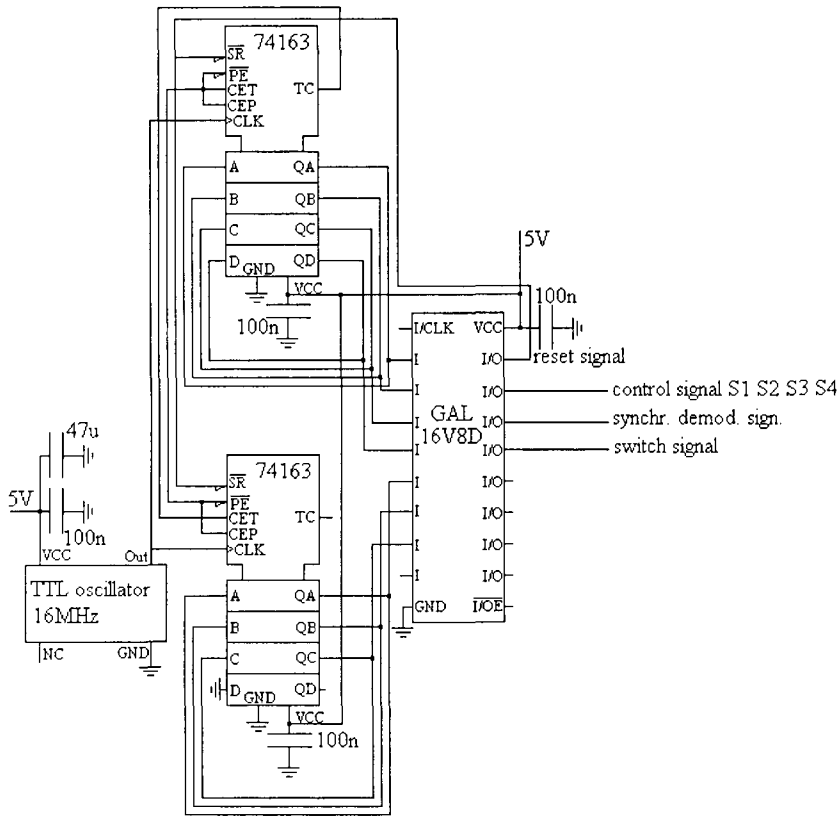

Figure 4-4 Electrical scheme of block timing electronics.

Figure 4-4 shows the electrical scheme of the block control electronics. Two synchronous 4-bit binary counters (type 74163A) are connected in cascade. The two 4-bit binary counters work as a 7-bit counter. The counters count the pulses of a 16 MHz oscillator. The counters are chosen because of the following specifications:

- Typical clock frequency 32 MHz
- Synchronous counting
- Internal look-ahead for fast counting
- Carry output for n-bit cascading
- Synchronous reset function

A GAL (=Generic Array Logic) is a device, which is capable of emulating a PAL (=Programmable Area Logic) architecture. A major advantage of a GAL is that the device can be reprogrammed. Features of the GAL 16V8D are:

- Reprogrammable
- Electrically erasable
- Programmable output polarity
- Maximum operating frequency 250 MHz
- Easy programmable with GAL-programmer

The 7 bit binary counter counts 128 pulses of the oscillator signal (16 MHz/128=125 kHz.). The output terminals of the 7 bit counter are connected with the input terminals of the GAL. The 7-bit binary counter is reset by the programmed logic of the GAL. The reset terminal of the 74163 is low active. A low level at the synchronous reset input sets all outputs of the 7-bit binary counter to low levels after the next positive going transition on the clock input (provided that the setup and hold time requirements for Synchronized Reset are met).

The GAL, counters and oscillator need 5 V supply voltage. The supply voltage is not directly connected with the positive supply voltage of the multiplexer because the power supply of the GAL could influence the adjustable voltage sources. The supply voltages are stabilized with 100 nF capacitors. The oscillator puts major demand on the supply voltage. The oscillator has additional capacitors located in the vicinity to stabilize the supply voltage demand.

4.5. Control signals

The GAL generates the 125 kHz clock signal for the multiplexer, the signal used to demodulate and the control signal for the analogue switch. Figure 4-5 shows the timing diagrams of the output signals of the block control electronic. The multiplexer requires a 125 kHz symmetrical clock signal that controls the switches internal switches.

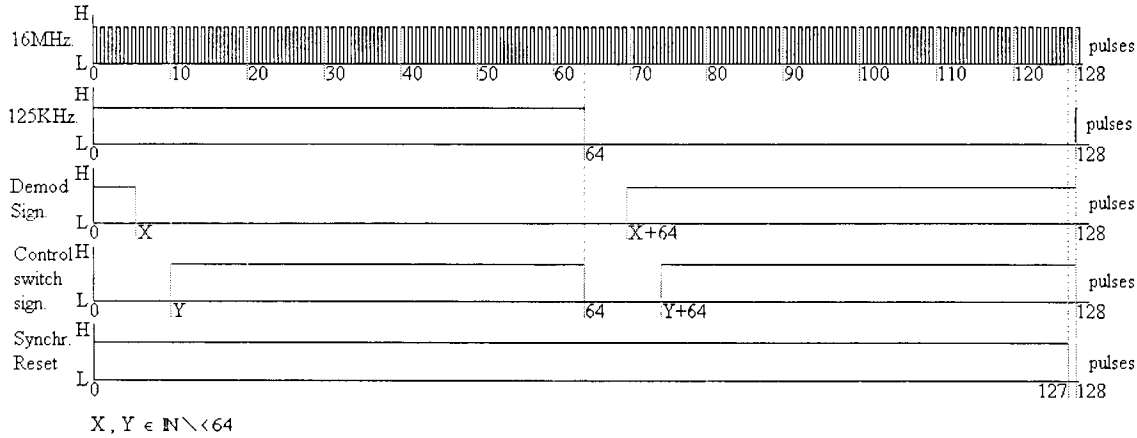

Figure 4-5 Timing diagram.

The switches in the controllable voltage sources and the buffer introduce a delay time between the output signal of the multiplexer (=125 kHz signal) and the input signal of the demodulator. This delay time must be taken into account for ***synchronous demodulation***. The 7-bit counter has 128 states. The logic of the GAL decides whether an output has to remain high or low during a state. One state corresponds with a time interval of approximately 62.5 nanoseconds.

Figure 4-5 shows the demodulation signal shifted X states compared to the 125 kHz clock signal of the multiplexer. The shift is necessary for synchronous demodulation. The value of X has to be experimentally determined. The phase difference between the input signal of the demodulator and the demodulation signal will be reduced to a minimum. Furthermore the demodulation signal has an additional phase shift of 180 degrees to compensate for the 180 degrees phase shift the integrator introduces.

The demodulation signal is a clock signal with voltage levels of 0 V or 5 V. To allow switching of gain stages of the demodulator to take place the voltage level of switching must be between 0 and 5 V. The voltage division at sel A input of the sensitive comparator of the demodulator ensures a constant voltage of 1.6 V at which the switching of gain stages takes place.

The signal that controls the analogue switch located at the output of the demodulator must close the switch when the output signal of the demodulator is smooth. The output signal of the demodulator is not smooth at the switching moments of the stages of the demodulator. The control signal of this switch is depicted in figure 4-5. The time that the switch is open must be experimentally determined. This signal has a frequency of 250 kHz because the demodulator switches two times every signal period.

4.6. Supply voltages

The electronic devices need ±15 V or ±5 V power supply. Positive and negative voltage regulators supply the necessary power for the components. The maximum output current of the voltage regulators is 1.5 A. All electronic components of the sensor require less current than 1.5 A. The supply voltages are stabilized with capacitors. Appendix A contains the electronic scheme of the entire measurement system.

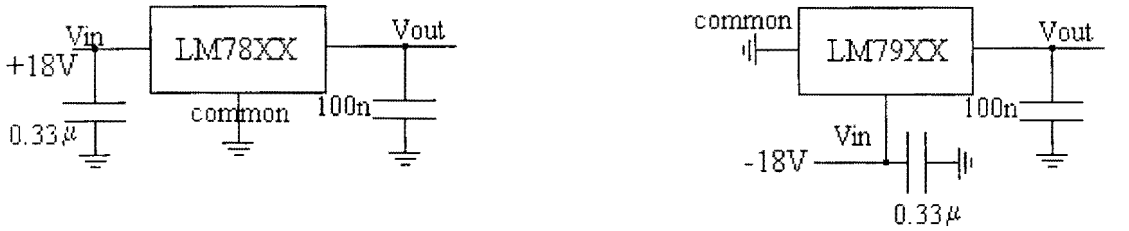

Figure 4-6a Positive power supply regulator. b Negative power supply regulator.
If XX == 05 |Vout| = 5V
If XX == 15 |Vout| = 15V

5. Practical implementation

5.1. Specifications of loudspeaker

A loudspeaker is needed to test the dynamic responses of the differential capacitive measurement system. The capacitive sensor has a maximum measuring range of approximately 10 millimeters. Furthermore the measurement system has a bandwidth of 20 kHz. The loudspeaker should not be too expensive and also have bandwidth of 20 kHz. We use a loudspeaker of the manufacture Monacor type SPH-165. Appendix B contains the technical datasheet of the loudspeaker. The loudspeaker has a linear displacement of $\pm$3.5 millimeters and a maximum displacement of $\pm$5 millimeters. The bandwidth of the loudspeaker is limited to 5 kHz. A wide bandwidth and a wide displacement range are contrary demands for a loudspeaker. We are satisfied with the wide displacement range of the loudspeaker.

5.2. Mechanical sensor construction

The capacitive sensor measures displacements with concentrically cylinder capacitors. See figure 5.1 for a detailed view of the cross-section of the mechanical construction. In equilibrium the concentric cylinder capacitors $C_{1\text{-}4}$, $C_{2\text{-}4}$ and $C_{3\text{-}4}$ are equal in size. The size of the capacitors in equilibrium must be approximately 1pF. This value is taken so the cylinder capacitive sensor corresponds with the capacitive sensor of the laser deflection system. The range of the capacitive sensor is 10 millimeters. The length $l_{1\text{-}4} + l_{2\text{-}4}$ of the concentric cylinder capacitors are equal the range of the capacitive sensor. This implies in equilibrium that $l_{1\text{-}4}$ is equal $l_{2\text{-}4}$, which is half the range of the sensor. Furthermore $l_{3\text{-}4}$ is equal $l_{1\text{-}4}$ in equilibrium.

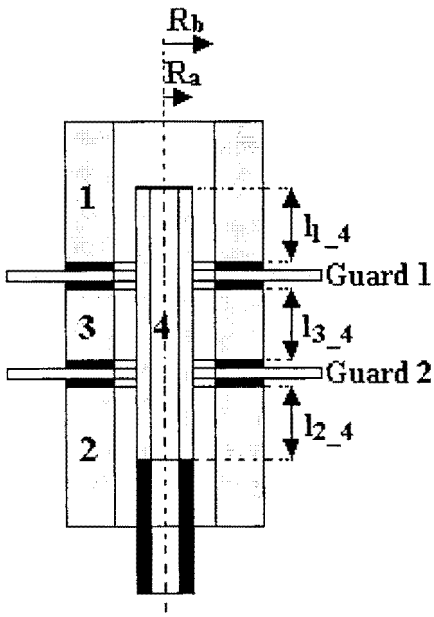

Figure 5-1 Cross-section of capacitive displacement sensor.
Grey area =*conducting material*
Black area = *non-conducting material*
White area = *air*

$$C_{1-4} = \frac{\varepsilon_0 \varepsilon_r 2\pi\, l_{1-4}}{\ln\left(\frac{R_b}{R_a}\right)} \tag{5.1}$$

$$10^{-12} = \frac{8.854 \cdot 10^{-12} \cdot 1 \cdot 2\pi \cdot 5 \cdot 10^{-3}}{\ln\left(\frac{R_b}{R_a}\right)} \Rightarrow R_b = 1.32 \cdot R_a \tag{5.2}$$

Formula 5.1 states the formula for calculating the capacity of the concentric cylinder capacitor. Entering all known variables in formula 5.1 leads to the result of a proportion of the radius R_a and R_b. The proportion of this radius implies that the capacitor values in equilibrium are approximately equal 1pF. R_a is equal 7 millimeters then R_b must be approximately 9 millimeters.

$$R_a = 7 \cdot 10^{-3} m$$
$$R_b = 1.32 \cdot 7 \cdot 10^{-3} \Rightarrow 9 \cdot 10^{-3} m$$

Cylinder 4 is attached with a non-conducting material to the diaphragm of the loudspeaker. Cylinder 4 is hollow from inside to minimize the additional moving mass that is added to the moving mass of the loudspeaker. The connection of the output terminal of the capacitive sensor with the input terminal of the buffer must be as short as possible. This is necessary to minimize the parasitic capacitor at the output terminal of the sensor. Furthermore the output voltage of the sensor must be buffered as soon as possible for a good signal to noise performance. A printed circuit board is integrated with cylinder 4 minimizing the connection. Appendix C contains the mechanical layout of the sensor. Furthermore details are shown how the moving cylinder is attached to the diaphragm of the loudspeaker.

5.3. Electronic implementation

Disturbance reduction
All electronic components are taken specifically because of their low noise performance. Most components are implemented in Surface Mounted Devices short SMD. The benefit of SMD is that these IC's have smaller parasitic capacities and para-inductions than standard IC's. All signals are transported with coaxial cables. This type of connection is much better for electric field shielding, since, as long as there is a connection between shield and ground, most of the noise current is simply shunted to ground. Furthermore coaxial cable have no parasitic capacitors and parasitic inductions because of the ***non-imaginary*** impedance.

Cage of Faraday
Tests of the capacitive measuring system revealed that the system had many disturbances. One of the major disturbances was a 50 Hz sinusoidal signal, which is the primary voltage supply of all electrical equipment. The current through the electronic equipment generates 50 Hz sinusoidal electrical fields. The metal wires and metal parts of the capacitive sensor receive these electrical fields, which disturbs the measurement. To eliminate this disturbance the measuring system has been put in a

Faraday cage. A Faraday cage is an earthed metallic wire or gauze screen enclosing electrical equipment to shield it from the influence of ***external electric fields***.

Figure 5-2 Differential capacitive measurement system in a Faraday cage.

Figure 5-2 shows the set-up of the differential capacitive measurement system in a Faraday cage. The influence of the 50 Hz external electrical fields has been eliminated. There was no 50 Hz signal present at the output of the measurement system.

Adjusting the potentiometers of the measuring system
Before any potentiometers are adjusted the electronic needs to be powered for 30 minutes for temperature effects. The potentiometers of the voltage reference sources must be adjusted first before other adjustments are made. With the potentiometers the positive and negative voltage reference sources can be adjusted exactly to respectively to +2.500 V and –2.500 V. For a good signal to noise ratio it is important that the reference voltage are maximal. This implies $\pm$ 2.500 V reference voltages. After that the potentiometer of the buffer needs to be adjusted to eliminate any dc offset voltage. This is not important because this dc offset voltage is modulated outside the pass-band of the low-pass filter.

The offset adjustment of the two input channels of the demodulator is accomplished by means of a differential and common-mode scheme. This facilitates fine adjustment of system errors in switched gain applications. With system input of the demodulator tied to zero, and a switching carrier waveform applied to the comparator, a low level square wave will appear at the output. The differential offset adjustment potentiometer can be used to null the amplitude of this square wave. The common-mode offset adjustment can be used to zero the residual dc output voltage. [ANA99]

Furthermore the dc offset of the amplifier of the second order filter must be adjusted such that the output signal of the filter is equal zero when the input signal is equal zero Volts. Finally the closed loop measurement system is adjusted with the dc offset voltage of the integrator amplifier. The input signal of the demodulator must be zero volts under all conditions.

Adjusting the control signals
The delay time between the input signal of the demodulator and the control signal of the multiplexer was measured. The measured delay time was approximately 130 nanoseconds. If the synchronous demodulation signal has its flanks two states later then the 125 kHz clock signal of the multiplexer then the two signals have a shift of 125 nanoseconds. This implies that the input signal of the demodulator will be synchronous demodulated. Further more the demodulation signal has an additional phase shift of 180 degrees (=64 states) to compensate the phase shift of the integration action of the controller.

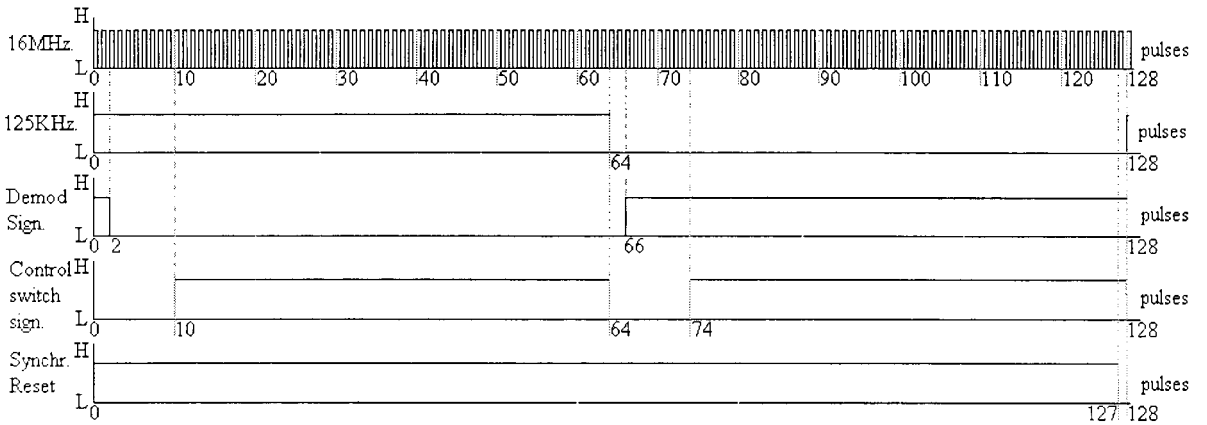

Figure 5-2 Implemented timing diagram.

Figure 5-2 shows the implemented timing diagram programmed into the GAL. The controlled switch at the output of the demodulator is open when the control switch signal is low and closed when the control switch signal is high. The time that the switch must be open is determined experimentally. If the switch is opened 10 states then the input signal of the switch is just smooth enough for further processing when the switch is closed. If the switch is closed sooner (<10 states) then the input signal of the switch contains many disturbances. If the switch is closed later (>10 states) the input signal of the switch was already smooth enough for further processing.

The switch is open if the 125 kHz signal is switching and if the demodulation signal is switching. After a few clock periods when the influence of this switching is negligible the switch is closed. The output information of the demodulator is used 84 percent of the time. Appendix D contains the state table of the implemented timing diagram. The logic expressions are given below. The bit value b_0 is the least significant bit. The line above a bit denotes the logic not operator.

$$125KHz\ clock := \overline{b}_6$$

$$demodulation\ signal := \overline{b}_6\overline{b}_5\overline{b}_4\overline{b}_3\overline{b}_2\overline{b}_1 + b_6\overline{b}_5\overline{b}_4\overline{b}_3\overline{b}_2b_1 + b_6\overline{b}_5\overline{b}_4b_3 + b_6\overline{b}_5b_4 + b_6b_5$$

$$\overline{control\ switch} := \overline{b}_6\overline{b}_5\overline{b}_4\overline{b}_3 + \overline{b}_6\overline{b}_5\overline{b}_4b_3\overline{b}_2\overline{b}_1 + b_6\overline{b}_5\overline{b}_4\overline{b}_3 + b_6\overline{b}_5\overline{b}_4b_3b_2\overline{b}_1$$

$$\overline{reset} := b_6b_5b_4b_3b_2b_1b_0$$

Investigation of temperature sensitivity of demodulator
An earlier report [GOO99] about the experimental differential capacitive displacement measurement system showed that the demodulator of the measurement system was the most temperature sensitive element. Therefore the demodulator in the current capacitive measurement system was tested for temperature sensitivity. After the electronics were powered for an hour ($T \approx 25$ °C) , the demodulator was cooled with cold spray. The temperature dropped to approximately 5°C. The measurement system worked according specifications. Then the measurement system was heated with a blow-drier to approximately 37°C. Close study of the system signals revealed that the output voltage of the capacitive sensor was not controlled to zero Volts. Further studies indicated that ***only*** the dc offset of the demodulator was drifted. Cooling the system with the cold spray brought the dc-offset of the demodulator back to its original value.

There are no commercially available demodulators that have the same characteristics as the AD630 and are less sensitive to temperature changes. To eliminate temperature offset drift of the demodulator the element should be kept at a constant low temperature. Further more cooling the demodulator results to lesser thermal noise. A Peltier element can cool an electronic device and keep it on a constant temperature. Appendix E contains information about the Peltier element.

The Peltier element keeps the temperature of the demodulator at a low level. The small temperature changes that may occur are small enough that there is no significant offset drift of the demodulator. A more detailed studie of the measurement systems performance revealed that the operational amplifiers of the filter and integrator have also a ***slight*** dc offset drift. The used operational amplifiers have already a low temperature drift of 5 μV per degree Celsius. Due to the practical lay out of the printed circuit board was it not possible to use a Peltier element. The Peltier element could keep the temperature of the operational amplifiers at a constant temperature. The influence of this temperature drift is minor and can be simply adjusted with the potentiometers. This can only be done if the temperature difference remains constant over a long time period. This is true for the measurement system.

6. Measured specifications of capacitive measurement system

6.1. Linear Variable Differential Transformer

To calibrate the differential capacitive measurement system reference measurements are needed. Because of the mechanical construction of the capacitive sensor it is not possible to use a simple measurement tool such as a measuring rod. Instead a *L*inear *V*ariable *D*ifferential *T*ransformer (*LVDT*) is used to measure displacements. The LVDT principal is that a movement of a core inside the transducer body is detected by a differential change in output on two secondary coils. The primary coil is being energized by an appropriate AC signal. With the core in a central position, the coupling from the primary to each secondary is equal an opposite and therefore cancel out, thus the resultant output voltage is zero.

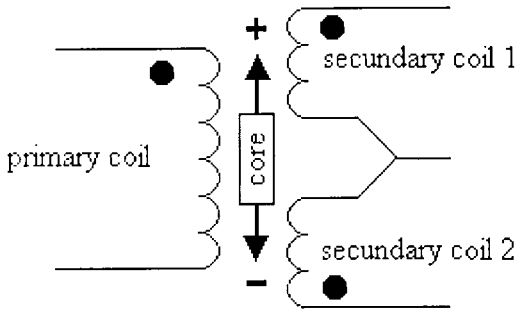

Figure 6-1 LVDT operating principle.

As the core is displaced further into one of the secondary coils its voltage increases proportionally and the other secondary voltage decreases, hence the output changes in magnitude and phase in proportion to movement in either direction from null. The LVDT is sensitive, reliable and repeatable. [SOL95] A spring push LVDT of Solartron metrology is used that has a range of 10 mm. Type AX/5.0/S supplied by Dimed N.V. Belgium. The specifications of the used LVDT are reported in table 6.1

Table 6.1 specifications of LVDT

PROPERTIES	
Sensitivity	1.874V/mm
Measuring range	± 5 mm
Resolution	0.25 µm
Linearity	5 µm
Repeatability	< 0.15 µm
Temperature coefficient	< 0.01 % measuring stroke/°C

The specifications of the LVDT are better then the expected specifications of the differential capacitive measurement system. For the calibration of the capacitive sensor we neglect the inaccuracy of the repeatability and the linearity of the LVDT. The specifications reported in table 6.1 are boundaries for the specifications of the capacitive measurement system.

6.2. Calibration of capacitive measurement system

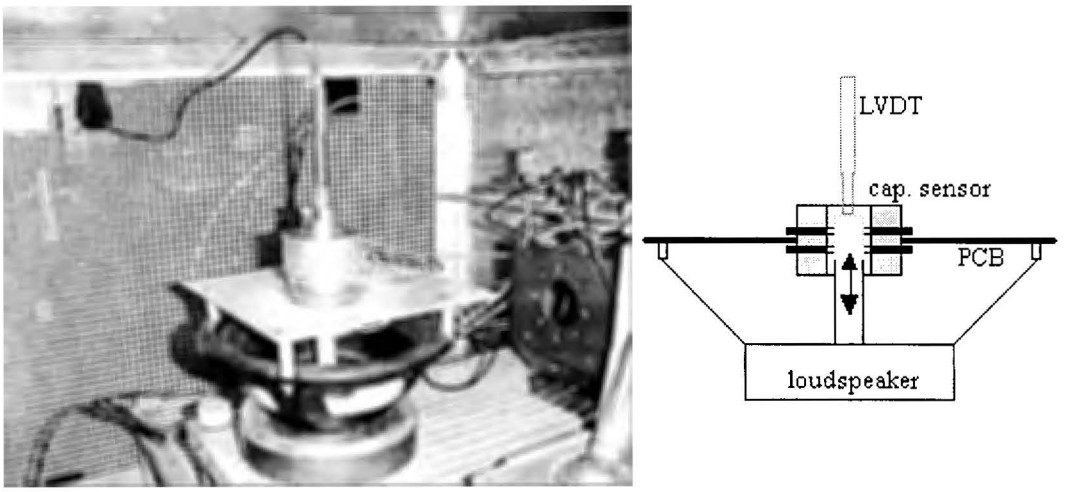

Figure 6-2 LVDT and differential capacitive sensor measure the displacement of the loudspeaker diaphragm.

The LVDT is positioned perpendicular above the loudspeaker diaphragm. Figure 6-2 shows the set-up of the differential capacitive sensor and the LVDT. The pen shape object in figure 6-2 is the LVDT. When the diaphragm of the loudspeaker moves the LVDT and capacitive sensor detect the displacement. Both sensors measure at the same location the displacement of the loudspeaker diaphragm. Both output voltage are measured simultaneously with a computer. Before the calibration measurement begins, both sensors are powered up for 30 minutes. This is done to warm up the sensors electronic to working temperature.

Measurement method
A triangle signal with a frequency of 0.001 Hz was the input signal of the loudspeaker. The amplitude and dc offset voltage of the triangle signal were chosen such that the displacement of the loudspeaker diaphragm covered the whole range of both sensors. Each second 10 samples were taken of the output voltages of the both measurement systems (LVDT and capacitive). The total measurement time for the calibration was approximately 7 hours.

Because the magnetic induction and rubber damping ring of the loudspeaker have hysteresse the displacement of the diaphragm of the loudspeaker is each time different for the same applied input voltage. This implies that the measured samples are taken randomly. A matlab routine was written to find similar samples of LVDT voltages from the measured results. The matlab routine creates a table were the first column is the value of the similar values of LVDT voltages. Columns 2 up to and including 11 are the samples of the capacitive measurement system that were taken at the same time with the similar voltages of the LVDT. Appendix F shows the written matlab code of the matlab routine.

Results calibration
Appendix G contains table G.1 that shows the result of the matlab routine. The averaged voltage of the capacitive measurement system of each row is calculated. The calculated averaged value is based on 10 measurement values. The measured noise is averaged which results to an improved signal to noise ratio by $\sqrt{10}$. The measured LVDT voltages are translated to displacement values. The result is a look up table were measured voltages measured with the capacitive measurement system are related to displacements. Appendix H contains the look up table. Figure 6-3 shows the calibration curve of the capacitive measurement system based on the look up table. The following observations can be made based on the calibration curve:

- There exists a 'linear' relation between measured displacement and output voltage of the capacitive measurement system.
- At the right far end of the curve a small non-linearity exists
- There is a difference between maximum and minimum value of the output voltage of the capacitive measurement system. A small dc offset voltage is integrated by the integration network, which results to a constant dc offset voltage.

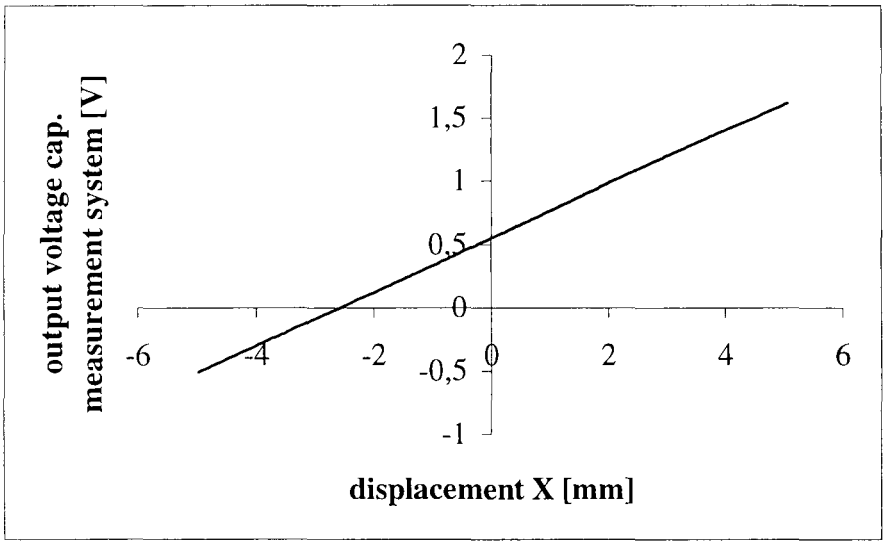

Figure 6-3 Calibration curve of differential capacitive measurement system.

Linearity
A linear function is fitted on the calibration curve such that the maximum difference between the output voltage of the linear function and the calibration curve is minimal. The linear function is given by formula 6.1.

$$Y = 0.21177 \cdot X + 0.552009 \qquad (6.1)$$

Y = output voltage differential capacitive measurement system [V]
X = displacement [mm]

The difference between the linear function Y and the calibration curve gives an indication of the non-linearity of the calibration curve. This difference is called delta and is depicted in figure 6-4. The following observations can be made from this curve:

- The maximum deviation between the function Y and the calibration curve is not more than 0.01 V $\rightarrow \approx 47$ µm.
- The deviation is positive as well as negative.
- The deviation is present in the whole range of the differential capacitive measurement system.
- The curve delta has at the far right end a sudden change in deviation.
- Between $\pm$ 3 mm exists a linear function.

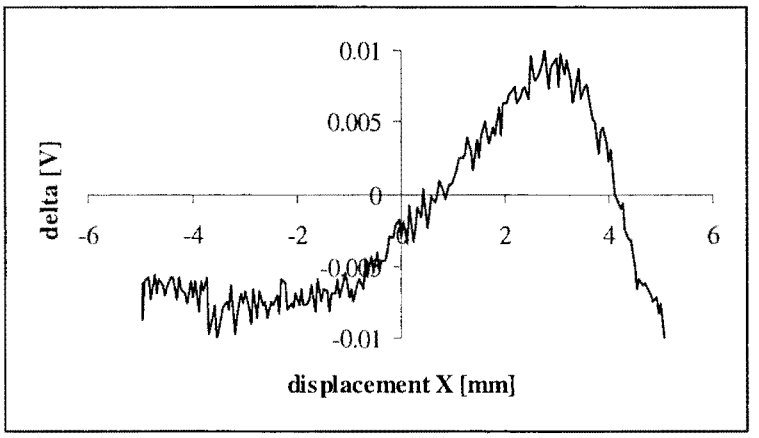

Figure 6-4 Non-linearity of calibration curve.

The fact that the calibration curve has some non-linearity's implies that the sensitivity of the capacitive measurement system is not constant. The systems sensitivity for the entire range is defined as the sensitivity of the nearest linear function that fits the calibration curve with the smallest maximum deviation. A 10 mV voltage difference between the linear curve and the calibration curve implies a 47 µm distance difference.

If the range of the capacitive measurement system is limited to $\pm$ 3 mm a better fitting linear function is found. The function Y' is the linear function valid for the range $\pm$ 3 mm. The maximum deviation between the output voltage of the function Y' and the calibration curve is not more than 3.5 mV, which corresponds with 16 µm. If the capacitive measurement system is not used at the far ends of its range a better linear relation exists between the output voltage of the measurement system and the displacement.

$$Y' = 0.2147 \cdot X + 0.5507 \qquad if\ -3\ mm \leq X \leq 3\ \text{mm} \tag{6.2}$$

Standard deviation
For each calculated averaged value of the output voltage of the capacitive measurement system the standard deviation is calculated. The standard deviation is given by formula 6.3.

$$\sigma_X = \sqrt{\sum_{i=1}^{N} \frac{(\bar{x} - x_i)^2}{N-1}} \tag{6.3}$$

σ_X := standard deviation

$\bar{x}$:= averaged value

x_i := value of i^{th} measurement

Table 6.2

	σ_X [mV]	σ_X [µm]
Maximum	4.22	20
Average	2.24	10.5

Table 6.2 shows the maximum and average calculated standard deviations in mV and µm. The values in µm are calculated with the sensitivity of the linear function Y. The maximum and averaged standard deviations are quite small. Appendix I contains the calculated standard deviations in V.

6.3. Resolution of capacitive measurement system

The resolution is the smallest interval between two adjacent discrete values the measurement system can measure. The range of the differential capacitive measurement system is 10^{-2} meters. The maximum output voltage of the measurement is at least 1000 mV, which are at least 10^3 steps. The disturbances and spike signals contribute to the instability of small voltages (<1000mV).

$$resolution = \frac{range}{\#steps} = \frac{10^{-2}}{10^3} \Rightarrow 10^{-5} m \tag{6.4}$$

The resolution of the differential capacitive measurement system is ***at least*** 10^{-5} m.

6.4. Reproducibility of capacitive measurement system

Reproducibility

Reproducibility is the closeness of agreement among repeated measurements of the output for the same value of input over a period of time. Because the magnetic induction and rubber damping ring of the loudspeaker have hysteresse which means that the same applied input voltage at different times does not result in the same displacement of the loudspeaker diaphragm. The LVDT also measured the displacements. The relation between LVDT voltage and output voltage of the capacitive measurement system was measured. A good reproducibility of the capacitive measurement system will give the same relation between LVDT voltage and output voltage of the capacitive measurement system.

Measurement method for measuring the reproducibility
The diaphragm of the loudspeaker moved 26 times up and down the whole range of the capacitive displacement measurement system. The input of the loudspeaker was a triangle signal with a frequency of 0.001 Hz. The amplitude and dc offset of the triangle signal were chosen such that the displacement of the loudspeaker diaphragm covered the whole range of the both sensors. The output voltage of the measurement system was sampled with a frequency of 1 Hz. If these measurements of 26 cycle movements result in the same relation between output voltages of the capacitive measurement system and LVDT the capacitive measurement system reproduces the same values.

Measured results of reproducibility

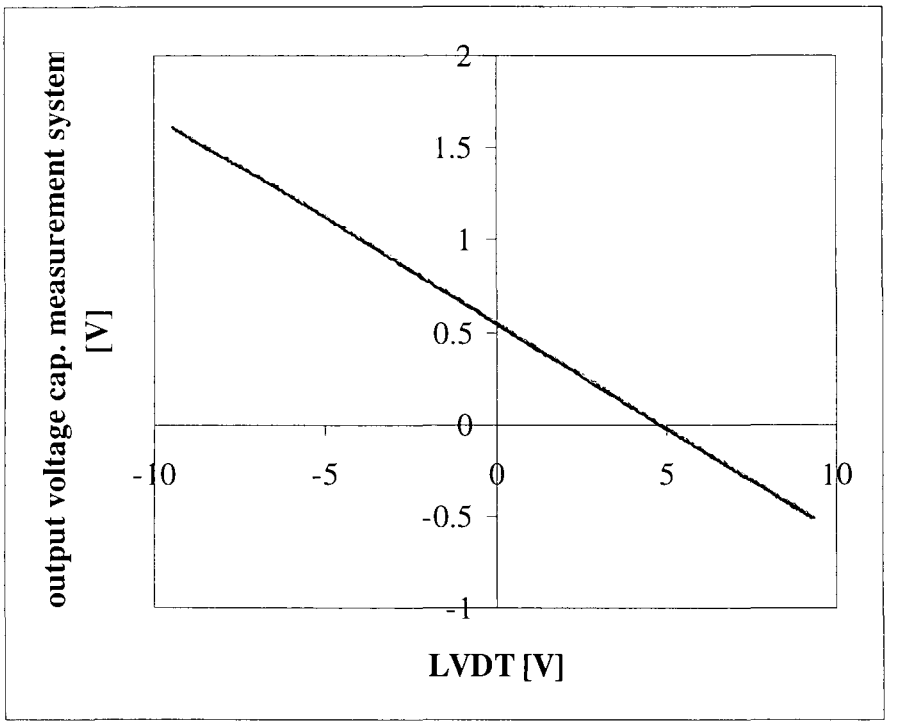

Figure 6-5 Repeated measured results.

Figure 6-5 shows 26 individual curves that describe independent the relation between measured output voltages measured with the LVDT and the capacitive measurement system. Each curve contains 1000 measured points. The following observations can be made from the curves depicted in figure 6-5:

- The relation between measured output voltages of the sensors repeats itself
- There only exist small deviations between different measurements.

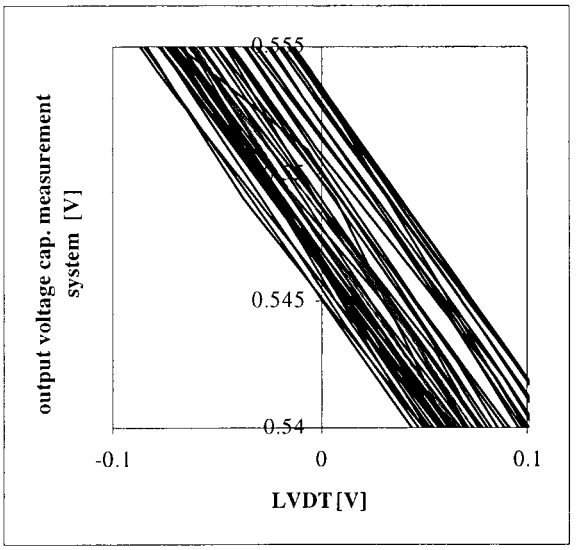

Figure 6-6 Magnification of repeated measured results.

Figure 6-6 shows a magnification of a part of the curves depicted in figure 6-5. The following observations can be made:

- The 26 depicted trajectories are parallel to each other.
- The maximum voltage difference between the averaged calculated trajectory and the measured trajectories is not more than 4 mV, which corresponds with a displacement difference of 19 μm.

Temperature drift of the amplifiers (NE5534) and/or disturbances may be the cause of the voltage differences between the trajectories. In chapter 7 the influences of disturbances and temperature drifts are discussed.

6.5. Inaccuracy

The absolute inaccuracy is given by formula 6.5:

$$\varepsilon_A = x_m - x_t \tag{6.5}$$

where

ε_A = absolute inaccuracy
x_m = measured value
x_t = true value

The absolute inaccuracy is defined as the difference between the true value and the measured value. The data used for obtaining the calibration curve was used for calculating the inaccuracy of the capacitive measurement system. See Appendix G for the data. Appendix J contains table J.1 that shows the calculated inaccuracy of the measurement. The inaccuracy is expressed in micrometers rather than Volts. This is done with the assumption that the measurement system has a sensitivity of 211mV/mm at the whole range. The ***maximum*** inaccuracy measured was 34 μm. The ***averaged*** inaccuracy of all measurements was approximately 8 μm. In chapter 7 possible causes of the inaccuracy are reported.

6.6. Signal to noise ratio

The signal to noise ratio is defined as:

$$\left(\frac{S}{N}\right) = 20^{10}\log\left(\frac{V_{signal\ peak-peak}}{V_{noise\ peak-peak}}\right) \tag{6.6}$$

The maximum and minimum signals of the measurement system are respectively 1.613 V and -0.508 V. A low-noise amplifier amplifies the noise at the output of the measurement system. The measured peak to peak voltage of the noise was 1 mV. This results to a signal to noise ratio of:

$$\left(\frac{S}{N}\right) = 66.5dB$$

The signal is 2121 times larger than the noise.

$$S = 2121 \cdot N$$

The capacitive measurement system has a range of 10 millimeters. The noise of the system results to a maximum inaccuracy of 4.7 µm. If all disturbances were to be eliminated except the noise, the system would have a resolution of 4.7 µm.

$$N = \frac{10^{-3}}{2121} \approx 4.7\,\mu m$$

6.7. Bandwidth

The calculated bandwidth of the measurement system is 20 kHz. The bandwidth of the measurement system could not be determined because:

- LVDT has a limited bandwidth of 300 Hz.
- The Loudspeaker has a bandwidth of 5 kHz.

The displacements of the loudspeaker diaphragm for frequencies higher than 18 kHz are so small that it was not possible to measure them accurately.

6.8. Conclusions of capacitive measurement system

The following conclusions can be made:

- The capacitive measurement system is almost linear
- The sensitivity of the capacitive system is 0.211 V/mm.
- The system has at least a resolution of 10^{-5} meters.
- The inaccuracy of the system is not greater than 34 µm
- Averaged inaccuracy of 8 µm.
- The capacitive measurement system has a signal to noise ratio of 66.5 dB. The noise contributes maximal 4.7 µm inaccuracy.
- The capacitive measurement system can detect displacements with a moving frequency of more than 18 kHz.

7. Sources of errors

7.1. List of critical components of the capacitive measurement system

demodulator

The demodulator (type AD630) is the most critical component of the measurement system.

- The demodulator is the component that limits the maximum operating frequency of the controllable voltage sources.
- The demodulator has a substantial dc offset temperature drift. Due to the dc offset temperature drift of the demodulator is the ac output voltage of the capacitive sensor no longer controlled to zero Volts. This implies that the measurement system does not work according to specifications. A heat pump is necessary to keep the temperature of the demodulator at a constant low level ensuring correct functioning of the measurement system.

amplifiers

The second most critical components of the measurement system are the operational amplifiers (type NE5534). The reason is also the dc offset temperature drift. The temperature drift of the amplifiers (type NE5534) result to a deterioration of the performance of the measurement system. The operational amplifiers (type NE5534) have already a low temperature drift. A heat pump may be necessary to cool the component.

multiplexer

The third most critical component of the measurement system is the multiplexer.

- The limited swing of voltage levels. When the output signals of the controllable voltage sources have larger amplitudes, results this to an increase of the signal to noise ratio. The multiplexer (type HEF4053) used cannot switch between two voltage levels that have a larger voltage difference of 5 Volts.
- The rise time. A decrease in rise time of the square wave signals results to lesser distortion at the output signal of the sensor.

A better demodulator and multiplexer that meet all requirements are not yet available.

7.2. Influence of low frequency disturbances

The influence of the 50 Hz electrical field was not measurable in the Faraday cage. The output signal of the measurement system contained low frequency disturbances. The main disturbance was a 250 Hz signal with a peak to peak value of approximately 0.8 mV_{p-p}. A voltage difference of 0.8 mV corresponds with a displacement difference of 3.8 μm. The cause of this disturbance was the fan that cools the heat sink. The power supply of the fan was ***indirectly*** connected with the power supply of the measurement system. A 0.33 μF capacitor was used to stabilize the output voltage of the voltage regulator that supplies the power for the fan. The 250 Hz disturbance can be eliminated by using a separate power source for the fan.

7.3. *Influence of non idealities on the systems performance*

Noise

The filter has eliminated the noise that is not located in the pass-band of the filter. The measured noise at the output of the measurement system was 1 mV_{p-p}. A 1 mV voltage difference corresponds with approximately 4.7 µm displacement difference. The noise contributes a maximum inaccuracy of 4.7 µm. This contribution cannot be easily reduced since all electrical components have been selected because of their low noise performance.

Internal resistance of the adjustable voltage source.

The switches of the adjustable voltage sources have an internal resistance value. The value of the internal resistance is somewhere between 50 Ω and 100 Ω. Figure 7.1 shows a drawing of a voltage source connected with one sensor input terminal.

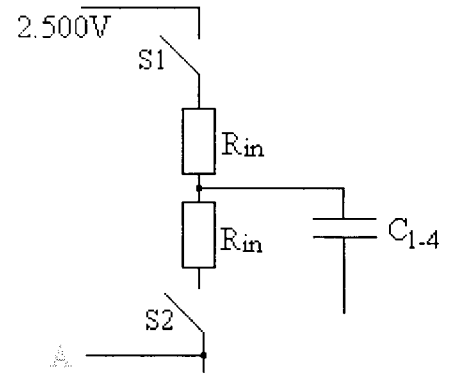

Figure 7-1 Controllable voltage source.

When the output voltage of the adjustable voltage source is switched between 2.500 V and the voltage level A the voltage level at capacitor C_{1-4} does not change immediately. The capacitor is charged. The charging of capacitor C_{1-4} is a first order system with a time constant τ.

$$\tau = R_{in} \cdot C_{1-4} \tag{7-1}$$

R_{in} := internal resistance of controllable voltage source.

The value of capacitor C_{1-4} is approximately 1 pF if no displacement has occurred. At the maximum positive range of the capacitive sensor the value of capacitor C_{1-4} is doubled and the value of C_{2-4} is reduced to zero. The maximum value of capacitor C_{1-4} is equal 2 pF. The maximum time constant is given:

$$\tau_{max} = R_{max} \cdot C_{1-4} = 2 \cdot 10^{-10}\ s \tag{7-2}$$

The modulation frequency of the system is 125 kHz. The maximum time constant is negligible compared to the period time of 8 µs. The influences of other resistances (wires, internal resistances of reference voltage sources, output impedance buffer ≈ 6 Ω, etc.) are small and negligible compared to the 100 Ω input resistance of the multiplexer.

Influence of parasitic capacitors C_{p4} and C_{p0}

The output voltage of the capacitive sensor is given by formula 7.3. Formula 7.3 was discussed in section 2.5.

$$V_3 = \frac{\{C_{1-4}C_{3-4} + C_{p5}(C_{p0} + C_{1-4} + C_{2-4} + C_{3-4})\}}{C_{3-4}(C_{p0} + C_{1-4} + C_{2-4}) + (C_{p4} + C_{p5} + C_{p6})(C_{p0} + C_{1-4} + C_{2-4} + C_{3-4})} V_1$$
$$+ \frac{\{C_{2-4}C_{3-4} + C_{p6}(C_{p0} + C_{1-4} + C_{2-4} + C_{3-4})\}}{C_{3-4}(C_{p0} + C_{1-4} + C_{2-4}) + (C_{p4} + C_{p5} + C_{p6})(C_{p0} + C_{1-4} + C_{2-4} + C_{3-4})} V_2 \quad (7\text{-}3)$$

The parasitic capacitors C_{p4} and C_{p0} reduce the sensitivity of the output voltage of the capacitive sensor. For simplicity all other non idealities are assumed not to exist. Parasitic capacitors values C_{p5} and C_{p6} are zero. The output voltage is then stated by formula 7.4.

$$V_3 = \frac{C_{1-4}C_{3-4}}{C_{3-4}(C_{p0} + C_{1-4} + C_{2-4}) + C_{p4}(C_{p0} + C_{1-4} + C_{2-4} + C_{3-4})} V_1$$
$$+ \frac{C_{2-4}C_{3-4}}{C_{3-4}(C_{p0} + C_{1-4} + C_{2-4}) + C_{p4}(C_{p0} + C_{1-4} + C_{2-4} + C_{3-4})} V_2 \quad (7\text{-}4)$$

In equilibrium (x =0) capacitors C_{1-4}, C_{2-4} and C_{3-4} are approximately equal to 1 pF. The estimation is that the maximum values of parasitic capacitors C_{p0} and C_{p4} are not larger than 0.1 pF. This is 10 percent of capacitor C_{3-4}.

Situation 1: all parasitic capacitors neglected. The output voltage is:

$$V_3^1 = \frac{1}{2}V_1 + \frac{1}{2}V_2 \quad (7\text{-}5)$$

Situation 2: all parasitic capacitor neglected except C_{p0} and C_{p4}. The output voltage is:

$$V_3^2 = \frac{1}{2.41}V_1 + \frac{1}{2.41}V_2 \quad (7\text{-}6)$$

The output voltage V_3 is approximately 20 percent ***less*** sensitive if parasitic capacitors C_{p0} and C_{p4} are not neglected. In the worse case scenario the measured results of the measurement system were substantially influenced due to parasitic capacitors C_{p0} and C_{p4}. Reducing capacitors C_{p0} and C_{p4} to insignificant values can in a best case scenario result to an increase of the output voltage of the measurement system with 20 percent.

If the sensitivity would increase with 20 percent and the measured errors would remain the same the accuracy would increase. Table 7.1 shows results. The averaged inaccuracy can be reduced with 1.6 μm while the maximum inaccuracy can be reduced with 7 μm.

Table 7.1

Sensitivity	211.77 mV/mm	211.77 + 20% mV/mm
maximum absolute inaccuracy	34 μm	27 μm
averaged absolute inaccuracy	8 μm	6.4 μm

This decrease in sensitivity is stated with the α factor. The α factor reduces the sensitivity of the Bessel transfer function and must be equal 0.8 for a sensitivity decrease of 20 percent. Formula 7.7 is the transfer function of the closed loop system. The formula has been discussed in section 3.5.

$$H_{system}(s)=\frac{c}{C_0}\frac{\alpha}{s^3R_1R_2R_3C_1C_2C_3+s^2(R_1R_3C_2C_3+R_2R_3C_2C_3)+sR_3C_3+\alpha} \qquad (7\text{-}7)$$

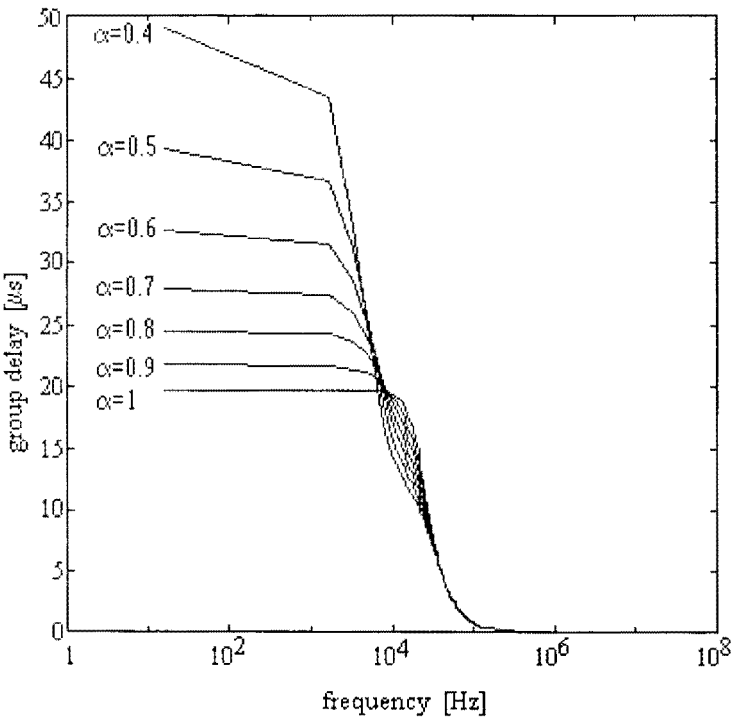

Figure 7-2 Group delay Bessel transfer function for several α values.

Figure 7.2 shows the group delay of the closed loop transfer function for several α values. α values larger than 0.5 have almost a constant delay time for frequencies in the pass-band. Only small deviations exist. If the α value is smaller than 0.5 the frequencies in the pass-band have substantially different delay times. This means that the output signal is distorted because each signal frequency inside the pass-band has a different delay time. The influence of an α value equal to 0.8 is negligible

Induction of cables

The voltage sources and sensor capacitors are connected in a closed loop. The current flowing through this loop induces a magnetic field. This magnetic field implies a certain induction in the closed loop. The induction of a wire that makes a circle R_0 and has a diameter a is approximately given by formula 7.8. This formula is used to approximate the inductance of the current loop.

$$L \approx \mu_0 R_0 \left\{ \ln\left(\frac{8R_0}{a} \right) - 2 \right\} \tag{7-8}$$

[LAA95]

where

L := inductance [Henry]
μ_0 := permeability [Henry m^{-1}]
R_0 :=radius of circle[m]
a :=diameter of wire [m]

The maximum inductance of the current loop can be calculated with formula 7.8. The wire has a diameter of 2 mm. The maximum radius of the current loop is approximately 0.04 m.

$$L_{max} \approx 150\,nH \tag{7-9}$$

The inductance and capacitors of the sensor form an oscillation circuit. The maximum capacity of the sensor is approximately 10 pF. The oscillation frequency is given by:

$$f_{oscilation} = \frac{1}{2\pi \sqrt{L_{max} C_{max}}} \approx 130\,MHz \tag{7-10}$$

The signal frequency of 125 kHz is 1040 times smaller then the oscillation frequency. The influence of the inductance is negligible.

Input bias current buffer

The input bias current of the buffer is maximum 2.5 nA. The dc voltage at the input terminal of the buffer is 0.5 V (= 2.5 nA · 200 MΩ). The demodulator modulates this dc signal outside the pass-band of the Bessel transfer function. This voltage level has no influence on the systems performance except when the dc signal is larger than the voltage swing of the buffer. The maximum voltage swing of the buffer is ± 15V which is much larger than the 0.5 V dc voltage .

Influence of integration network on Bessel transfer function

The integrator of the capacitive measurement system has an additional resistance parallel to the integrator capacitor. This resistance is necessary to limit the integration action when the system is in saturation.

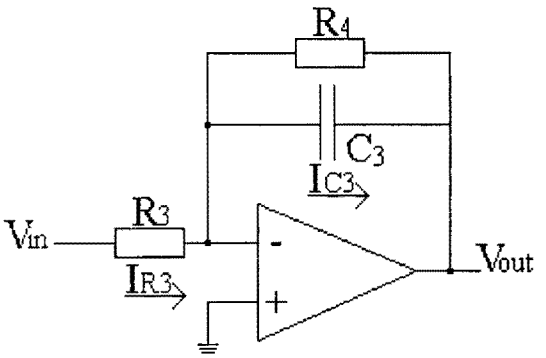

Figure 7-3 Integration network.

The transfer function is given by formula 7.11.

$$\frac{V_{uit}}{V_{in}} = -\frac{R_4}{sC_3R_3R_4 + R_3} \tag{7-11}$$

$$\text{If } R_4 >> R_3 \rightarrow \frac{V_{uit}}{V_{in}} \approx -\frac{R_4}{sC_3R_3R_4} = -\frac{1}{sC_3R_3} \tag{7-12}$$

The closed loop transfer function changes due to the additional resistance R_4. The transfer function of the integration network is almost the same as an integrator if the value of resistance R_4 is much larger then the value of resistance R_3. Resistor R_4 (=1 MΩ) is indeed much larger than resistor R_3 (=1962 Ω). The influence of the additional resistor R_4 is minimal on the Bessel transfer function.

Influence integration network on final error

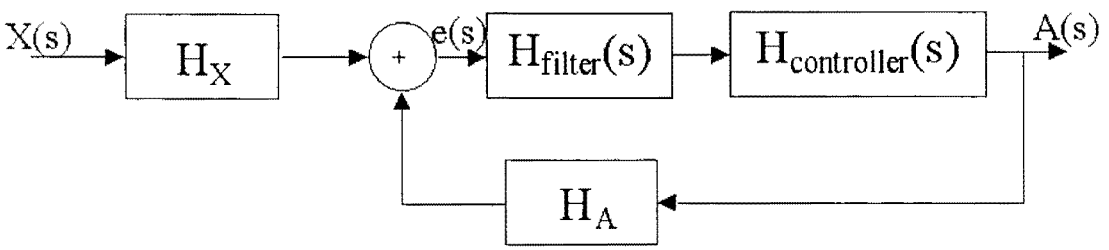

Figure 7-4 Block diagram measurement system.

Figure 7.4 shows the block diagram of the measurement system. The error transfer function is given by formula 7.13.

$$\frac{e(s)}{X(s)} = \frac{H_X}{1 - H_{controller}(s) \cdot H_{filter}(s) \cdot H_A} \tag{7-13}$$

The transfer functions were discussed in chapter 3:

$$H_{controller}(s) = -\frac{R_4}{sR_3R_4C_3 + R_3} \tag{7-14}$$

$$H_{filter}(s) = \frac{1}{s^2R_1R_2C_1C_2 + s[R_1C_2 + R_2C_2] + 1} \tag{7-15}$$

$$H_X = \alpha\frac{c}{C_0} \tag{7-16}$$

$$H_A = \alpha \tag{7-17}$$

Substituting formulas 7.14 up to and including 7.17 in formula 7.13 gives the following result.

$$\frac{e(s)}{X(s)} = \alpha\frac{c}{C_0} \cdot \frac{(sR_3R_4C_3 + R_3) \cdot (s^2R_1R_2C_1C_2 + s[R_1C_2 + R_2C_2] + 1)}{(sR_3R_4C_3 + R_3) \cdot (s^2R_1R_2C_1C_2 + s[R_1C_2 + R_2C_2] + 1) + \alpha R_4} \tag{7-18}$$

The final value theorem states:

$$\lim_{t \to \infty} e(t) = \lim_{s \to 0} s \cdot \frac{e(s)}{X(s)} \cdot X(s) \tag{7-19}$$

This leads to:

$$e_{ss} = \lim_{s \to 0} s \cdot \frac{1}{s} \cdot \alpha\frac{c}{C_0} \frac{s^3(...) + s^2(...) + s(...) + R_3}{s^3(...) + s^2(...) + s(...) + R_3 + \alpha R_4} = \alpha\frac{c}{C_0}\frac{R_3}{R_3 + \alpha R_4} \tag{7-20}$$

Assumption made that :

$\alpha = 1$ and $\frac{c}{C_0} = 0.2$

$R_3 = 1962\ \Omega$
$R_4 = 1\ M\Omega$

The final steady state error value is:

$$e_{ss} \approx 4 \cdot 10^{-4} \tag{7-21}$$

A 0.4 mV final error corresponds with a displacement inaccuracy of 1.9 μm. Increasing resistor value R4 decreases the final steady state error value.

Influence of offset drift of demodulator

The demodulator is cooled with a heat pump and does not have any dc offset voltage drift. There is no inaccuracy of the temperature drift of the demodulator.

Influence input bias current of filter

The filter input terminal is 625 nanoseconds (=10 states) disconnected with the output of the demodulator when the analogue switch is opened. The capacity at the output of the switch supplies the input bias current for the amplifier. This can be modelled as a shown in figure 7.5. The 100 Ω resistance is the internal resistance of the switch. When the switch is opened. The 1.2 nF capacitor supplies the input current for the amplifier.

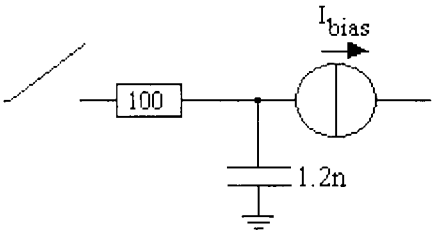

Figure 7-5 Model of switch and input bias current filter.

The assumption is made that the input voltage of the switch does not change. Figure 7.6 shows the voltage level of the capacitor. When the switch is closed the capacitor is recharged. When the switch is opened the capacitor supplies the input bias current of the amplifier. The voltage level of the capacitor drops ΔV. After the switch is closed the capacitor is recharged again.

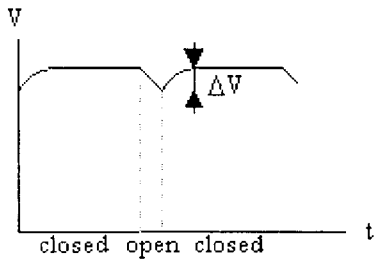

Figure 7-6 Voltage curve.

Formula 7.22 gives the voltage drop of the capacitor. The input bias current is 2.5 nA and independent of time.

$$\Delta V = \frac{1}{C}\int Idt \tag{7-22}$$

$$\Delta V = \frac{1}{1.2\cdot 10^{-9}} \int_0^{625\cdot 10^{-9}} 2.5\cdot 10^{-9} dt \approx 1.3\mu V \tag{7-23}$$

The voltage drop is approximately 1.3 μV. This voltage drop can be neglected compared to noise of 1 mV_{p-p}. The capacitor is recharged. The time constant of the first order system for recharging is 120 ns. This also negligible compared to 8 μs period time.

Influence offset drift of amplifiers

The influence of the offset voltage of the filter amplifier was measured. Table 7.2 reports the measured results. A 100 μV offset voltage gives an inaccuracy of approximately 1.8 μm.

Table 7.2

Offset voltage filter [μV]	Output voltage [mV]	Measured displacement [μm]
0	-200	94.5
100	-204	96.3

The offset temperature drift of the amplifier NE5534 is typical 5 μV/°C. The temperature variations of a complete cycle (=24 hours) in a room will not be more than 10 °C. The maximum total offset drift is 50 μV. A 0.9 μm inaccuracy is the result of the 50 μV increase in offset voltage. The two amplifiers can induce a maximum inaccuracy of approximately 1.8 μm due to temperature drift.

Influence analogue switch

The analogue switch located at the output of the demodulator is opened 10 cycles then closed for 54 cycles after which the process repeats itself. In a worse case scenario the input signal of the analogue switch changes at the same moment that the switch is opened. It takes 625 nanoseconds before this information reaches the rest of the system. The measurement system has a maximum response delay of approximately 0.63 μs. The bandwidth of the system is 20 kHz. The influence of this delay is not more than 1.25 percent on the minimum period time. The accuracy of the measurement system increases because disturbances such as spike signals are eliminated.

Humidity changes

Humidity changes do not have any influence on the systems performance. A higher humidity influences the dielectric constant of air named ε_r. Because the measurement system measures differential the influence of the dielectric constant is self canceling.

7.4. Contributions to uncertainty

Table 7.3 lists the influences of several causes to the uncertainty of the measurement system. The most dominant factor of the inaccuracy is the influence of noise. This is the noise of all electronic components. All components used for the measurement system have been selected because of their low noise specifications. There is no component used that has a substantial larger noise influence than all other electronic components. Further developments in integrated circuit technology may lead to components that have less noise.

The second most dominant factor is the influence of low frequency disturbances. The main cause of this disturbances was the fan. Using a separate supply source for the fan will eliminate the 250 Hz disturbance at the output of the measurement system. The influence of parasitic capacitors C_{p4} can be eliminated further. This can be done by additional guarding the output of the sensor.

The steady state error contributes a 1.9 μm uncertainty. Using a higher resistance value for R_4 will decrease the contributed uncertainty. Cooling the amplifiers of the integrator and filter will lead to further improvement of the systems performance.

Table 7.3

Influence of sources on the inaccuracy	Uncertainty [μm]
Noise	4.7
Low frequency disturbance	3.8
Steady state error	1.9
Sensitivity decrease due to parasitic capacitors C_{p0} and C_{p4}	1.6 $\Rightarrow$ 7
Offset drift amplifiers	1.8

8. Loudspeaker

8.1. Theory

A systematic diagram of a loudspeaker is represented in figure 8-1. A voltage applied across the loudspeaker input terminals pushes current through the voice coil. The voice coil is positioned in the magnetic field created by the permanent magnet. The passage of current through the coil wires creates the driving force that moves the attached diaphragm. The movement of the diaphragm generates the acoustic pressure response. Electrical energy is transformed to mechanical energy which is transformed to acoustic energy.

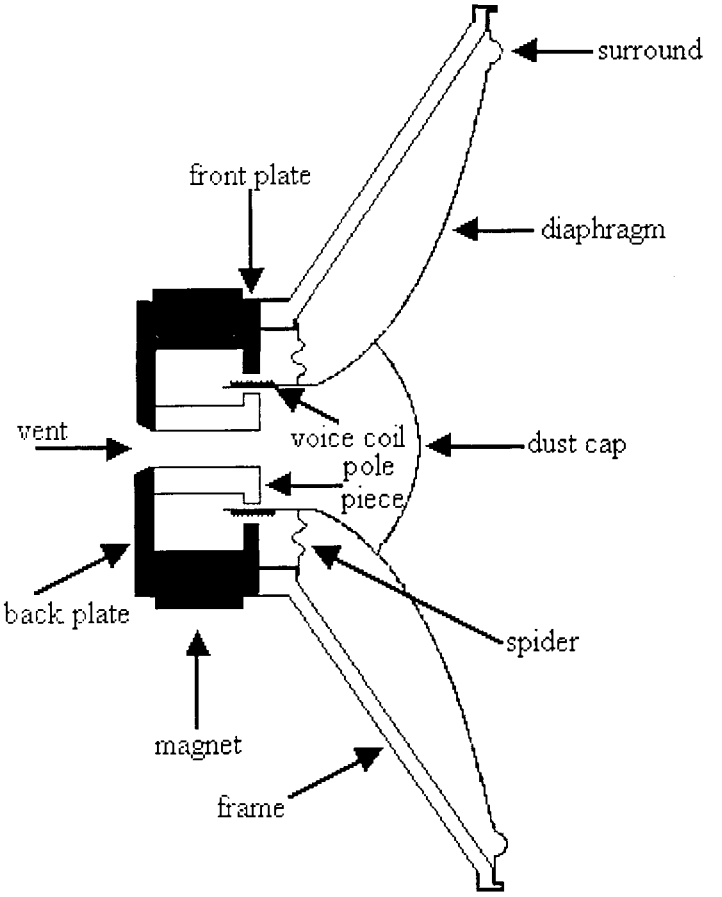

Figure 8-1 Diagram of loudspeaker.

The diaphragm is attached to the loudspeaker frame by the spider and the surround. These create compliance (inverse of stiffness) and damping the loudspeaker system. Both the magnetic induction and rubber damping of the loudspeaker diaphragm have hysterese. The position hysterese of the rubber damping is not audible because sound is the result of movement (=speed) of the loudspeaker diaphragm and not the position of the diaphragm of the loudspeaker.

At low frequency, the loudspeaker response can be modeled as a simple mass-spring-damper shown in figure 8-2. For higher frequencies the model must be extended with vibration components. The electrical dynamics of the loudspeaker can be modeled with an inductor, a resistor and a voltage source. [LAN98] Appendix B contains the specifications of the loudspeaker.

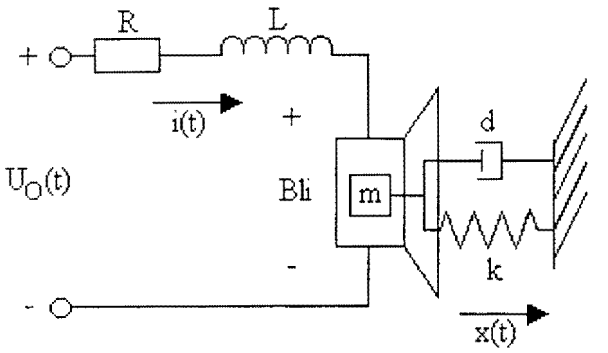

Figure 8-2 Electrical / mechanical model of loudspeaker.

Definitions:

m	= movable mass of loudspeaker
d	= damping factor of loudspeaker
k	= stiffness or compliance^{-1} factor of loudspeaker
Bl	= force constant of loudspeaker
R	= resistance of voice coil
L	= inductance of voice coil
$x(t)$	= displacement of diaphragm as a function of time
$i(t)$	= current flowing through voice coil as a function of time
$U_O(t)$	= input voltage of loudspeaker as a function of time

8.2. Current to displacement relation

The relationship between current flowing through the voice coil and the displacement of the diaphragm is calculated by using Newton's laws of motion.

$$m\ddot{x}(t) + d\dot{x}(t) + kx(t) = Bli(t) \tag{8.1}$$

The Laplace transforms are:

$$X(s) = \ell(x(t)) \tag{8.2}$$

$$I(s) = \ell(i(t)) \tag{8.3}$$

The transfer function that describes the relationship between current flowing through the voice coil and the displacement of the diaphragm is given by formula 8.4.

$$H(s)_{current\_displacement} = \frac{X(s)}{I(s)} = \frac{Bl}{ms^2 + ds + k} \tag{8.4}$$

The transfer function $H(s)_{current\_displacement}$ is a second order system. The bode diagram has the characteristics of a second order low-pass filter.

8.3. Voltage to displacement relation

Using Kirchhoff's law gives:

$$U_0(t) = Ri(t) + L\dot{i}(t) + Bl\dot{x}(t) \tag{8.5}$$

The Laplace transforms of $U_0(t)$ is:

$$U_0(s) = \ell(U_0(t)) \tag{8.6}$$

Combining formula 8.5 with formulas 8.2, 8.3 and 8.6 results to:

$$U_0(s) = (sL + R)I(s) + sBlX(s) \tag{8.7}$$

Combining formula 8.4 and 8.7 results to the transfer function that describes the relation between the input voltage applied to the input terminals of the loudspeaker and the displacement of the diaphragm.

$$H(s)_{voltage\_displacement} = \frac{X(s)}{U_0(s)} = \frac{Bl}{s^3mL + s^2(mR + dL) + s(dR + kL + Bl^2) + kR} \tag{8.8}$$

The transfer function $H(s)_{voltage\_displacement}$ is a third order system. The complexity of the model increases if the loudspeaker is voltage driven rather then current driven.

8.4. Nonlinear behavior of the loudspeaker

The major physical causes for the nonlinear transduction in electro dynamical loudspeakers appear to be:

- The displacement dependent mechanical stiffness of the suspension
- The displacement dependent force factor
- The displacement dependent self-inductance of the voice coil

The force deflection characteristic of the loudspeaker cone suspension can be approximated by a polynomial:

$$F_m = \alpha x(t) + \beta x(t)^2 + \gamma x(t)^3 \tag{8.9}$$

Where F_{in} indicates the applied force which causes the displacement x(t). Formula 8.1 must then be rewritten as:

$$m\ddot{x}(t) + d\dot{x}(t) + \alpha x(t) + \beta x(t)^2 + \gamma x(t)^3 = Bli(t) \tag{8.10}$$

For high frequency signals the derivative of the position (=speed) is higher than for low frequency signals. At high frequencies the derivatives are large enough so that the effect of the non-linearity $(=\beta x(t)^2+\gamma x(t)^3)$ in formula 8.10 is weak and the equation is more linear. At low frequencies the derivatives are small so that the effect of the non-linearity is strong and formula 8.10 is more nonlinear. This is why the distortion is

more severe at low frequencies for a loudspeaker with suspension non-linearity. Furthermore the greater the displacement the greater the influence is of the suspension non-linearity. Another way of thinking is that non-linearity's introduce higher harmonic signals. Higher frequencies introduce higher harmonics, which are more damped because each practical system has a low-pass band.

Another source of harmonic distortion is the non-uniform flux density. The flux density is not a constant; instead it is a function of the displacement. This non-linearity effects both the electrical as mechanical circuit. The movement of the voice coil out of the radial magnetic field changes the inductance of the voice coil. The inductance is related to the displacement. For small displacements the voice coil does not leave the magnetic field of the permanent magnet but for large displacement the voice coil leaves the magnetic field of the permanent magnet. This introduces a non-linearity. [GAO91]

8.5. Current control

As mentioned in section 8.2 when the loudspeaker is current driven the transfer function is a second order transfer function. A voltage driven loudspeaker has a third order transfer function. A main reason why the loudspeaker should be current driven rather than voltage driven is that the non-linearity of the voice coil L is not present in the transfer function $H(s)_{current\_displacement}$. By choosing a current driven interface with the loudspeaker a non-linear term is no longer present.

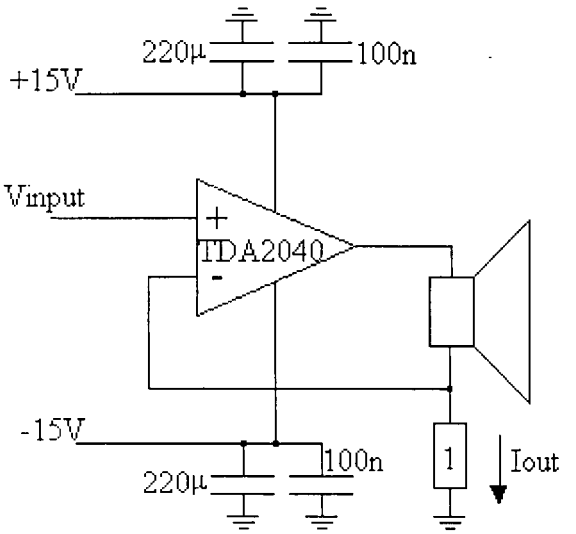

Figure 8-3 Voltage controlled current interface.

Figure 8-3 shows the electrical scheme of the voltage controlled current interface for the loudspeaker. The input bias current of the operational amplifier is assumed to be negligible. The following relations can be derived:

$$V_+ = V_{input} \tag{8.11}$$

$$I_{out} = \frac{V_-}{1} \tag{8.12}$$

$$V_+ = V_- \tag{8.13}$$

$$V_{input} = I_{out} \tag{8.14}$$

The input voltage of the operational amplifier controls the current through the voice coil of the loudspeaker. The maximum current flowing through the voice coil is 1A. The power amplifier (type: TDA2040) is used to supply the necessary current to the loudspeaker. The power amplifier can maximally supply 3A. The capacitors depicted in figure 8-3 are to stabilize the supply voltages.

8.6. Measured step responses of loudspeaker

The step response of a system gives a good impression of the systems dynamics. For several step input currents of the loudspeaker the displacement of the diaphragm is measured with the capacitive measurement system.

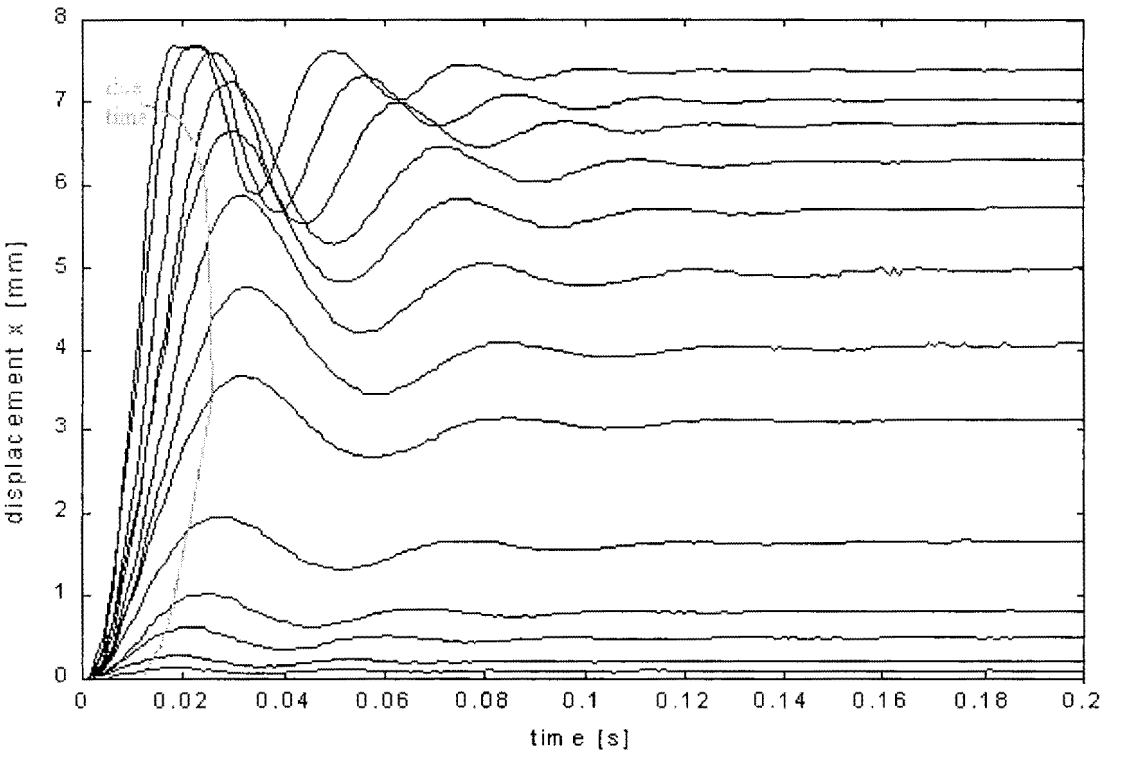

Figure 8-4 Measured step responses of the loudspeaker.

Figure 8-4 shows the measured step responses. The input current of the loudspeaker was respectively: 0.01, 0.02, 0.035, 0.05, 0.075, 0.1, 0.125, 0.15, 0.175, 0.2, 0.25, 0.3 and 0.4A. The following observation can be made:

- The rise time and also peak time of the measured step responses increase if the input current increases until a maximum is reached. After that the rise time and peak time decrease if the input current increases further.
- The step response of input current 0.4 A shows saturation. The maximum deviation of the loudspeaker diaphragm is the reason for this saturation.

The peak and rise time are related to the undamped natural frequency of the system. The transfer function is given by formula 8.4 The undamped natural frequency and damping ratio are respectively:

$$\omega_n = \sqrt{\frac{k}{m}} \tag{8.15}$$

$$\varsigma = \frac{d}{2\sqrt{km}} \tag{8.16}$$

The undamped natural frequency depends on the movable mass and the stiffness of the diaphragm. Since the movable mass is constant the reason of the non-linearity of the peak and rise times are related to the stiffness.

8.7. Model identification

Data acquisition

The poles that are related to the non-linear stiffness change due to the displacement of the diaphragm. It is not possible to identify a linear model that accurately describes the complete range. The movement range of the diaphragm is divided into 4 sections. For each section a model will be identified. Sections 2 and 3 are located in the linear range of the loudspeaker. Sections 1 and 4 are located in the non-linear range of the loudspeaker. For small displacements in sections 1 and 4 a linear model can be found. The look up table of the capacitive measurement is adjusted such that an input current of 0 A corresponds with 0 mm displacement. The minimum and maximum boundary of the displacement range of the loudspeaker are respectively –1 and 9 mm.

The input of the loudspeaker is generated by a digital random number generator. The variance and frequency of the input current signals are respectively 0.02 and 100 Hz. The mean value for section 1 to 4 are respectively 0, 0.05, 0.1 and 0.15. The variance of the input current signal is chosen small because for small displacements the dynamics of the loudspeaker is linear. For large displacements the loudspeaker has many non-linearity's which are difficult to identify and analyze.

The measuring time and the sampling time determine respectively the minimum frequency and maximum frequency boundary for which the model extracted out of the acquired data is valid. The measuring time was 4 seconds and the sampling time was 0.001 second. The frequency boundaries of the data are respectively 0.25 Hz and 1 kHz. The captured data sets are divided into two groups:

- Data for **identification**
- Data for **validation** of the identified models

Output error model

The output error model is an easy model to identify a process with. The formula for an output error model is given by formula 8.17. The formula states that white noise is supposed to be additive to the output.

$$y(k) = \frac{b_1 z^{-1} + b_2 z^{-2} + .. + b_{nb} z^{-nb}}{1 + f_1 z^{-1} + f_2 z^{-2} + .. + f_{nf} z^{-nf}} u(k) + e(k) \tag{8.17}$$

where

z := shift operator
$e(k)$:= white noise
$u(k)$:= input
$y(k)$:= output

[BOS94]

Model fitting

The transfer function $H(s)_{current\_displacement}$ is a second order transfer function. The identification data has been fitted with a second order transfer function (two poles and 1 or 2 zeros). The data was best fitted with a transfer function that had two poles and one zero. The following 4 second order model were extracted from the data for identification. Formula 8.19 to 8.22 are the transfer functions of the models. Table 8-1 gives the fit of the matlab compare routine. The fit is given by formula 8.18. A low fit means that the simulated output of the model is almost equal to the measured output.

$$FIT = \frac{norm(Yh - Y)}{sqrt(length(Y))} \tag{8.18}$$

where

Yh := model output
Y := measured output
$norm$:= largest value

Table 8.1

MODEL	FIT
1	$8.8437 \cdot 10^{-5}$
2	$1.6281 \cdot 10^{-4}$
3	$1.4779 \cdot 10^{-4}$
4	$1.4008 \cdot 10^{-4}$

If x ≈ 0.6 mm

$$H(z)_{OE1} = \frac{-4.486 \cdot 10^{-4} z + 7.053 \cdot 10^{-4}}{z^2 - 1.919 z + 0.9457} \tag{8.19}$$

If x ≈ 2.9 mm

$$H(z)_{OE2} = \frac{-8.745 \cdot 10^{-4} z + 1.134 \cdot 10^{-3}}{z^2 - 1.928 z + 0.9408} \tag{8.20}$$

If x ≈ 4.6 mm

$$H(z)_{OE3} = \frac{-8.467 \cdot 10^{-4} z + 1.099 \cdot 10^{-3}}{z^2 - 1.92z + 0.9318} \tag{8.21}$$

If x ≈ 7.4 mm

$$H(z)_{OE4} = \frac{-5.67 \cdot 10^{-4} z + 7.472 \cdot 10^{-4}}{z^2 - 1.911z + 0.9315} \tag{8.22}$$

With the matlab function compare the simulated output is compared with the measured output of the validation data. Figure 8-5 shows the result of the compare routine. The simulated data represents the measured data quite well for all 4 models. The two data streams of each model only have a substantial deviation at the beginning, because the simulated model has different initial conditions than the actual initial conditions of the measured data.

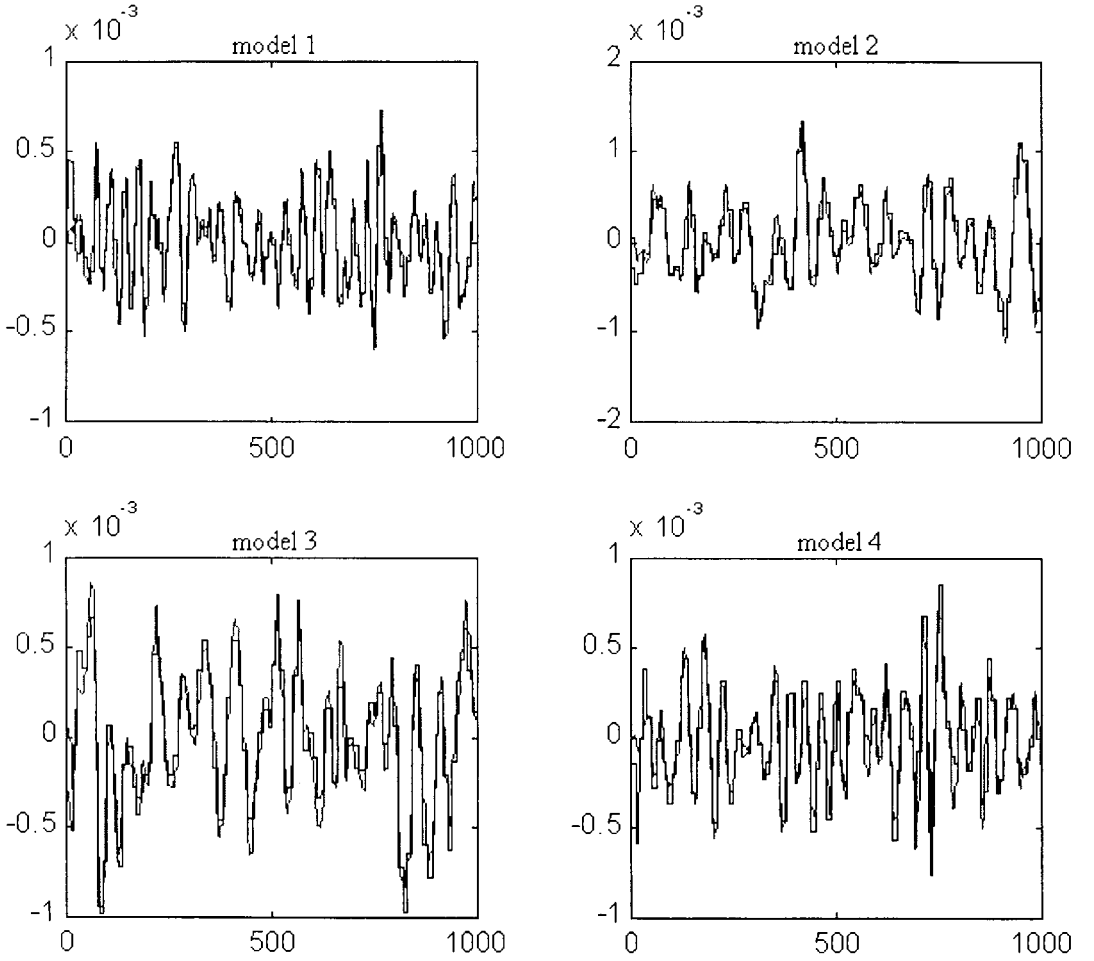

Figure 8-5 Comparing simulated output with measured output.

8.8. Step responses of output error models

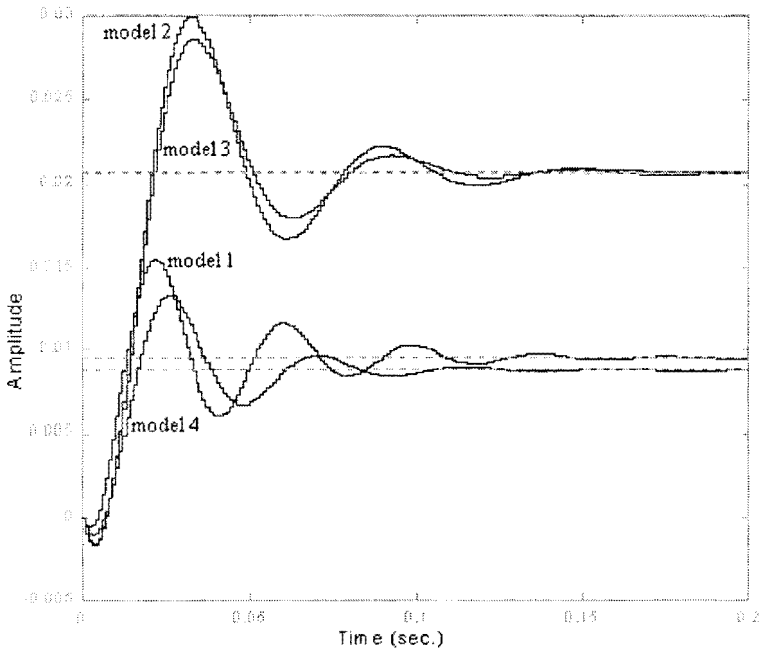

Figure 8-7 Step responses of the output error models.

Figure 8-7 shows the step responses of the four output error models. The following observations can be made:

- The step responses of models 2 and 3 are almost the same. The models are valid in the linear area of the displacement of the loudspeaker diaphragm.
- The step responses of models 1 and 4 have different final values and different peak times. Model 1 is valid in the non-linear range located around x=0.6 mm. Model 4 is valid in the non-linear range located around x=7.4 mm.
- Large deviations in the final values of the step responses of the models located in the linear and non-linear range. In the non-linear range saturation of the magnetic induction and rubber damping are possible sources of these deviations.
- All output error step responses have an initial undershoot. The cause of this undershoot is a non-minimum phase zero that is identified with the output error model. The cause of this non-minimum phase is not due of the loudspeaker characteristics but because of the digital signal processor used for capturing the data.

Based on the identified models a controller shall be designed in the next chapter.

9. Controller

9.1. Controller types

There exist several controller design methods:

- PID controller
- Dead beat controller
- Robust controller
- LQG controller

Due to limited time a simple controller was designed to control the displacement of the loudspeaker diaphragm. It is possible to design a controller for each output error model. Each controller controls the system in its range that it is designed for. The major disadvantage is the switching between different controllers. The problem lies in the initial states of the controller that is switched on. It takes some time before the transient is died out. Furthermore it is difficult to realize an uninterrupted transition. [DAM95] Since no special constraints are given for the controller a simple controller is designed that is stable and valid for the entire range of the loudspeaker displacement. The controller is designed for the linear range of the loudspeaker displacement.

9.2. Controller design

Controller requirements:

- Always stable
- No final error
- Not more than 20 percent overshoot

No final error implies that an integrator is required. The poles of the closed loop system should lie within the unity circle in the z-domain to ensure stability. A general controller is designed. An integrator pole is positioned in z =1 to remove a systematic final error. The poles of the models valid in the linear range of the loudspeaker displacement have been cancelled out with zero's. Furthermore an additional pole is added to realize a proper system. This additional pole is placed such that the closed loop poles of the system do not have more than 20 percent overshoot. The maximum gain factor of the actuator is 100. If the gain factor of the actuator would be larger the actuator will certainly saturate. The controller is given by formula 9.1.

$$C(z) = 100\frac{z^2 - 1.928z + 0.9407}{z^2 - 1.71z + 0.71} \tag{9.1}$$

Figure 9.1 shows the root locus of the closed loop system for each of the four output error models. The poles of the models valid in the non-linear range of the loudspeaker displacement are not compensated by the numerator of the controller C(z). The two system poles located on the real axis have a damping factor equal to one 1, which implies no overshoot of the control response. This will certainly result to a slower response of the controller. The poles in the linear range are compensated quite well and will result to a quick response of the controller.

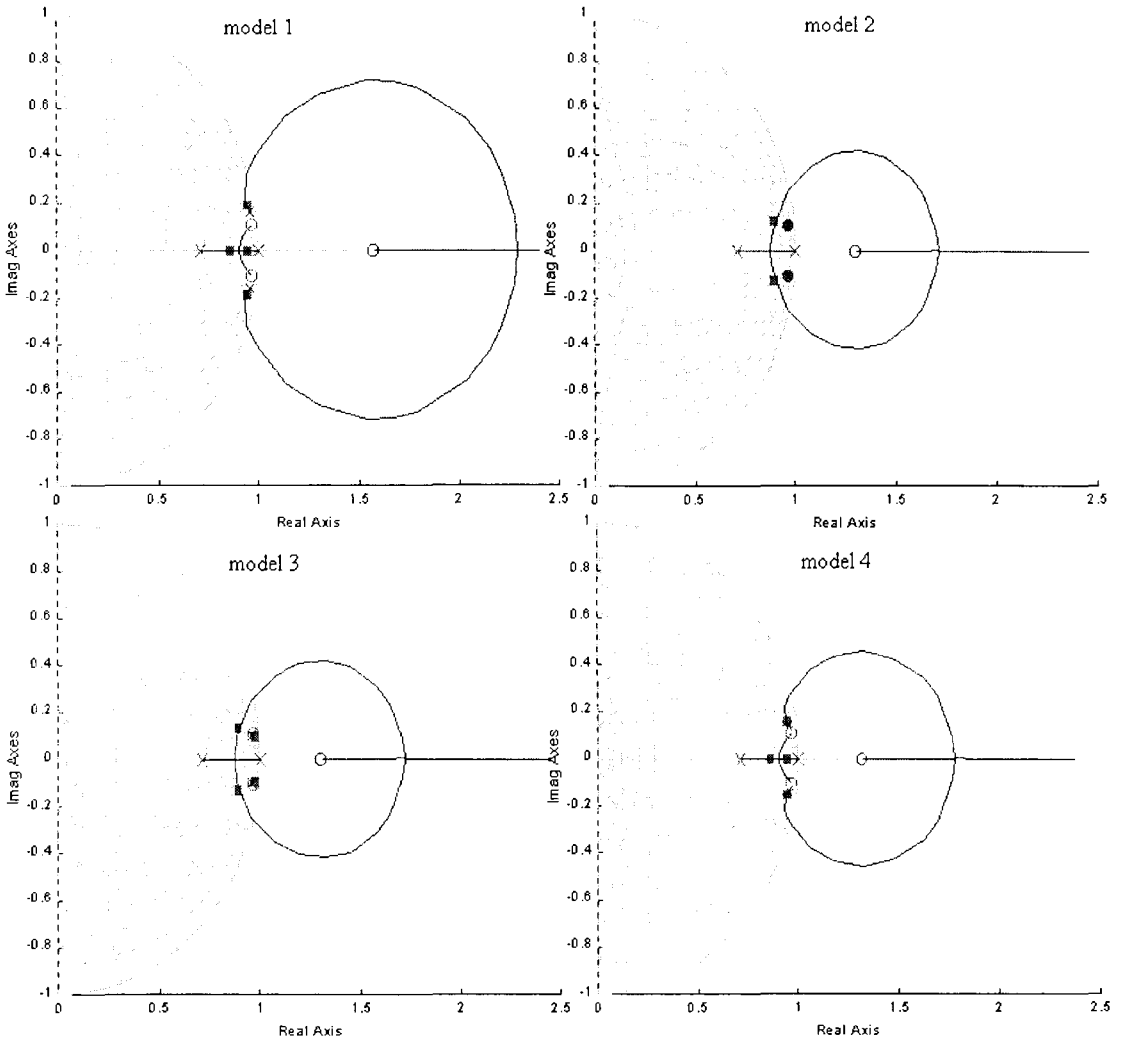

Figure 9-1 Root locus closed loop system.

Figure 9.2 shows the response of the controller for all four output error models. The step responses of the closed loop system in the linear range are quite fast. The initial undershoot of the step responses is the cause of a non-minimum phase zero. In the non-linear range the responses are indeed slower. The output of the controller is limited with a saturation function. This saturation is necessary to limit the maximum current that flows through the voice coil of the loudspeaker. The boundaries of the saturation are –0.5A and +0.5A. This saturation will cause a windup problem.

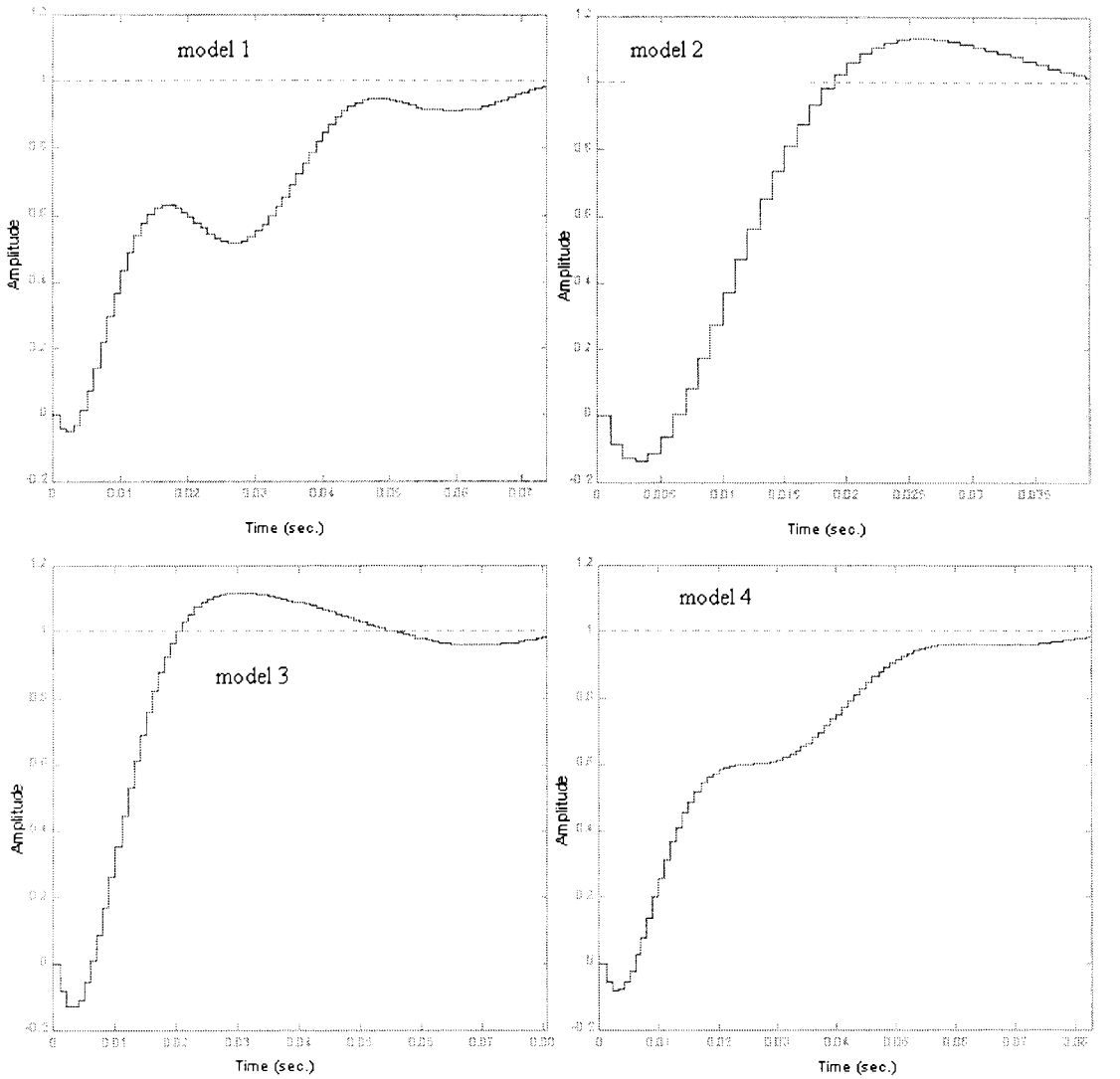

Figure 9-2 Step response of the closed loop system.

9.3.Anti windup

Theory

In the classic control theory calculates a controller C(s) an actuator signal u(t) based on the error signal e(t). The windup phenomenon occurs when the controlling signal u(t) delivered by the controller is not in agreement with the output signal $u^R(t)$ of the actuator. This can occur if a non-linearity is introduced into the control loop such as a saturation. The difference between the two signals can cause a considerable degradation in the performance of the control loop, even long after the cause of the trouble has vanished. [HAN80]

A general description of the SISO linear controller:

$$\dot{x}(t) = Ax(t) + Me(t) \tag{9.2}$$

$$u(t) = Bx(t) + Ne(t) \tag{9.3}$$

where

$x(t)$ = state vector of controller
$e(t)$ = control error signal
$u(t)$ = controlling signal

In the presence of a windup cause the same control structure as defined by formula 9.2 and 9.3 is used but the actual error signal e(t) is substituted with an other input signal $e^R(t)$ chosen in such a way that the resulting output signal u(t) of the controller is equal $u^R(t)$. As soon as the windup disappears the controller should be described by formula 9.2 and 9.3. For the equations of the conditioned controller:

$$\dot{x}(t) = Ax(t) + Me^R(t) \tag{9.4}$$

$$u^R(t) = Bx(t) + Ne^R(t) \tag{9.5}$$

For unconditioned situation

$$u(t) = Bx(t) + Ne(t) \tag{9.6}$$

This implies that:

$$e^R(t) = e(t) + \frac{u^R(t) - u(t)}{N} \tag{9.7}$$

Transfer function unconditioned controller:

$$C(s) = \frac{U(s)}{E(s)} = B(Is - A)^{-1}M + N \tag{9.8}$$

Definition

$$C_\infty := \lim_{s \to \infty} C(s) = N \tag{9.9}$$

This results to:

$$U(s) = C(s)\left(E(s) - \left(\frac{1}{C_\infty} - \frac{1}{C(s)} \right)\left(U(s) - U^R(s)\right) \right) \tag{9.10}$$

in which

$$E^R(s) = \left(\frac{1}{C_\infty} - \frac{1}{C(s)} \right)\left(U(s) - U^R(s)\right) \tag{9.11}$$

and

$$Q(s) := \left(\frac{1}{C_\infty} - \frac{1}{C(s)} \right) \tag{9.12}$$

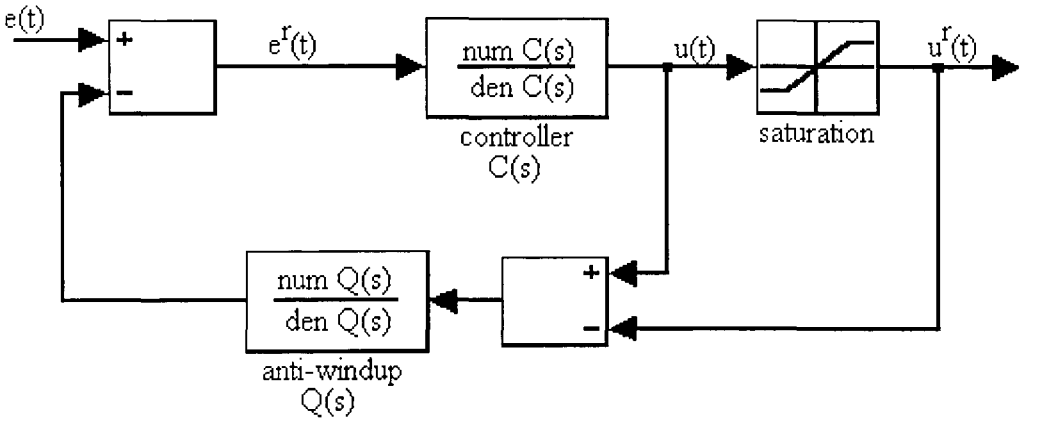

Figure 9-3 Anti-windup scheme for controller.

The control signal u(t) depends not only on the error signal e(t) but also on the difference $u^R(t)$-u(t). The block diagram is depicted in figure 9.3. The transfer function of the inner loop which appears in the block diagram is:

$$\frac{U(s)}{U^R(s)} = -\frac{C_\infty}{C(s)} + 1 \tag{9.13}$$

As the unconditioned controller is stable, the inner loop will also be stable if the unconditioned controller is a minimum phase system. This means no zeros in the right half plane of the s-domain.

In practice

The anti-windup for the discrete domain is analogues as for the s-domain only discrete transfer function are used in the anti-windup model. Formula 9.1 states the transfer function of the controller. The anti-windup is calculated as:

$$\lim_{z \to \infty} C(z) = \lim_{z \to \infty} 100 \frac{z^2 - 1.928z + 0.9407}{z^2 - 1.71z + 0.71} = 100 \tag{9.14}$$

$$Q(z) = \frac{1}{C_\infty} - \frac{1}{C(z)} = \frac{2z^2 - 3.638z + 1.651}{100z^2 - 192.8z + 94.07} \tag{9.15}$$

The poles and zeros of the Q(z) are:

Poles: $0.964 \pm 0.1068i$
Zeros: 0.9506 and 0.8684

The transfer function Q(z) has no zeros outside the unity gain circle which implies that the transfer function has no non-minimum phase zeros. Conclusion the inner loop is stable.

9.4. Controlling performance

The controller and anti-windup are implemented in a digital signal processor (=Dspace). A look up table transforms the measured output voltage of the capacitive measurement system to displacements. The outputs of the look-up table and the block reference signal are divided by 1000 to ensure that the error signal is in meters rather than millimeters.

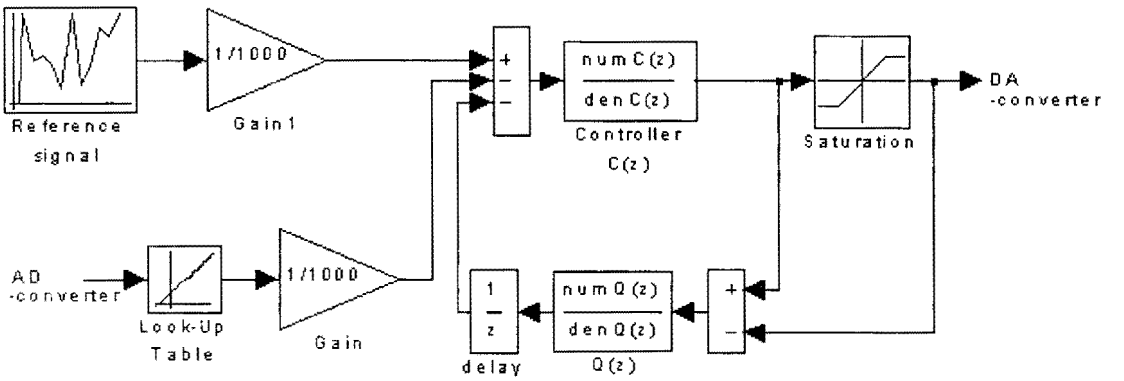

Figure 9-4 Implemented block diagram in Dspace.

The block saturation saturates the output signal of the controller above 0.5 A and below –0.5 A to respectively 0.5 A and –0.5 A. The inner loop of the anti windup has an additional small delay (0.0005 sec). This delay is necessary because the Dspace cannot implement algebraic loops.

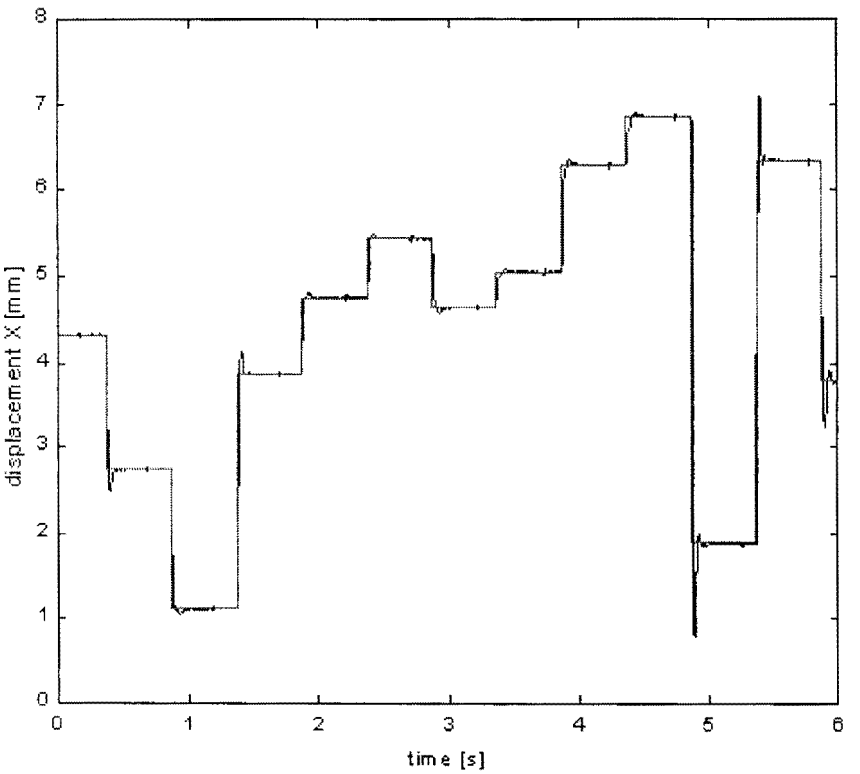

Figure 9-5 Reference signal and measured output signal.

Figure 9.5 shows the reference signal and the measured output signal. The following observations can be made:

- No final error
- Less overshoot

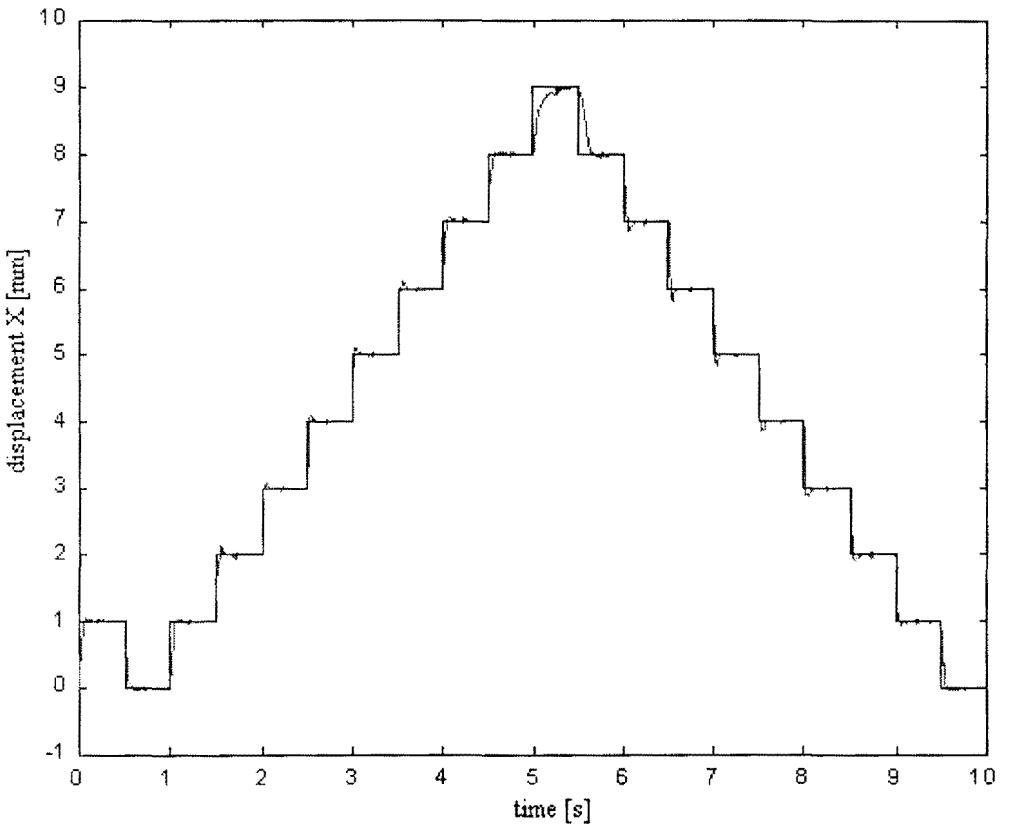

Figure 9-6 Measured output signal response.

Figure 9.6 shows the measured output signal and the reference signal. The step responses of the reference signal are followed with less overshoot by the displacement of the loudspeaker diaphragm. The step response at 9 mm displacement has a longer settling time because the controller was not optimal designed for the far ends of the range of the loudspeaker diaphragm. The controller works according requirements mentioned in section 9.2.

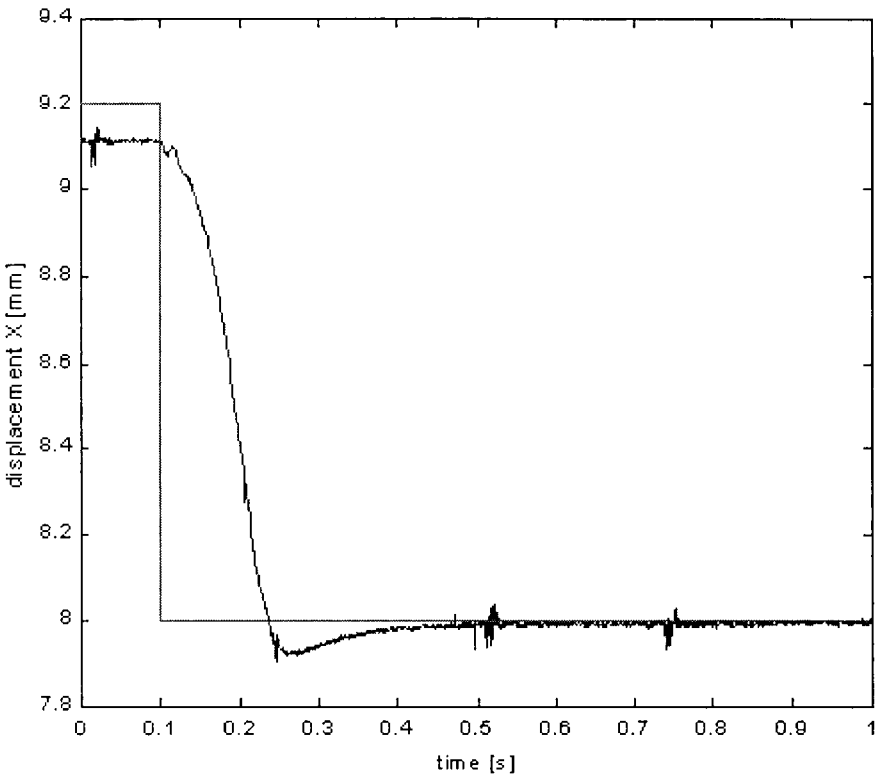

Figure 9-7 Anti windup performance.

The output signal of the controller is saturated if the displacement is larger than 9.1 mm. The anti windup ensures that the integration action of the controller is 'switched off'. Figure 9.7 shows a final error between the reference signal and the output signal of the look up table. When the reference signal (=displacement [mm]) drops below 9.1 mm the integration action of the controller is 'switched on'. After 0.5 seconds the final error is zero. The switching between the two controllers, controller with integration action and controller without integration action, is the cause for the long time that the final value has been reached. The initial states of the controller that is switched on are not correct and it will take some time before the effect of this incorrect states is negligible. The disturbances that can be seen in figure 9.6 are related to the noise disturbances of the DA and AD-converters and must not be seen as disturbances of the capacitive measurement system.

10. Conclusions and recommendations

10.1. Conclusions

The capacitive measurement system has a resolution of at least 10^{-5}m. A 1 mm displacement of the loudspeaker diaphragm results in a 211 mV voltage difference at the output of the capacitive measurement system. A calibration curve was measured. Based on this calibration curve a look up table was found for the measurement system. The calibration curve has a good linearity. The maximum deviation between the calibration curve and the closest linear function is not more than 47 μm. This is a small deviation compared to the maximum range (=10^{-2} m) of the measurement system.

The most critical components of the measurement system are in descending order of importance:

- Demodulator
- Amplifiers
- Multiplexer

The demodulator and amplifiers should be kept at a constant low temperature to eliminate temperature offset drift. The temperature offset drift deteriorates the performance of the measurement system. Replacing these components through components with better specifications will result to a substantially increase of the signal to noise ratio and a reduction of the inaccuracy of the measurement system due to temperature variations. Unfortunately such components are not yet available.

The averaged inaccuracy of the measurement system is 8 μm. The main sources that have an influence on the inaccuracy of the measurement system are in descending order of importance:

- Noise
- Low frequency disturbances
- Steady state error integration network
- Sensitivity change due to parasitic capacitor C_{p0} and C_{p4}
- Temperature offset drift of amplifiers

The controller that controls the displacement of the loudspeaker diaphragm is:

- Stable
- No final error
- Anti windup

The anti windup of the controller ensures that the integration action of the controller is 'switched off' when the control signal is saturated. The integration action will be 'switched on' when the control output signal is not saturated.

10.2. Recommendations

The main cause of the low frequency disturbances can be reduced. The cause of this disturbance is the fan that cools the Peltier element. Using a separate supply source for the fan eliminates the 250 Hz disturbance. This will definitely lead to an increase of the accuracy of the measurement system. Reducing the noise contribution of the electrical components will be difficult. All electronic components are chosen because of their low noise performance. Cooling the amplifiers with a heat pump eliminates the temperature drift of the amplifiers and increases the accuracy. The heat pump can be simply implemented until an amplifier has been found that has better low noise and low temperature drift specifications than the amplifier NE5534.

The developments in integrated circuit technology should be carefully followed. Improved electrical components that have a wider bandwidth, better rise time and lesser noise should be investigated. A wider bandwidth, lesser noise and faster rise time improve the performance of the measurement system.

Appendix A

Electronic scheme of capacitive measurement system

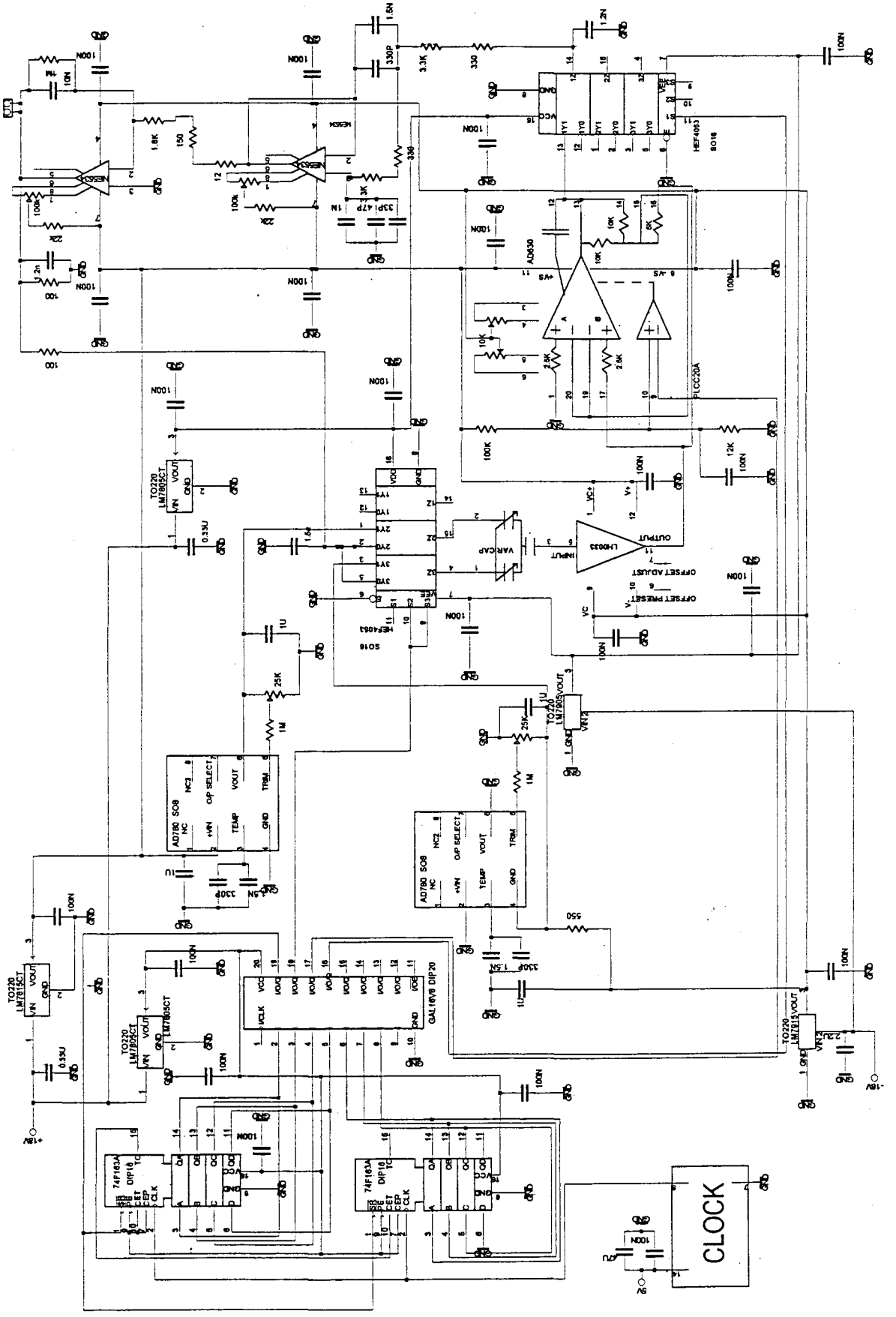

Appendix B

Table B.1 specifications loudspeaker SPH-165

IMPEDANZ (Z)	8	OHM
Resonanzefrequenz (fs)	33	Hz.
Max. frequenzbereich	F3-5000	Hz.
Empf. Trennfreq. (fmax.)	3500	Hz.
Max. Belastbastbarkeit	100	Wmax
Nennbelstbakeit (P)	50	Wrms
Mittl. Schalldr. (1W/1m)	89	dB
Nachgiebigkeit (Cms)	1.22	mm/N
Bewegte Masse (Mms)	16	g
Mech. Widerstand (Rms)	1.6	Kg/s
Mechanische Gute (Qms)	2.02	
Elektrische Gute (Qes)	0.23	
Gesamtegute (Qts)	0.21	
Aquivalentvolumen (Vas)	36	l
Gleichstromwiderst. (Re)	6.5	Ohm
Schwingspulenindukt. (Le)	1.1	mH
Schwingspulendurchmesser	35.5	mm
Schwingspulentrager	Alu	
Schwingspulenwick.-Hohe	15	mm
Luftspalthohe	8	mm
Lineare Auslenkung	$\pm$3.5	mm
Eff. Membranflache (Sd)	137	cm^2
Verschiebevolumen (Vd)	48	cm
Kraftfaktor (B· L)	9.7	Tm
Referenz-Wirkungsgrad (No)	0.5	%
Magnetdurchmesser	120	mm
Magnetgewicht	29.5	oz.
Einbouwoffnung (diamesser)	142	mm
Einbautiefe	89	mm
Abmessungen (diamesser)	165	mm
Gewicht	2.32	Kg
Bassreflex	>10	L

Appendix C

Mechanical lay-out of differential capacitive sensor and loudspeaker

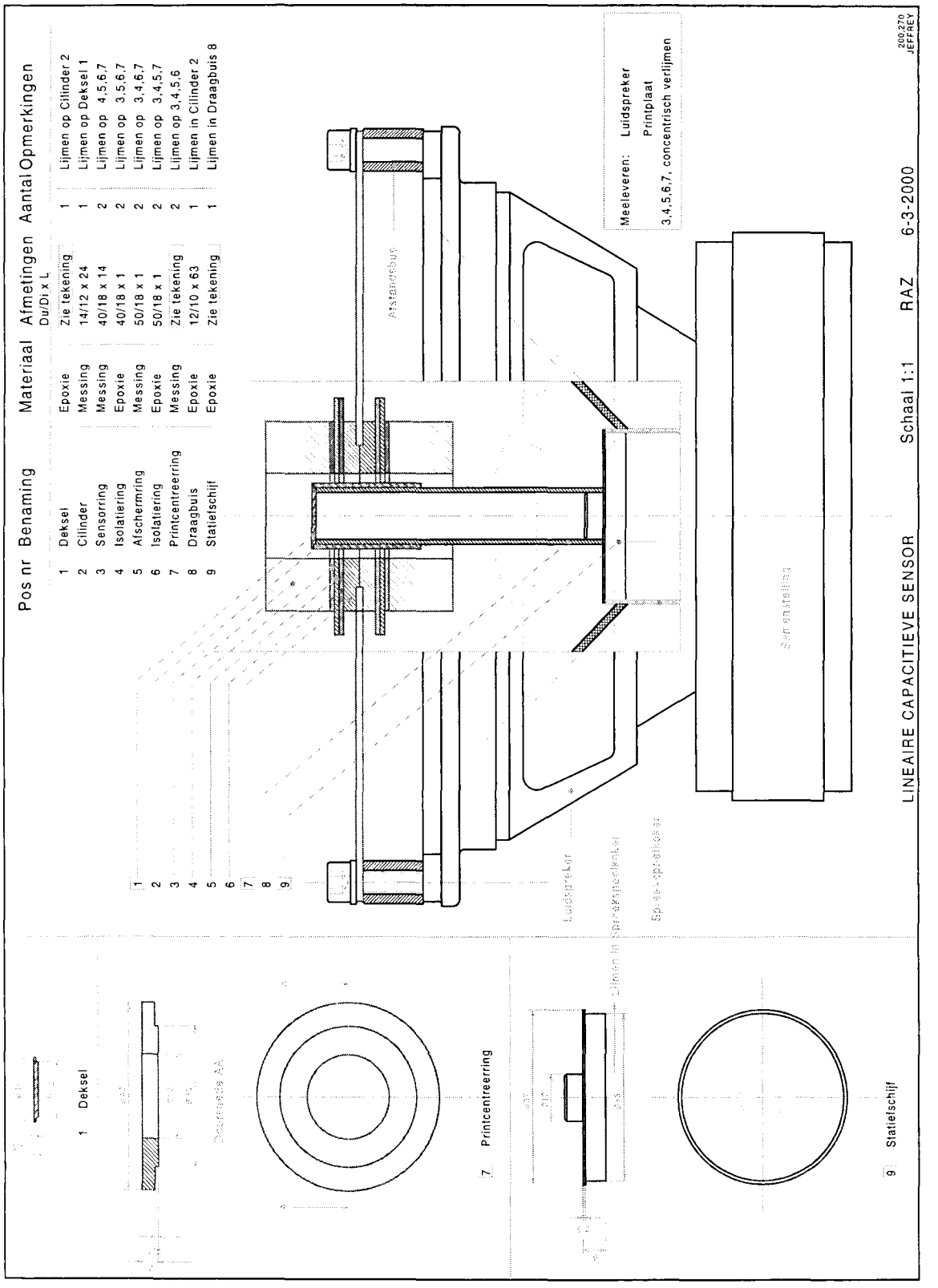

Appendix D

Table D.1 state table of implemented timing diagram

STATE	BINARY NUMBER	125KHZ CLOCK	SYNCHRONOUS RESET	DEMODULATION	CONTROL SWITCH
0	0000000	H	L	H	L
1	0000001	H	L	H	L
2	0000010	H	L	L	L
3	0000011	H	L	L	L
4	0000100	H	L	L	L
5	0000101	H	L	L	L
6	0000110	H	L	L	L
7	0000111	H	L	L	L
8	0001000	H	L	L	L
9	0001001	H	L	L	L
10	0001010	H	L	L	H
11	0001011	H	L	L	H
12	0001100	H	L	L	H
13	0001101	H	L	L	H
14	0001110	H	L	L	H
15	0001111	H	L	L	H
16	0010000	H	L	L	H
17	0010001	H	L	L	H
18	0010010	H	L	L	H
19	0010011	H	L	L	H
20	0010100	H	L	L	H
21	0010101	H	L	L	H
22	0010110	H	L	L	H
23	0010111	H	L	L	H
24	0011000	H	L	L	H
25	0011001	H	L	L	H
26	0011010	H	L	L	H
27	0011011	H	L	L	H
28	0011100	H	L	L	H
29	0011101	H	L	L	H
30	0011110	H	L	L	H
31	0011111	H	L	L	H
32	0100000	H	L	L	H
33	0100001	H	L	L	H
34	0100010	H	L	L	H
35	0100011	H	L	L	H
36	0100100	H	L	L	H
37	0100101	H	L	L	H
38	0100110	H	L	L	H
39	0100111	H	L	L	H
40	0101000	H	L	L	H
41	0101001	H	L	L	H
42	0101010	H	L	L	H
43	0101011	H	L	L	H
44	0101100	H	L	L	H
45	0101101	H	L	L	H
46	0101110	H	L	L	H
47	0101111	H	L	L	H
48	0110000	H	L	L	H
49	0110001	H	L	L	H

Continu 1 table D.1 state table of implemented timing diagram

STATE	BINARY NUMBER	125KHZ CLOCK	SYNCHRONOUS RESET	DEMODULATION	CONTROL SWITCH
50	0110010	H	L	L	H
51	0110011	H	L	L	H
52	0110100	H	L	L	H
53	0110101	H	L	L	H
54	0110110	H	L	L	H
55	0110111	H	L	L	H
56	0111000	H	L	L	H
57	0111001	H	L	L	H
58	0111010	H	L	L	H
59	0111011	H	L	L	H
60	0111100	H	L	L	H
61	0111101	H	L	L	H
62	0111110	H	L	L	H
63	0111111	H	L	L	H
64	1000000	L	L	L	L
65	1000001	L	L	L	L
66	1000010	L	L	H	L
67	1000011	L	L	H	L
68	1000100	L	L	H	L
69	1000101	L	L	H	L
70	1000110	L	L	H	L
71	1000111	L	L	H	L
72	1001000	L	L	H	L
73	1001001	L	L	H	L
74	1001010	L	L	H	H
75	1001011	L	L	H	H
76	1001100	L	L	H	H
77	1001101	L	L	H	H
78	1001110	L	L	H	H
79	1001111	L	L	H	H
80	1010000	L	L	H	H
81	1010001	L	L	H	H
82	1010010	L	L	H	H
83	1010011	L	L	H	H
84	1010100	L	L	H	H
85	1010101	L	L	H	H
86	1010110	L	L	H	H
87	1010111	L	L	H	H
88	1011000	L	L	H	H
89	1011001	L	L	H	H
90	1011010	L	L	H	H
91	1011011	L	L	H	H
92	1011100	L	L	H	H
93	1011101	L	L	H	H
94	1011110	L	L	H	H
95	1011111	L	L	H	H
96	1100000	L	L	H	H
97	1100001	L	L	H	H
98	1100010	L	L	H	H
99	1100011	L	L	H	H
100	1100100	L	L	H	H

Continu 2 table D.1 state table of implemented timing diagram

STATE	BINARY NUMBER	125KHZ CLOCK	SYNCHRONOUS RESET	DEMODULATION	CONTROL SWITCH
101	1100101	L	L	H	H
102	1100110	L	L	H	H
103	1100111	L	L	H	H
104	1101000	L	L	H	H
105	1101001	L	L	H	H
106	1101010	L	L	H	H
107	1101011	L	L	H	H
108	1101100	L	L	H	H
109	1101101	L	L	H	H
110	1101110	L	L	H	H
111	1101111	L	L	H	H
112	1110000	L	L	H	H
113	1110001	L	L	H	H
114	1110010	L	L	H	H
115	1110011	L	L	H	H
116	1110100	L	L	H	H
117	1110101	L	L	H	H
118	1110110	L	L	H	H
119	1110111	L	L	H	H
120	1111000	L	L	H	H
121	1111001	L	L	H	H
122	1111010	L	L	H	H
123	1111011	L	L	H	H
124	1111100	L	L	H	H
125	1111101	L	L	H	H
126	1111110	L	L	H	H
127	1111111	L	H	H	H

Appendix E

Principle of Peltier element

The flow of an electric current through the junction of two ***dissimilar*** conductors can either cool or heat this junction depending on the direction of the current. Heat generating or absorption rates are proportional to the magnitude of the current and also the temperature of the junction. Practical Peltier Effect Heat pumps consist of many couples of dissimilar conductors connected electrically in series and thermally in parallel. When the device is connected to a dc source, heat will be absorbed at one end of the device, cooling it, while heat is rejected at the other end, where the temperature rises. [Reference RS97] See figure E-1 . Reversing the current reverses the flow of heat. At the hot side, the heat must be removed through the use of a heat sink. The heat delivered to the hot side of the device includes the 'pumped' heat plus the electrical power dissipated within the heat pump.

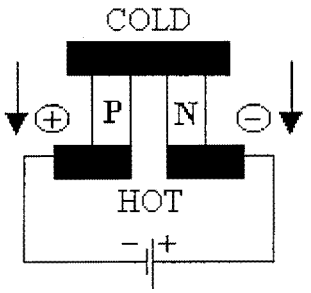

Figure E.1 Single dissimilar conductor couple of a heat pump.

The demodulator is cooled with a heat pump. The heat at the hot side of the Peltier device is removed with a heat sink. The heat sink is cooled with a fan. Heat conducting paste is pasted between heat pump and the package of the demodulator and between the heat pump and the heat sink. The heat conducting paste will optimize the heat transfer from the package of the demodulator to the heat sink.

Heat pump operation

Definitions:

Q_c = the amount of heat absorbed at the cold face [W]
Q_{max} = maximum amount of heat that can be absorbed at cold face [W]
I_{opt} = optimum current (most efficient input current required for a given ΔT) [A]
I_{max} = input current resulting in greatest ΔT [A]
ΔT = temperature difference between cold and hot surface of heat pump [°C]

continu appendix E

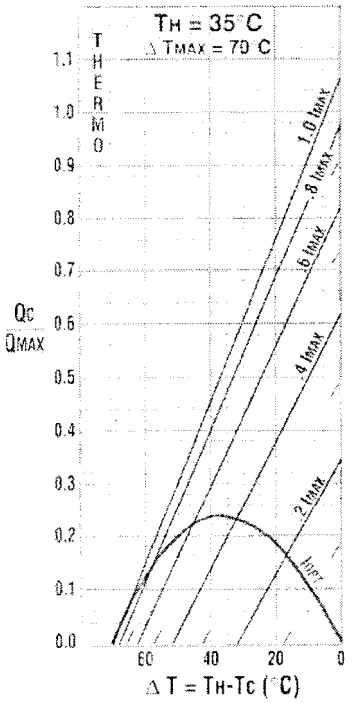

Figure E.2 Selection / Performance Graph.

The internal power dissipation of the demodulator (AD630) is 600mW, which is the amount of heat the heat pump, must absorb at the cold side. The temperature difference must be approximately 25°C. The selection/Performance graphs depicted in figure E.2 gives at the crossing of $\Delta T=25°C$ and I-curves a I_{opt} current of $0.25I_{max}$. The appropriated $Q_c/Q_{max} = 0.2$. This results that Q_{max} is equal 3W. The maximum current ($=I_{max}$) of the heat pump is 3.9A. The operation current ($=I_{opt}$) used for the heat pump is 1A.

Appendix F

Matlab code

```
%program to read data in delimited format
%input file dat.xls
%output file sort.xls
%22-6-2000
%auteur J.H.P.M. Goossens

Matrix=dlmread('dat.xls','\t');     %reads an excel file called dat.xls
[m,n]=size(Matrix);                 %number of samples is equal m
b=sortrows(Matrix,3);               %sorts Matrix ascending based on kolom 3
min_aantal_samples = 10;            %minimum count of samples
rij=1;                              %first or second row
dlm='\t';
z=1;

NEWLINE = sprintf('\n');            % delimiter defaults to Comma for CSV
dlm = sprintf(dlm);                 % Handles special characters.

% open the file
if strncmp(computer,'MAC',3)
  fid = fopen('sort.xls' ,'wt');
else
  fid = fopen('sort.xls' ,'wb');
end

if fid == (-1), error(['Could not open file ' sort.xls]); end

for k=1:m
  k=z;
  r=b(k,3);
  [i,j,v]=find(b(:,3) == r);    %i contains row of samples with equal values LVDT
  [mi,ni]=size(i);              %mi contains the number of samples b is equal r
   if mi >= 10                  %number of equal LVDT values greater than 10
      a=b(i(1),3);
      c=b(i(1),rij);
      d=b(i(2),rij);
      e=b(i(3),rij);
      f=b(i(4),rij);
      g=b(i(5),rij);
      h=b(i(6),rij);
      j=b(i(7),rij);
      q=b(i(8),rij);
      y=b(i(9),rij);
```

continu Matlab code

```
    z=b(i(10),rij);
    opslaan= [ a c d e f g h j q y z];      %values are stored in vector opslaan
    [br,bc] = size(opslaan);
      for i = 1:br
       for j = 1:bc
        if(opslaan(i,j) ~= 0)
          str = num2str(opslaan(i,j));
          fwrite(fid, str, 'uchar');
         end
        if(j < bc)
          fwrite(fid, dlm, 'uchar');
        end
       end
       fwrite(fid, NEWLINE, 'char'); % this may \r\n for DOS
      end
    end;
    z=k+mi;
    if z >= m
      break
    end;
end;

% close files
fclose(fid);
```

Appendix G

Table G.1 results of matlab routine

LVDT [V]	1 [V]	2 [V]	3 [V]	4 [V]	5 [V]	6 [V]	7 [V]	8 [V]	9 [V]	10 [V]
-9,485	1,614	1,614	1,614	1,614	1,613	1,613	1,614	1,614	1,614	1,613
-9,4	1,607	1,607	1,607	1,607	1,607	1,606	1,606	1,606	1,607	1,606
-9,3	1,595	1,595	1,595	1,595	1,595	1,595	1,594	1,595	1,594	1,593
-9,2	1,585	1,585	1,585	1,585	1,585	1,585	1,585	1,584	1,584	1,582
-9,1	1,573	1,573	1,574	1,573	1,573	1,573	1,573	1,573	1,572	1,572
-9	1,562	1,561	1,563	1,563	1,563	1,562	1,562	1,562	1,561	1,561
-8,9	1,551	1,551	1,551	1,552	1,552	1,551	1,551	1,551	1,551	1,552
-8,8	1,54	1,541	1,541	1,54	1,54	1,541	1,54	1,54	1,54	1,54
-8,7	1,531	1,53	1,53	1,529	1,529	1,528	1,528	1,528	1,529	1,527
-8,6	1,518	1,519	1,517	1,519	1,517	1,519	1,517	1,517	1,518	1,518
-8,5	1,507	1,507	1,507	1,506	1,507	1,507	1,505	1,505	1,505	1,504
-8,4	1,497	1,497	1,497	1,497	1,496	1,497	1,496	1,496	1,495	1,494
-8,3	1,488	1,487	1,488	1,486	1,488	1,487	1,486	1,486	1,485	1,486
-8,2	1,478	1,477	1,477	1,476	1,475	1,475	1,475	1,474	1,474	1,474
-8,1	1,468	1,466	1,465	1,465	1,465	1,464	1,464	1,464	1,464	1,463
-8	1,457	1,455	1,457	1,455	1,457	1,457	1,454	1,454	1,454	1,454
-7,9	1,446	1,445	1,445	1,445	1,444	1,444	1,443	1,443	1,442	1,44
-7,8	1,434	1,435	1,434	1,433	1,433	1,433	1,432	1,433	1,432	1,432
-7,7	1,425	1,423	1,423	1,423	1,422	1,421	1,422	1,421	1,421	1,42
-7,6	1,414	1,414	1,415	1,415	1,414	1,414	1,413	1,414	1,413	1,413
-7,5	1,405	1,404	1,402	1,402	1,402	1,403	1,401	1,401	1,399	1,399
-7,4	1,394	1,395	1,393	1,393	1,392	1,391	1,391	1,39	1,389	1,389
-7,3	1,383	1,383	1,383	1,382	1,382	1,381	1,381	1,38	1,38	1,38
-7,2	1,372	1,371	1,372	1,371	1,371	1,369	1,37	1,369	1,367	1,368
-7,1	1,363	1,36	1,357	1,357	1,355	1,356	1,357	1,355	1,355	1,356
-7	1,352	1,352	1,349	1,349	1,348	1,347	1,346	1,346	1,346	1,346
-6,9	1,341	1,34	1,34	1,338	1,336	1,336	1,335	1,335	1,334	1,334
-6,8	1,33	1,329	1,328	1,328	1,328	1,327	1,326	1,326	1,325	1,325
-6,7	1,319	1,318	1,318	1,317	1,317	1,317	1,316	1,316	1,315	1,314
-6,6	1,308	1,307	1,307	1,306	1,306	1,305	1,304	1,303	1,304	1,303
-6,5	1,298	1,295	1,294	1,293	1,293	1,293	1,292	1,291	1,291	1,291
-6,4	1,286	1,286	1,285	1,285	1,284	1,285	1,284	1,282	1,282	1,281
-6,3	1,275	1,275	1,273	1,271	1,271	1,27	1,27	1,269	1,268	1,268
-6,2	1,265	1,262	1,259	1,258	1,258	1,258	1,257	1,258	1,258	1,257
-6,1	1,253	1,252	1,251	1,252	1,248	1,247	1,248	1,247	1,247	1,247
-6,001	1,243	1,241	1,242	1,24	1,239	1,238	1,238	1,238	1,238	1,238
-5,9	1,232	1,229	1,229	1,228	1,227	1,227	1,225	1,225	1,225	1,224
-5,8	1,22	1,218	1,219	1,218	1,217	1,217	1,217	1,216	1,214	1,215

Continu 1 table G.1 results of matlab routine

LVDT [V]	1 [V]	2 [V]	3 [V]	4 [V]	5 [V]	6 [V]	7 [V]	8 [V]	9 [V]	10 [V]
-5,7	1,207	1,207	1,206	1,205	1,202	1,203	1,202	1,201	1,202	1,201
-5,6	1,199	1,197	1,197	1,195	1,195	1,194	1,192	1,192	1,191	1,191
-5,5	1,186	1,185	1,184	1,184	1,184	1,182	1,181	1,18	1,18	1,18
-5,4	1,174	1,173	1,172	1,172	1,171	1,17	1,17	1,169	1,169	1,169
-5,3	1,161	1,16	1,159	1,158	1,158	1,158	1,158	1,155	1,157	1,158
-5,2	1,153	1,152	1,152	1,15	1,151	1,15	1,147	1,148	1,147	1,148
-5,099	1,142	1,142	1,138	1,138	1,137	1,136	1,135	1,136	1,136	1,134
-4,999	1,13	1,127	1,126	1,125	1,125	1,124	1,125	1,123	1,124	1,123
-4,901	1,119	1,118	1,114	1,113	1,113	1,114	1,112	1,112	1,112	1,111
-4,8	1,107	1,105	1,104	1,103	1,103	1,101	1,101	1,1	1,1	1,099
-4,7	1,094	1,095	1,095	1,095	1,094	1,094	1,091	1,09	1,09	1,089
-4,6	1,082	1,081	1,08	1,078	1,078	1,078	1,076	1,078	1,077	1,076
-4,5	1,072	1,072	1,072	1,068	1,068	1,066	1,066	1,066	1,065	1,065
-4,4	1,061	1,06	1,058	1,057	1,056	1,056	1,056	1,054	1,054	1,054
-4,301	1,049	1,048	1,046	1,046	1,046	1,045	1,043	1,043	1,041	1,041
-4,201	1,037	1,036	1,035	1,035	1,031	1,032	1,032	1,031	1,031	1,031
-4,099	1,026	1,026	1,024	1,024	1,023	1,021	1,02	1,021	1,021	1,021
-3,9	1,002	1,002	1,002	1	1,001	0,999	0,999	0,997	0,998	0,996
-3,8	0,991	0,99	0,99	0,989	0,989	0,986	0,987	0,986	0,985	0,985
-3,701	0,98	0,98	0,979	0,978	0,977	0,974	0,975	0,974	0,975	0,974
-3,6	0,967	0,966	0,963	0,962	0,963	0,963	0,962	0,963	0,961	0,959
-3,499	0,956	0,957	0,957	0,954	0,953	0,952	0,952	0,952	0,952	0,949
-3,401	0,944	0,942	0,941	0,94	0,941	0,94	0,939	0,939	0,939	0,939
-3,3	0,934	0,933	0,933	0,929	0,929	0,929	0,927	0,927	0,927	0,928
-3,2	0,923	0,921	0,917	0,916	0,917	0,916	0,916	0,916	0,915	0,914
-3,1	0,91	0,909	0,908	0,907	0,906	0,906	0,906	0,904	0,905	0,904
-3	0,899	0,899	0,898	0,897	0,895	0,896	0,894	0,895	0,893	0,894
-2,901	0,887	0,887	0,887	0,885	0,883	0,882	0,881	0,883	0,881	0,881
-2,801	0,875	0,874	0,87	0,872	0,87	0,871	0,87	0,869	0,869	0,87
-2,703	0,865	0,863	0,864	0,863	0,863	0,859	0,859	0,859	0,859	0,858
-2,601	0,849	0,85	0,849	0,849	0,847	0,846	0,847	0,848	0,845	0,845
-2,502	0,842	0,84	0,84	0,838	0,838	0,838	0,837	0,836	0,834	0,833
-2,401	0,831	0,83	0,831	0,829	0,827	0,826	0,825	0,824	0,825	0,824
-2,299	0,819	0,819	0,818	0,813	0,812	0,814	0,814	0,813	0,812	0,812
-2,203	0,807	0,807	0,807	0,806	0,804	0,801	0,802	0,801	0,8	0,8
-2,094	0,795	0,796	0,794	0,792	0,789	0,791	0,79	0,789	0,789	0,786
-2	0,781	0,783	0,782	0,782	0,782	0,78	0,779	0,775	0,779	0,775
-1,902	0,772	0,77	0,769	0,768	0,768	0,767	0,766	0,766	0,766	0,766
-1,801	0,758	0,757	0,757	0,757	0,757	0,756	0,755	0,755	0,755	0,754
-1,701	0,749	0,746	0,747	0,746	0,743	0,744	0,745	0,744	0,742	0,743

Continu 2 table G.1 results of matlab routine

LVDT	1	2	3	4	5	6	7	8	9	10
[V]	[V]	[V]	[V]	[V]	[V]	[V]	[V]	[V]	[V]	[V]
-1,6	0,737	0,734	0,733	0,733	0,732	0,731	0,732	0,731	0,732	0,729
-1,505	0,726	0,724	0,724	0,724	0,722	0,723	0,722	0,722	0,718	0,718
-1,4	0,714	0,715	0,714	0,712	0,714	0,709	0,709	0,708	0,708	0,708
-1,299	0,701	0,703	0,699	0,7	0,698	0,699	0,697	0,696	0,697	0,697
-1,209	0,69	0,69	0,688	0,689	0,687	0,688	0,687	0,688	0,687	0,686
-1,1	0,68	0,675	0,677	0,675	0,677	0,676	0,676	0,676	0,675	0,674
-0,991	0,667	0,666	0,665	0,662	0,662	0,662	0,661	0,661	0,662	0,659
-0,901	0,655	0,655	0,653	0,648	0,651	0,652	0,651	0,649	0,651	0,65
-0,794	0,645	0,643	0,642	0,644	0,643	0,643	0,643	0,641	0,638	0,639
-0,695	0,633	0,633	0,63	0,629	0,629	0,629	0,627	0,626	0,628	0,625
-0,598	0,621	0,621	0,62	0,619	0,619	0,618	0,618	0,618	0,617	0,616
-0,501	0,611	0,609	0,609	0,609	0,608	0,603	0,606	0,604	0,602	0,601
-0,403	0,599	0,596	0,599	0,594	0,593	0,593	0,593	0,593	0,592	0,59
-0,302	0,588	0,588	0,589	0,587	0,586	0,585	0,583	0,582	0,583	0,582
-0,201	0,575	0,574	0,572	0,571	0,571	0,571	0,571	0,569	0,57	0,569
-0,096	0,565	0,564	0,564	0,562	0,561	0,56	0,559	0,559	0,558	0,557
-0,012	0,555	0,554	0,552	0,552	0,55	0,549	0,548	0,548	0,548	0,547
0,107	0,541	0,541	0,538	0,541	0,538	0,539	0,536	0,536	0,536	0,535
0,2	0,531	0,531	0,53	0,53	0,529	0,528	0,525	0,525	0,522	0,521
0,301	0,519	0,519	0,518	0,516	0,515	0,513	0,513	0,512	0,513	0,511
0,403	0,507	0,507	0,508	0,504	0,504	0,501	0,501	0,502	0,501	0,5
0,498	0,497	0,495	0,497	0,494	0,487	0,491	0,49	0,49	0,49	0,487
0,612	0,481	0,481	0,479	0,479	0,479	0,477	0,478	0,477	0,475	0,476
0,7	0,472	0,472	0,471	0,468	0,468	0,467	0,467	0,468	0,467	0,463
0,801	0,462	0,459	0,459	0,457	0,456	0,456	0,455	0,454	0,451	0,453
0,897	0,451	0,45	0,449	0,448	0,447	0,447	0,442	0,445	0,445	0,442
1,03	0,434	0,434	0,432	0,431	0,429	0,43	0,429	0,428	0,428	0,427
1,096	0,428	0,428	0,426	0,425	0,424	0,424	0,421	0,421	0,421	0,421
1,212	0,415	0,415	0,414	0,412	0,405	0,408	0,407	0,406	0,406	0,405
1,289	0,406	0,404	0,403	0,403	0,4	0,403	0,403	0,4	0,399	0,398
1,396	0,392	0,391	0,39	0,384	0,388	0,388	0,388	0,386	0,385	0,384
1,506	0,379	0,379	0,377	0,377	0,375	0,374	0,376	0,374	0,375	0,374
1,604	0,37	0,367	0,367	0,361	0,363	0,363	0,365	0,363	0,364	0,363
1,696	0,359	0,353	0,353	0,353	0,353	0,353	0,352	0,352	0,351	0,35
1,798	0,346	0,344	0,343	0,342	0,342	0,342	0,341	0,341	0,341	0,341
1,891	0,335	0,331	0,334	0,333	0,331	0,329	0,331	0,33	0,329	0,328
2,003	0,324	0,322	0,322	0,322	0,321	0,32	0,315	0,32	0,319	0,317
2,09	0,314	0,313	0,312	0,31	0,31	0,309	0,308	0,307	0,308	0,307
2,209	0,3	0,299	0,298	0,294	0,294	0,295	0,294	0,294	0,292	0,292
2,303	0,289	0,288	0,287	0,287	0,287	0,286	0,284	0,285	0,284	0,282

Continu 3 table G.1 results of matlab routine

LVDT [V]	1 [V]	2 [V]	3 [V]	4 [V]	5 [V]	6 [V]	7 [V]	8 [V]	9 [V]	10 [V]
2,397	0,277	0,277	0,276	0,276	0,275	0,273	0,273	0,272	0,272	0,272
2,505	0,267	0,265	0,263	0,261	0,26	0,261	0,262	0,261	0,26	0,26
2,603	0,251	0,251	0,247	0,251	0,251	0,251	0,25	0,248	0,25	0,247
2,693	0,245	0,246	0,245	0,243	0,237	0,24	0,241	0,239	0,238	0,236
2,8	0,228	0,228	0,23	0,226	0,233	0,231	0,232	0,23	0,229	0,223
2,896	0,221	0,217	0,221	0,216	0,218	0,217	0,217	0,216	0,216	0,214
2,997	0,21	0,21	0,207	0,209	0,209	0,207	0,205	0,205	0,207	0,205
3,097	0,199	0,198	0,197	0,197	0,191	0,19	0,194	0,193	0,19	0,19
3,21	0,186	0,184	0,184	0,184	0,183	0,183	0,183	0,181	0,181	0,18
3,302	0,176	0,175	0,174	0,173	0,172	0,169	0,171	0,169	0,168	0,168
3,404	0,164	0,164	0,162	0,161	0,16	0,158	0,16	0,156	0,156	0,157
3,497	0,155	0,148	0,152	0,15	0,149	0,148	0,149	0,149	0,145	0,146
3,6	0,143	0,141	0,141	0,14	0,14	0,137	0,136	0,137	0,137	0,134
3,701	0,13	0,13	0,129	0,127	0,127	0,126	0,126	0,123	0,122	0,121
3,803	0,114	0,119	0,114	0,118	0,116	0,117	0,115	0,114	0,114	0,113
3,903	0,106	0,106	0,106	0,102	0,103	0,103	0,103	0,1	0,101	0,101
3,997	0,098	0,095	0,097	0,092	0,091	0,094	0,089	0,091	0,091	0,089
4,091	0,087	0,083	0,085	0,081	0,08	0,08	0,081	0,081	0,081	0,078
4,199	0,074	0,074	0,073	0,073	0,072	0,069	0,072	0,069	0,07	0,067
4,297	0,064	0,063	0,06	0,061	0,062	0,062	0,06	0,058	0,057	0,058
4,402	0,052	0,051	0,045	0,048	0,048	0,045	0,045	0,043	0,044	0,042
4,5	0,04	0,039	0,038	0,038	0,037	0,036	0,036	0,035	0,035	0,03
4,601	0,027	0,027	0,028	0,025	0,025	0,024	0,023	0,021	0,023	0,021
4,698	0,018	0,017	0,017	0,014	0,013	0,014	0,011	0,013	0,009	0,01
4,799	0,006	0,004	0,003	0	0,001	0,001	0,001	-0,002	0	-0,003
4,9	-0,006	-0,006	-0,008	-0,009	-0,007	-0,01	-0,01	-0,01	-0,011	-0,015
5	-0,019	-0,017	-0,02	-0,02	-0,02	-0,021	-0,022	-0,021	-0,023	-0,024
5,099	-0,028	-0,029	-0,029	-0,029	-0,032	-0,031	-0,031	-0,033	-0,035	-0,033
5,2	-0,04	-0,046	-0,042	-0,048	-0,043	-0,044	-0,045	-0,044	-0,045	-0,045
5,302	-0,05	-0,052	-0,052	-0,052	-0,053	-0,053	-0,054	-0,06	-0,054	-0,057
5,403	-0,066	-0,063	-0,069	-0,066	-0,068	-0,07	-0,068	-0,068	-0,068	-0,069
5,5	-0,073	-0,075	-0,079	-0,075	-0,076	-0,076	-0,076	-0,082	-0,081	-0,081
5,599	-0,085	-0,087	-0,085	-0,09	-0,085	-0,088	-0,088	-0,089	-0,088	-0,089
5,7	-0,096	-0,097	-0,097	-0,099	-0,099	-0,1	-0,104	-0,101	-0,101	-0,103
5,8	-0,107	-0,107	-0,108	-0,109	-0,109	-0,112	-0,11	-0,114	-0,112	-0,115
5,901	-0,12	-0,12	-0,121	-0,121	-0,121	-0,123	-0,128	-0,126	-0,127	-0,125
6	-0,138	-0,131	-0,134	-0,135	-0,135	-0,139	-0,135	-0,137	-0,138	-0,136
6,1	-0,142	-0,141	-0,141	-0,143	-0,143	-0,145	-0,143	-0,144	-0,146	-0,148
6,199	-0,152	-0,153	-0,153	-0,156	-0,157	-0,16	-0,157	-0,16	-0,157	-0,16
6,299	-0,163	-0,164	-0,167	-0,168	-0,168	-0,168	-0,169	-0,168	-0,169	-0,169

Continu 4 table G.1 results of matlab routine

LVDT [V]	1 [V]	2 [V]	3 [V]	4 [V]	5 [V]	6 [V]	7 [V]	8 [V]	9 [V]	10 [V]
6,4	-0,175	-0,177	-0,179	-0,179	-0,178	-0,179	-0,18	-0,181	-0,181	-0,182
6,5	-0,188	-0,188	-0,189	-0,191	-0,19	-0,19	-0,191	-0,191	-0,195	-0,198
6,601	-0,201	-0,198	-0,202	-0,204	-0,21	-0,205	-0,205	-0,203	-0,206	-0,207
6,7	-0,209	-0,211	-0,214	-0,212	-0,214	-0,213	-0,213	-0,214	-0,215	-0,214
6,8	-0,22	-0,221	-0,222	-0,226	-0,224	-0,226	-0,231	-0,229	-0,225	-0,224
6,9	-0,231	-0,235	-0,238	-0,237	-0,239	-0,237	-0,239	-0,238	-0,24	-0,241
7	-0,243	-0,243	-0,243	-0,243	-0,243	-0,244	-0,246	-0,248	-0,246	-0,249
7,1	-0,254	-0,254	-0,254	-0,258	-0,257	-0,258	-0,258	-0,259	-0,259	-0,26
7,2	-0,266	-0,266	-0,266	-0,266	-0,267	-0,268	-0,271	-0,268	-0,27	-0,269
7,3	-0,283	-0,277	-0,279	-0,279	-0,28	-0,282	-0,281	-0,282	-0,286	-0,282
7,4	-0,291	-0,288	-0,288	-0,288	-0,29	-0,29	-0,291	-0,29	-0,293	-0,293
7,5	-0,299	-0,3	-0,301	-0,301	-0,303	-0,302	-0,303	-0,31	-0,304	-0,304
7,6	-0,31	-0,311	-0,31	-0,312	-0,311	-0,312	-0,316	-0,316	-0,316	-0,315
7,7	-0,322	-0,323	-0,324	-0,328	-0,325	-0,326	-0,326	-0,326	-0,327	-0,33
7,8	-0,333	-0,334	-0,336	-0,337	-0,337	-0,336	-0,336	-0,338	-0,338	-0,338
7,9	-0,345	-0,345	-0,345	-0,346	-0,346	-0,347	-0,348	-0,351	-0,351	-0,349
8	-0,358	-0,356	-0,356	-0,357	-0,357	-0,357	-0,357	-0,358	-0,359	-0,362
8,1	-0,368	-0,367	-0,369	-0,372	-0,369	-0,373	-0,373	-0,373	-0,371	-0,372
8,2	-0,378	-0,38	-0,379	-0,38	-0,379	-0,381	-0,382	-0,381	-0,382	-0,382
8,3	-0,391	-0,39	-0,39	-0,39	-0,391	-0,392	-0,396	-0,393	-0,392	-0,392
8,4	-0,401	-0,402	-0,401	-0,404	-0,404	-0,404	-0,406	-0,405	-0,405	-0,405
8,5	-0,412	-0,414	-0,414	-0,414	-0,416	-0,416	-0,417	-0,418	-0,417	-0,417
8,6	-0,423	-0,423	-0,424	-0,424	-0,425	-0,429	-0,426	-0,429	-0,43	-0,429
8,7	-0,435	-0,436	-0,437	-0,437	-0,436	-0,436	-0,437	-0,44	-0,439	-0,437
8,8	-0,446	-0,451	-0,449	-0,449	-0,448	-0,449	-0,448	-0,452	-0,451	-0,45
8,9	-0,46	-0,457	-0,46	-0,457	-0,458	-0,46	-0,459	-0,461	-0,46	-0,461
9	-0,471	-0,472	-0,47	-0,472	-0,471	-0,471	-0,474	-0,475	-0,473	-0,474
9,1	-0,481	-0,481	-0,481	-0,481	-0,483	-0,481	-0,482	-0,484	-0,485	-0,482
9,2	-0,494	-0,494	-0,492	-0,494	-0,494	-0,494	-0,494	-0,493	-0,494	-0,494
9,3	-0,505	-0,508	-0,508	-0,508	-0,509	-0,508	-0,508	-0,506	-0,506	-0,511
9,327	-0,508	-0,508	-0,508	-0,508	-0,508	-0,508	-0,509	-0,508	-0,508	-0,508

Appendix H

Look up table H.1

X [mm]	Diff. Cap. [V]
-5.061	1.6137
-5.016	1.6066
-4.962	1.5946
-4.909	1.5845
-4.855	1.5729
-4.802	1.562
-4.749	1.5513
-4.695	1.5403
-4.642	1.5289
-4.589	1.5179
-4.535	1.506
-4.482	1.4962
-4.429	1.4867
-4.375	1.4755
-4.322	1.4648
-4.268	1.4554
-4.215	1.4437
-4.162	1.4331
-4.108	1.4221
-4.055	1.4139
-4.002	1.4018
-3.948	1.3917
-3.895	1.3815
-3.842	1.37
-3.788	1.3571
-3.735	1.3481
-3.681	1.3369
-3.628	1.3272
-3.575	1.3167
-3.521	1.3053
-3.468	1.2931
-3.415	1.284
-3.361	1.271
-3.308	1.259
-3.255	1.2492
-3.202	1.2395
-3.148	1.2271
-3.094	1.2171
-3.041	1.2036
-2.988	1.1943

X [mm]	Diff. Cap. [V]
-3.041	1.2036
-2.988	1.1943
-2.934	1.1826
-2.881	1.1709
-2.828	1.1582
-2.774	1.1498
-2.720	1.1374
-2.667	1.1252
-2.615	1.1138
-2.561	1.1023
-2.508	1.0927
-2.454	1.0784
-2.401	1.068
-2.347	1.0566
-2.295	1.0448
-2.241	1.0331
-2.187	1.0227
-2.081	0.9996
-2.027	0.9878
-1.974	0.9766
-1.921	0.9629
-1.867	0.9534
-1.814	0.9404
-1.760	0.9296
-1.707	0.9171
-1.654	0.9065
-1.600	0.896
-1.548	0.8837
-1.494	0.871
-1.442	0.8612
-1.387	0.8475
-1.335	0.8376
-1.281	0.8272
-1.226	0.8146
-1.175	0.8035
-1.117	0.7911
-1.067	0.7798
-1.014	0.7678
-0.961	0.7561
-0.907	0.7449

X [mm]	Diff. Cap. [V]
-0.853	0.7324
-0.803	0.7223
-0.747	0.7111
-0.693	0.6987
-0.645	0.688
-0.586	0.6761
-0.528	0.6627
-0.480	0.6515
-0.423	0.6421
-0.370	0.6289
-0.319	0.6187
-0.267	0.6062
-0.215	0.5942
-0.161	0.5853
-0.107	0.5713
-0.051	0.5609
-0.006	0.5503
0.057	0.5381
0.106	0.5272
0.160	0.5149
0.215	0.5035
0.265	0.4918
0.326	0.4782
0.373	0.4683
0.427	0.4562
0.478	0.4466
0.549	0.4302
0.584	0.4239
0.646	0.4093
0.687	0.4019
0.744	0.3876
0.803	0.376
0.855	0.3646
0.905	0.3529
0.959	0.3423
1.009	0.3311
1.068	0.3202
1.115	0.3098
1.178	0.2952
1.228	0.2859

Continu look up table H.1

X [mm]	Diff. Cap. [V]
1.279	0.2743
1.336	0.262
1.389	0.2497
1.437	0.241
1.494	0.229
1.545	0.2173
1.599	0.2074
1.652	0.1939
1.712	0.1829
1.762	0.1715
1.816	0.1598
1.866	0.1491
1.921	0.1386
1.974	0.1261
2.029	0.1154
2.082	0.1031
2.132	0.0927
2.183	0.0817
2.240	0.0713
2.292	0.0605
2.348	0.0463
2.401	0.0364
2.455	0.0244
2.506	0.0136
2.560	0.0011
2.614	-0.0092
2.668	-0.0207
2.720	-0.031
2.774	-0.0442
2.829	-0.0537
2.883	-0.0675
2.934	-0.0774
2.987	-0.0874
3.041	-0.0997
3.094	-0.1103
3.148	-0.1232
3.201	-0.1358
3.255	-0.1436
3.307	-0.1565
3.361	-0.1673
3.415	-0.1791
3.468	-0.1911
3.522	-0.2041
3.575	-0.2129
3.628	-0.2248
3.681	-0.2375
3.735	-0.2448
3.788	-0.2571
3.842	-0.2677
3.895	-0.2811
3.948	-0.2902
4.002	-0.3027
4.055	-0.3129
4.108	-0.3257
4.162	-0.3363
4.215	-0.3473
4.268	-0.3577
4.322	-0.3707
4.375	-0.3804
4.429	-0.3917
4.482	-0.4037
4.535	-0.4155
4.589	-0.4262
4.642	-0.437
4.695	-0.4493
4.749	-0.4593
4.802	-0.4723
4.855	-0.4821
4.909	-0.4937
4.962	-0.5077
4.977	-0.5081

Appendix I

Table I.1 standard deviations

Average Cap. [V]	σ_X [mV]
1,6137	0,48
1,6066	0,52
1,5946	0,70
1,5845	0,97
1,5729	0,57
1,562	0,82
1,5513	0,48
1,5403	0,48
1,5289	1,20
1,5179	0,88
1,506	1,15
1,4962	1,03
1,4867	1,06
1,4755	1,43
1,4648	1,40
1,4554	1,43
1,4437	1,77
1,4331	0,99
1,4221	1,45
1,4139	0,74
1,4018	1,93
1,3917	2,06
1,3815	1,27
1,37	1,70
1,3571	2,56
1,3481	2,38
1,3369	2,64
1,3272	1,69
1,3167	1,49
1,3053	1,77
1,2931	2,18
1,284	1,76
1,271	2,58
1,259	2,54
1,2492	2,49
1,2395	1,90
1,2271	2,47
1,2171	1,79
1,2036	2,41
1,1943	2,79
1,1826	2,27
1,1709	1,79
1,1582	1,62

Average Cap. [V]	σ_X [mV]
1,1498	2,20
1,1374	2,72
1,1252	2,10
1,1138	2,66
1,1023	2,54
1,0927	2,41
1,0784	2,01
1,068	2,94
1,0566	2,46
1,0448	2,74
1,0331	2,38
1,0227	2,21
0,9996	2,17
0,9878	2,25
0,9766	2,50
0,9629	2,28
0,9534	2,59
0,9404	1,65
0,9296	2,72
0,9171	2,77
0,9065	2,01
0,896	2,16
0,8837	2,58
0,871	2,05
0,8612	2,62
0,8475	1,78
0,8376	2,76
0,8272	2,82
0,8146	2,91
0,8035	3,03
0,7911	3,14
0,7798	2,86
0,7678	2,04
0,7561	1,29
0,7449	2,13
0,7324	2,12
0,7223	2,58
0,7111	2,96
0,6987	2,16
0,688	1,33
0,6761	1,66
0,6627	2,50
0,6515	2,32

Average Cap. [V]	σ_X [mV]
0,6421	2,18
0,6289	2,64
0,6187	1,64
0,6062	3,49
0,5942	2,94
0,5853	2,67
0,5713	1,95
0,5609	2,77
0,5503	2,79
0,5381	2,33
0,5272	3,71
0,5149	2,96
0,5035	2,95
0,4918	3,74
0,4782	1,99
0,4683	2,75
0,4562	3,22
0,4466	3,10
0,4302	2,49
0,4239	2,85
0,4093	4,22
0,4019	2,51
0,3876	2,84
0,376	1,94
0,3646	2,67
0,3529	2,38
0,3423	1,64
0,3311	2,28
0,3202	2,66
0,3098	2,49
0,2952	2,82
0,2859	2,13
0,2743	2,11
0,262	2,36
0,2497	1,70
0,241	3,59
0,229	2,94
0,2173	2,21
0,2074	2,01
0,1939	3,60
0,1829	1,79
0,1715	2,95
0,1598	3,01

Continu table I.1

Average Cap. [V]	σ_X [mV]
0,1491	2,85
0,1386	2,80
0,1261	3,21
0,1154	2,01
0,1031	2,23
0,0927	3,16
0,0817	2,63
0,0713	2,41
0,0605	2,32
0,0463	3,33
0,0364	2,80
0,0244	2,46
0,0136	3,06
0,0011	2,69
-0,0092	2,70
-0,0207	2,00
-0,031	2,26
-0,0442	2,20
-0,0537	2,87
-0,0675	2,01
-0,0774	3,10
-0,0874	1,84
-0,0997	2,63
-0,1103	2,83
-0,1232	3,05
-0,1358	2,35
-0,1436	2,22
-0,1565	3,03
-0,1673	2,11
-0,1791	2,08
-0,1911	3,14
-0,2041	3,35
-0,2129	1,79
-0,2248	3,43
-0,2375	2,84
-0,2448	2,30
-0,2571	2,28
-0,2677	1,83
-0,2811	2,51
-0,2902	1,87
-0,3027	3,06
-0,3129	2,56
-0,3257	2,36
-0,3363	1,70
-0,3473	2,36
-0,3577	1,77
-0,3707	2,26
-0,3804	1,43
-0,3917	1,83
-0,4037	1,77
-0,4155	1,90
-0,4262	2,78
-0,437	1,49
-0,4493	1,77
-0,4593	1,49
-0,4723	1,64
-0,4821	1,45
-0,4937	0,67
-0,5077	1,70
-0,5081	0,32

Appendix J

Table J.1 measured inaccuracy

error 1 [µm]	error 2 [µm]	error 3 [µm]	error 4 [µm]	error 5 [µm]	error 6 [µm]	error 7 [µm]	error 8 [µm]	error 9 [µm]	error 10 [µm]
1,42	1,42	1,42	1,42	3,31	3,31	1,42	1,42	1,42	3,31
1,89	1,89	1,89	1,89	1,89	2,83	2,83	2,83	1,89	2,83
1,89	1,89	1,89	1,89	1,89	1,89	2,83	1,89	2,83	7,56
2,36	2,36	2,36	2,36	2,36	2,36	2,36	2,36	2,36	11,81
0,47	0,47	5,19	0,47	0,47	0,47	0,47	0,47	4,25	4,25
0,00	4,72	4,72	4,72	4,72	0,00	0,00	0,00	4,72	4,72
1,42	1,42	1,42	3,31	3,31	1,42	1,42	1,42	1,42	3,31
1,42	3,31	3,31	1,42	1,42	3,31	1,42	1,42	1,42	1,42
9,92	5,19	5,19	0,47	0,47	4,25	4,25	4,25	0,47	8,97
0,47	5,19	4,25	5,19	4,25	5,19	4,25	4,25	0,47	0,47
4,72	4,72	4,72	0,00	4,72	4,72	4,72	4,72	4,72	9,44
3,78	3,78	3,78	3,78	0,94	3,78	0,94	0,94	5,67	10,39
6,14	1,42	6,14	3,31	6,14	1,42	3,31	3,31	8,03	3,31
11,81	7,08	7,08	2,36	2,36	2,36	2,36	7,08	7,08	7,08
15,11	5,67	0,94	0,94	0,94	3,78	3,78	3,78	3,78	8,50
7,56	1,89	7,56	1,89	7,56	7,56	6,61	6,61	6,61	6,61
10,86	6,14	6,14	6,14	1,42	1,42	3,31	3,31	8,03	17,47
4,25	8,97	4,25	0,47	0,47	0,47	5,19	0,47	5,19	5,19
13,69	4,25	4,25	4,25	0,47	5,19	0,47	5,19	5,19	9,92
0,47	0,47	5,19	5,19	0,47	0,47	4,25	0,47	4,25	4,25
15,11	10,39	0,94	0,94	0,94	5,67	3,78	3,78	13,22	13,22
10,86	15,58	6,14	6,14	1,42	3,31	3,31	8,03	12,75	12,75
7,08	7,08	7,08	2,36	2,36	2,36	2,36	7,08	7,08	7,08
9,44	4,72	9,44	4,72	4,72	4,72	0,00	4,72	14,17	9,44
27,86	13,69	0,47	0,47	9,92	5,19	0,47	9,92	9,92	5,19
18,42	18,42	4,25	4,25	0,47	5,19	9,92	9,92	9,92	9,92
19,36	14,64	14,64	5,19	4,25	4,25	8,97	8,97	13,69	13,69
13,22	8,50	3,78	3,78	3,78	0,94	5,67	5,67	10,39	10,39
10,86	6,14	6,14	1,42	1,42	1,42	3,31	3,31	8,03	12,75
12,75	8,03	8,03	3,31	3,31	1,42	6,14	10,86	6,14	10,86
23,14	8,97	4,25	0,47	0,47	0,47	5,19	9,92	9,92	9,92
9,44	9,44	4,72	4,72	0,00	4,72	0,00	9,44	9,44	14,17
18,89	18,89	9,44	0,00	0,00	4,72	4,72	9,44	14,17	14,17
28,33	14,17	0,00	4,72	4,72	4,72	9,44	4,72	4,72	9,44
17,94	13,22	8,50	13,22	5,67	10,39	5,67	10,39	10,39	10,39
16,53	7,08	11,81	2,36	2,36	7,08	7,08	7,08	7,08	7,08
23,14	8,97	8,97	4,25	0,47	0,47	9,92	9,92	9,92	14,64
13,69	4,25	8,97	4,25	0,47	0,47	0,47	5,19	14,64	9,92
16,06	16,06	11,33	6,61	7,56	2,83	7,56	12,28	7,56	12,28
22,19	12,75	12,75	3,31	3,31	1,42	10,86	10,86	15,58	15,58
16,06	11,33	6,61	6,61	6,61	2,83	7,56	12,28	12,28	12,28
14,64	9,92	5,19	5,19	0,47	4,25	4,25	8,97	8,97	8,97
13,22	8,50	3,78	0,94	0,94	0,94	0,94	15,11	5,67	0,94

Continu 1 table J.1 measured inaccuracy

error 1 [µm]	error 2 [µm]	error 3 [µm]	error 4 [µm]	error 5 [µm]	error 6 [µm]	error 7 [µm]	error 8 [µm]	error 9 [µm]	error 10 [µm]
15,11	10,39	10,39	0,94	5,67	0,94	13,22	8,50	13,22	8,50
21,72	21,72	2,83	2,83	1,89	6,61	11,33	6,61	6,61	16,06
22,67	8,50	3,78	0,94	0,94	5,67	0,94	10,39	5,67	10,39
24,55	19,83	0,94	3,78	3,78	0,94	8,50	8,50	8,50	13,22
22,19	12,75	8,03	3,31	3,31	6,14	6,14	10,86	10,86	15,58
6,14	10,86	10,86	10,86	6,14	6,14	8,03	12,75	12,75	17,47
17,00	12,28	7,56	1,89	1,89	1,89	11,33	1,89	6,61	11,33
18,89	18,89	18,89	0,00	0,00	9,44	9,44	9,44	14,17	14,17
20,78	16,06	6,61	1,89	2,83	2,83	2,83	12,28	12,28	12,28
19,83	15,11	5,67	5,67	5,67	0,94	8,50	8,50	17,94	17,94
18,42	13,69	8,97	8,97	9,92	5,19	5,19	9,92	9,92	9,92
15,58	15,58	6,14	6,14	1,42	8,03	12,75	8,03	8,03	8,03
11,33	11,33	11,33	1,89	6,61	2,83	2,83	12,28	7,56	17,00
15,11	10,39	10,39	5,67	5,67	8,50	3,78	8,50	13,22	13,22
16,06	16,06	11,33	6,61	1,89	12,28	7,56	12,28	7,56	12,28
19,36	14,64	0,47	4,25	0,47	0,47	4,25	0,47	8,97	18,42
12,28	17,00	17,00	2,83	1,89	6,61	6,61	6,61	6,61	20,78
17,00	7,56	2,83	1,89	2,83	1,89	6,61	6,61	6,61	6,61
20,78	16,06	16,06	2,83	2,83	2,83	12,28	12,28	12,28	7,56
27,86	18,42	0,47	5,19	0,47	5,19	5,19	5,19	9,92	14,64
16,53	11,81	7,08	2,36	2,36	2,36	2,36	11,81	7,08	11,81
14,17	14,17	9,44	4,72	4,72	0,00	9,44	4,72	14,17	9,44
15,58	15,58	15,58	6,14	3,31	8,03	12,75	3,31	12,75	12,75
18,89	14,17	4,72	4,72	4,72	0,00	4,72	9,44	9,44	4,72
17,94	8,50	13,22	8,50	8,50	10,39	10,39	10,39	10,39	15,11
7,08	11,81	7,08	7,08	2,36	7,08	2,36	2,36	11,81	11,81
20,78	11,33	11,33	1,89	1,89	1,89	2,83	7,56	17,00	21,72
17,94	13,22	17,94	8,50	0,94	5,67	10,39	15,11	10,39	15,11
20,78	20,78	16,06	7,56	12,28	2,83	2,83	7,56	12,28	12,28
16,53	16,53	16,53	11,81	2,36	11,81	7,08	11,81	16,53	16,53
18,42	23,14	13,69	4,25	9,92	0,47	5,19	9,92	9,92	24,08
5,67	15,11	10,39	10,39	10,39	0,94	3,78	22,67	3,78	22,67
19,83	10,39	5,67	0,94	0,94	3,78	8,50	8,50	8,50	8,50
8,97	4,25	4,25	4,25	4,25	0,47	5,19	5,19	5,19	9,92
19,36	5,19	9,92	5,19	8,97	4,25	0,47	4,25	13,69	8,97
21,72	7,56	2,83	2,83	1,89	6,61	1,89	6,61	1,89	16,06
17,47	8,03	8,03	8,03	1,42	3,31	1,42	1,42	20,31	20,31
13,69	18,42	13,69	4,25	13,69	9,92	9,92	14,64	14,64	14,64
10,86	20,31	1,42	6,14	3,31	1,42	8,03	12,75	8,03	8,03
9,44	9,44	0,00	4,72	4,72	0,00	4,72	0,00	4,72	9,44
18,42	5,19	4,25	5,19	4,25	0,47	0,47	0,47	5,19	9,92
20,31	15,58	10,86	3,31	3,31	3,31	8,03	8,03	3,31	17,47
16,53	16,53	7,08	16,53	2,36	2,36	2,36	11,81	2,36	7,08

Continu 2 table J.1 measured inaccuracy

error 1 [µm]	error 2 [µm]	error 3 [µm]	error 4 [µm]	error 5 [µm]	error 6 [µm]	error 7 [µm]	error 8 [µm]	error 9 [µm]	error 10 [µm]
13,69	4,25	0,47	8,97	4,25	4,25	4,25	5,19	19,36	14,64
19,36	19,36	5,19	0,47	0,47	0,47	8,97	13,69	4,25	18,42
10,86	10,86	6,14	1,42	1,42	3,31	3,31	3,31	8,03	12,75
22,67	13,22	13,22	13,22	8,50	15,11	0,94	10,39	19,83	24,55
22,67	8,50	22,67	0,94	5,67	5,67	5,67	5,67	10,39	19,83
12,75	12,75	17,47	8,03	3,31	1,42	10,86	15,58	10,86	15,58
17,47	12,75	3,31	1,42	1,42	1,42	1,42	10,86	6,14	10,86
19,36	14,64	14,64	5,19	0,47	4,25	8,97	8,97	13,69	18,42
22,19	17,47	8,03	8,03	1,42	6,14	10,86	10,86	10,86	15,58
13,69	13,69	0,47	13,69	0,47	4,25	9,92	9,92	9,92	14,64
17,94	17,94	13,22	13,22	8,50	3,78	10,39	10,39	24,55	29,28
19,36	19,36	14,64	5,19	0,47	8,97	8,97	13,69	8,97	18,42
16,53	16,53	21,25	2,36	2,36	11,81	11,81	7,08	11,81	16,53
24,55	15,11	24,55	10,39	22,67	3,78	8,50	8,50	8,50	22,67
13,22	13,22	3,78	3,78	3,78	5,67	0,94	5,67	15,11	10,39
17,47	17,47	12,75	1,42	1,42	6,14	6,14	1,42	6,14	25,03
27,39	13,22	13,22	3,78	0,94	0,94	5,67	10,39	24,55	15,11
20,78	16,06	11,33	6,61	1,89	1,89	21,72	7,56	7,56	21,72
17,94	17,94	8,50	3,78	5,67	0,94	5,67	10,39	10,39	15,11
19,36	19,36	9,92	5,19	0,47	0,47	13,69	13,69	13,69	13,69
26,92	26,92	22,19	12,75	20,31	6,14	10,86	15,58	15,58	20,31
19,36	9,92	5,19	5,19	8,97	5,19	5,19	8,97	13,69	18,42
20,78	16,06	11,33	17,00	1,89	1,89	1,89	7,56	12,28	17,00
14,17	14,17	4,72	4,72	4,72	9,44	0,00	9,44	4,72	9,44
25,50	11,33	11,33	17,00	7,56	7,56	1,89	7,56	2,83	7,56
28,80	0,47	0,47	0,47	0,47	0,47	4,25	4,25	8,97	13,69
17,47	8,03	3,31	1,42	1,42	1,42	6,14	6,14	6,14	6,14
18,42	0,47	13,69	8,97	0,47	9,92	0,47	5,19	9,92	14,64
17,94	8,50	8,50	8,50	3,78	0,94	24,55	0,94	5,67	15,11
19,83	15,11	10,39	0,94	0,94	3,78	8,50	13,22	8,50	13,22
22,67	17,94	13,22	5,67	5,67	0,94	5,67	5,67	15,11	15,11
14,64	9,92	5,19	5,19	5,19	0,47	8,97	4,25	8,97	18,42
12,75	12,75	8,03	8,03	3,31	6,14	6,14	10,86	10,86	10,86
23,61	14,17	4,72	4,72	9,44	4,72	0,00	4,72	9,44	9,44
6,14	6,14	12,75	6,14	6,14	6,14	1,42	8,03	1,42	12,75
18,89	23,61	18,89	9,44	18,89	4,72	0,00	9,44	14,17	23,61
4,72	4,72	4,72	14,17	18,89	9,44	14,17	4,72	0,00	28,33
17,47	1,42	17,47	6,14	3,31	1,42	1,42	6,14	6,14	15,58
12,28	12,28	1,89	7,56	7,56	1,89	11,33	11,33	1,89	11,33
24,08	19,36	14,64	14,64	13,69	18,42	0,47	4,25	18,42	18,42
14,64	5,19	5,19	5,19	0,47	0,47	0,47	8,97	8,97	13,69
21,25	16,53	11,81	7,08	2,36	11,81	2,36	11,81	16,53	16,53
19,83	19,83	10,39	5,67	0,94	8,50	0,94	17,94	17,94	13,22

Continu 3 table J.1 measured inaccuracy

error 1 [µm]	error 2 [µm]	error 3 [µm]	error 4 [µm]	error 5 [µm]	error 6 [µm]	error 7 [µm]	error 8 [µm]	error 9 [µm]	error 10 [µm]
27,86	5,19	13,69	4,25	0,47	5,19	0,47	0,47	19,36	14,64
20,78	11,33	11,33	6,61	6,61	7,56	12,28	7,56	7,56	21,72
18,42	18,42	13,69	4,25	4,25	0,47	0,47	14,64	19,36	24,08
6,61	17,00	6,61	12,28	2,83	7,56	1,89	6,61	6,61	11,33
13,69	13,69	13,69	5,19	0,47	0,47	0,47	14,64	9,92	9,92
25,03	10,86	20,31	3,31	8,03	6,14	17,47	8,03	8,03	17,47
25,03	6,14	15,58	3,31	8,03	8,03	3,31	3,31	3,31	17,47
12,75	12,75	8,03	8,03	3,31	10,86	3,31	10,86	6,14	20,31
16,53	11,81	2,36	2,36	7,08	7,08	2,36	11,81	16,53	11,81
26,92	22,19	6,14	8,03	8,03	6,14	6,14	15,58	10,86	20,31
17,00	12,28	7,56	7,56	2,83	1,89	1,89	6,61	6,61	30,22
12,28	12,28	17,00	2,83	2,83	1,89	6,61	16,06	6,61	16,06
20,78	16,06	16,06	1,89	2,83	1,89	12,28	2,83	21,72	17,00
23,14	13,69	8,97	5,19	0,47	0,47	0,47	14,64	5,19	19,36
15,11	15,11	5,67	0,94	10,39	3,78	3,78	3,78	8,50	27,39
8,03	17,47	3,31	3,31	3,31	1,42	6,14	1,42	10,86	15,58
14,17	9,44	9,44	9,44	4,72	0,00	0,00	9,44	18,89	9,44
19,83	8,50	10,39	17,94	5,67	0,94	3,78	0,94	3,78	3,78
17,47	8,03	8,03	8,03	3,31	3,31	1,42	29,75	1,42	15,58
7,08	21,25	7,08	7,08	2,36	11,81	2,36	2,36	2,36	7,08
20,78	11,33	7,56	11,33	6,61	6,61	6,61	21,72	17,00	17,00
11,33	1,89	11,33	12,28	11,33	2,83	2,83	7,56	2,83	7,56
17,47	12,75	12,75	3,31	3,31	1,42	20,31	6,14	6,14	15,58
15,58	15,58	10,86	6,14	6,14	8,03	1,42	17,47	8,03	22,19
15,11	15,11	10,39	10,39	10,39	0,94	22,67	13,22	17,94	8,50
10,39	22,67	8,50	3,78	3,78	15,11	3,78	5,67	10,39	0,94
7,56	12,28	12,28	2,83	2,83	6,61	2,83	1,89	11,33	20,78
21,25	16,53	16,53	2,36	2,36	16,53	2,36	16,53	2,36	16,53
20,31	15,58	1,42	3,31	3,31	3,31	8,03	3,31	8,03	8,03
19,36	9,92	0,47	0,47	5,19	0,47	4,25	8,97	8,97	13,69
14,64	14,64	9,92	0,47	5,19	5,19	0,47	0,47	18,42	32,58
14,64	28,80	9,92	0,47	27,86	4,25	4,25	5,19	8,97	13,69
18,42	8,97	5,19	4,25	5,19	0,47	0,47	5,19	9,92	5,19
22,67	17,94	13,22	5,67	3,78	5,67	29,28	19,83	0,94	3,78
30,69	11,81	2,36	2,36	7,08	2,36	7,08	2,36	11,81	16,53
8,50	8,50	8,50	8,50	8,50	3,78	5,67	15,11	5,67	19,83
14,64	14,64	14,64	4,25	0,47	4,25	4,25	8,97	8,97	13,69
8,03	8,03	8,03	8,03	3,31	1,42	15,58	1,42	10,86	6,14
8,97	19,36	9,92	9,92	5,19	4,25	0,47	4,25	23,14	4,25
3,78	10,39	10,39	10,39	0,94	0,94	3,78	0,94	13,22	13,22
17,47	12,75	8,03	8,03	1,42	3,31	1,42	34,47	6,14	6,14
13,69	8,97	13,69	4,25	8,97	4,25	14,64	14,64	14,64	9,92
17,47	12,75	8,03	10,86	3,31	1,42	1,42	1,42	6,14	20,31

Continu 4 table J.1 measured inaccuracy

error 1 [µm]	error 2 [µm]	error 3 [µm]	error 4 [µm]	error 5 [µm]	error 6 [µm]	error 7 [µm]	error 8 [µm]	error 9 [µm]	error 10 [µm]
15,58	10,86	1,42	3,31	3,31	1,42	1,42	8,03	8,03	8,03
10,86	10,86	10,86	6,14	6,14	1,42	3,31	17,47	17,47	8,03
1,42	8,03	8,03	3,31	3,31	3,31	3,31	1,42	6,14	20,31
12,75	17,47	8,03	6,14	8,03	10,86	10,86	10,86	1,42	6,14
11,33	1,89	6,61	1,89	6,61	2,83	7,56	2,83	7,56	7,56
3,31	8,03	8,03	8,03	3,31	1,42	20,31	6,14	1,42	1,42
12,75	8,03	12,75	1,42	1,42	1,42	10,86	6,14	6,14	6,14
16,53	7,08	7,08	7,08	2,36	2,36	7,08	11,81	7,08	7,08
15,11	15,11	10,39	10,39	5,67	13,22	0,94	13,22	17,94	13,22
9,44	4,72	0,00	0,00	4,72	4,72	0,00	14,17	9,44	0,00
15,58	8,03	1,42	1,42	6,14	1,42	6,14	12,75	8,03	3,31
3,31	10,86	3,31	10,86	6,14	3,31	1,42	8,03	3,31	8,03
6,14	1,42	10,86	1,42	6,14	6,14	8,03	12,75	3,31	8,03
5,19	5,19	5,19	5,19	4,25	5,19	0,47	8,97	13,69	0,47
1,42	1,42	8,03	1,42	1,42	1,42	1,42	3,31	1,42	1,42
12,75	1,42	1,42	1,42	6,14	1,42	1,42	8,03	8,03	15,58
0,47	0,47	0,47	0,47	0,47	0,47	4,25	0,47	0,47	0,47

Appendix K

Reference list:

ACH00 *Vicktor M.G. van Acht*
Magnetically levitated 6 DOF mirror
Thesis report
2000

ANA99 *Analog Devices*
Datasheet Balanced Modulator/Demodulator AD630
www.analog.com

BOS94 *Paul P.J. van den Bosch and A.C. van der Klauw*
Modeling, Identification and Simulation of Dynamical Systems
CRC Press, Inc.
1994

DAM95 *Ad A.H. Damen*
Introductie Regelaars ontwerp addendum
Collegedictaat
Technische Universiteit Eindhoven
November 1995

FRA94 *Gene F. Franklin, J. David Powell and Abbas Emami-Naeini*
Feedback control of dynamic systems
Work student series
Addison-Wesley Publishing Company, Inc.
1994 third edition

GAO91 *Franklin X.Y. Gao and W. Martin Snelgrove*
Adaptive linearization of a loudspeaker
IEEE 1991

GOO99 *Jeffrey H.P.M. Goossens*
Differentieel capacitief positie sensor systeem met 1 vrijheidsgraad
Stageverslag
Technische Universiteit Eindhoven
Departement of electrical engineering
Measurement and Control section
September 1999

HAN80 *Raymond J.L. Hanus*
A new technique for preventing control windup
Journal A, volume 21, no 1, 1980

Continu reference list

LAA95 *P.C.T van der Laan*
Velden in de Elektrotechniek
Collegedictaat
Technische Universiteit Eindhoven
January 1995

LAN98 *Steven A. Lane and Robert L. Clark*
Improving loudspeaker performance for active noise control applications
Journal of the audio engineering society, volume 46, issue 6, 1998

RS97 *Datasheet*
Peltier effect heat pumps
March 1997

SCH97 *Hans Schurer, Alex G.J. Nijmeijer, Mark A. Boer, Cornelis H. Slump and Otto E. Herrmann*
Identification and compensation of the electrodynamic transducer nonlinearities
IEEE 1997

SOL95 *Solartron metrology*
User leaflet of boxed inline conditioning module
Issue 3 may 1995

SUA96 *Kendall L. Su*
Analog filters
London: Chapman & Hall 1996